

AN ABSTRACT OF THE THESIS OF

Robert H. Simon for the Ph.D. in Chemical Engineering
(Name) (Degree) (Major)

Date Thesis presented November 3, 1948

Title Heat Transfer in Beds of Fluidized Solids

Abstract Approved [REDACTED]
(Major Professor)

A study of heat transfer in beds of fluidized solids has been made in order to supply some of the basic information which was lacking when the wartime fluid catalytic cracking plants were built. Although a number of papers on fluidization of solids have been written in the past several years, with the exception of some preliminary experiments on indirect heat transfer by Parent, Yagol, and Steiner, nothing has been published on heat transfer in beds of fluidized solids.

In this thesis, equipment was designed and constructed for this purpose. A technique was developed which permitted a general study of the behavior of fluidized beds with respect to heat flow; and the magnitude of the coefficient of heat transfer between the upward flowing gas and the wall, with and without the presence of solid particles, was determined. In addition, an attempt was made to determine the coefficient of heat transfer between the gas and the solid particles.

The apparatus consisted essentially of two four inch tubes: one was sheet metal, ten feet high, insulated, and preceded by an air heater. A rotatable screen defined the bottom of the fluidized bed and seventeen thermocouples measured temperatures at various points in the gas stream, in the bed, in the metal tube, and in the insulation. The other tube was glass, ten feet high, and was used for visual observation of materials in order that their behavior in the metal tube might be known. Air velocities were measured by two thin-plate orifices.

Runs were made on 3A Catalyst, Ottawa Standard Silica Sand, wood charcoal, Utah hard coal, and with an empty tube. The particles ranged in size from -270 mesh to 8 mesh. In attempting to determine the coefficient of heat transfer between the air and the particles, hot air was introduced suddenly into the bed of fluidized solids and temperature measurements were made throughout the unsteady state portion of the run. It was hoped that the rate of heat flow to the solid could be calculated by difference between the input and the losses to the metal and the insulation but, partly because of unaccountable losses and partly because of the close approach to equilibrium between air and solid at the top of the bed, this method was unsuccessful. However, this did not affect the experimentation to determine the coefficient of heat transfer between the air and the metal wall.

The calculations of this latter value were based on combining the measured rate of heat flow through the insulation, after steady state had been reached,

with the resistance concept. The results are summarized below.

Coefficient of Heat Transfer between Air and Tube Wall

<u>Material Fluidized</u>	<u>Approximate Avg. Particle Size</u>	<u>Mass Velocity lb per hr-sq ft</u>	<u>Coefficient of Heat Transfe Btu per hr-sq ft-°F</u>
3A Catalyst	150 mesh	193	22
Sand	40 mesh	813	13
Coal	20 mesh	809	5.2
Coal	20 mesh	636	4.5
Coal	20 mesh	635	4.5
Charcoal	20 mesh	548	3.2
Empty Tube	---	637	0.89
Empty Tube	---	636	0.74

The following conclusions were drawn:

1. The film coefficient of heat transfer between the air and the tube wall is much greater when fluidized solids are present than when absent.
2. The film coefficient increases with increasing mass velocity. In fact, it increases at about the same rate as the mass velocity.
3. The film coefficient increases with decreasing particle size. The increase is at least proportional to the particle size and may be much greater than that.

It is recommended that further extensive experimental work be carried out on the coefficient of heat transfer between the air stream and the tube wall and that an attempt be made to determine the coefficient of heat transfer between the air and the fluidized particles using continuous feed and discharge of the particles.

HEAT TRANSFER IN BEDS
OF FLUIDIZED SOLIDS

by

Robert Haskell Simon

A THESIS

Submitted to


OREGON STATE COLLEGE

in partial fulfillment of
the requirements for the
degree of


DOCTOR OF PHILOSOPHY

October 1948


APPROVED:



Head of Department of Chemical Engineering
In Charge of Major



Chairman of School Graduate Committee



Dean of Graduate School

ACKNOWLEDGMENT

The author wishes to acknowledge his indebtedness to Professor J.S. Walton for his guidance throughout this thesis. He also desires to express his gratitude to the other members of the staff of the Chemical Engineering Department for their helpful suggestions, to Professor S.H. Graf for the loan of equipment and to O. Levenspiel for his assistance in constructing the apparatus.

EATON'S
CORRASABLE
BOND
U.S.A.
BERKSHIRE

TABLE OF CONTENTS

	Page
Introduction	1
Literature Survey	2
Scope	6
Procedure	8
Method of Attack	8
Equipment	8
Preliminary Operations	12
First Heating Runs	17
Improved Apparatus	21
Apparatus	25
Results and Discussion	38
Fluidization	38
Theory	39
Typical Calculations	45
Schmidt Method	53
Coefficient of Heat Transfer between Air and Tube Wall	60
Steady State Heat Flow	64
Coefficient of Heat Transfer between Air and Solid	73
Conclusions	82
Recommendations	84
Appendix	85
Additional Equipment Data	85

TABLE OF CONTENTS CONTINUED

	Page
Orifice Calibration	86
Thermocouple Calibration	94
Temperature vs Millivolts for Iron-Constantan Thermocouple	96
Fluidization Characteristics of 14 to 28 Mesh Utah Coal	97
Net Pressure Drop	99
Tyler Standard Sieves	102
Density of Particles	103
Apparent Density of Particles	104
Average Particle Size	105
Specific Heat of Utah Coal	107
Steady State Runs with Empty Tube	108
Calculation of Film Coefficient between the Outside of the Insulation and the Room	112
Unsteady State Run with Empty Tube	113
Unsteady State Runs with Coal	115
Unsteady State Cooling Runs	135
Suction Thermocouple Operation	146
Temperature Drop Through the Metal Wall	147
Longitudinal Flow of Heat	148
Flow of Heat Through Fittings	149
Schmidt Method	150
Accuracy of Results	155

Table of Nomenclature

- a Subscript, indicating air.
- A_g Area of outside of metal wall, square feet.
- A_i Area of insulation normal to the heat flow, square feet.
- A_s Total surface area of the particles in the bed, square feet.
- A_T Cross-sectional area of the tube, square feet.
- A_w Inside surface area of the metal tube, square feet.
- A' Total mean area of the particles in the bed, square feet.
- C_p Specific heat, Btu per lb - $^{\circ}\text{F}$.
- G Mass velocity, lb per (hour) (square foot).
- G' GA_T , mass velocity lbs per hr.
- h_g Coefficient of heat transfer between the outside of the metal and the inside of the insulation, Btu per (hour) (square foot) ($^{\circ}\text{F}$).
- h_r Coefficient of heat transfer between the outside of the insulation and the room, Btu per (hour) (square foot) ($^{\circ}\text{F}$).
- h_s Coefficient of heat transfer between the air and the particles, Btu per (hour) (square foot) ($^{\circ}\text{F}$).
- h_w Coefficient of heat transfer between the air and the tube wall, Btu per (hour) (square foot) ($^{\circ}\text{F}$).
- i Subscript, indicating insulation.
- K Thermal conductivity, Btu per (hour) (square foot) ($^{\circ}\text{F}$ per foot).
- l Distance, in the direction of the flow of heat, feet
- m Subscript, indicating metal.
- N Depth of bed, feet.
- P_1 Pressure, upstream of the orifice, inches of mercury.

- ΔP Pressure drop across the orifice, inches of water.
- $q \frac{dQ}{d\theta}$, rate of heat flow, Btu per hr
- Q Quantity of heat, Btu.
- r Radial distance from center of tube, feet.
- r' Distance from center of tube to inside of insulation, feet.
- s Subscript, indicating solid particles.
- t Temperature, $^{\circ}\text{F}$.
- t_d Gas temperature at entrance of bed, $^{\circ}\text{F}$.
- t_e Gas temperature at exit from bed, $^{\circ}\text{F}$.
- t' Temperature at inside of insulation, $^{\circ}\text{F}$.
- t'' Insulation temperature $\frac{1}{4}$ inch out from metal wall, $^{\circ}\text{F}$.
- $t_1, t_2, \text{etc.}$ Temperature at the thermocouples indicated by the subscript, $^{\circ}\text{F}$.
- t_o Room temperature, $^{\circ}\text{F}$.
- T average temperature of all the particles, $^{\circ}\text{F}$.
- TC Abbreviation for thermocouple.
- U_s Overall coefficient of heat transfer between the air and the particles, Btu per (hour) (square foot) ($^{\circ}\text{F}$).
- w Subscript, indicating tube wall.
- W Weight, pounds.
- x Distance, feet.
- $\alpha = \frac{K}{\rho C_p}$, thermal diffusivity, square feet per hour.
- Δ_s Temperature difference between the air and the center of a particle, $^{\circ}\text{F}$.
- Δ_w Temperature difference between the air and the metal wall, $^{\circ}\text{F}$.
- ρ Density, pounds per cubic foot.

ρ_0 Density of the air in the orifice, pounds per cubic foot.

θ Time, hours.

HEAT TRANSFER IN BEDS OF FLUIDIZED SOLIDS

INTRODUCTION

This thesis was undertaken in order to supply information on the transmission of heat in beds of fluidized solids. Specifically, quantitative data are presented which show rates of heat transfer between beds of solid and the retaining wall of the bed. Some qualitative information is also submitted on the rate of heat transfer between the fluidized solids and air passing upwardly through the bed.

Although the technique of fluidization of solids has been known for seventy years, it did not attain industrial importance until the early part of World War II. At that time, a number of plants were built for the catalytic cracking of petroleum, using a process developed by the Standard Oil Development Company. This process was at first called 'jiggling' and, later, 'fluidization of solids' - terms which were very descriptive of the action of the solids. The essential idea was that a bed of fine solids - in this case catalyst - was suspended in a rising gas stream, leading to intimate contact between gas and solid. Under the pressure of wartime, these plants were built with little basic information. This thesis was written in order to supply some of that information.

Literature Survey

During the past few years, a number of papers have been written on fluidization of solids. With few exceptions, they have been concerned with either catalytic cracking of petroleum in fluidized beds or the flow characteristics of fluidized solids. As far as is known, the only information published on heat transfer in beds of fluidized solids has appeared in the following articles:

1. Kalbach, in his three papers (1,2,3) reviewing fluidization and discussing the information necessary for the design of fluidized equipment, mentioned the rapid transfer of heat as one of the chief advantages.

2. Kite and Roberts (4) discussed non-catalytic fluidization. Among possible uses they listed "---heat transfer operations wherein sensible heat is transferred from solid to gas phase or the reverse." They have applied this to the preheating of limestone in a stepwise calciner employing fluidization. However, no data were given. They also mentioned the uniformity of temperature in fluidized beds, a point emphasized by Dr. Warren K. Lewis in an address when receiving the Priestly Medal in 1947.

1. Kalbach, J.C. Improving Solids-Gas Contact by Fluidization, Chemical Engineering 51:94-8, June 1944.
2. Kalbach, J.C. Fluidization in Chemical Reactions, Chemical Engineering 54:105-8, Jan. 1947.
3. Kalbach, J.C. Handling Solids-Gas Reactions by Fluidization, Chemical Engineering 54:136-8, Feb. 1947.
4. Kite, R.P. and Roberts, E.J. Fluidization in Non-Catalytic Reactions, Chemical Engineering 54:112-5, Dec. 1947.

3. Thomas and Hoekstra (5), in the course of a study of the catalytic cracking of gas oil, passed air through a bed of hot, spent catalyst in a two-inch pipe. The pipe was located in a thermostatted block. Temperatures were measured at four points in the bed and one above the bed by means of thermocouples inserted in a well. Heat was supplied by the burning carbonaceous deposit. No heat balances were given and no heat transfer rates calculated.

4. Parent, Yagol, and Steiner (6) carried out some preliminary experiments on indirect heat transfer in a steam-jacketed copper tube. They measured the inlet and outlet temperatures of nitrogen flowing at approximately 0.4 and 0.5 feet per second through the empty tube and again with -70 + 325 mesh coke present. At the lower velocity their heat transfer coefficient was 3 per cent lower when fluidized solids were present than when absent, whereas at the higher velocity the coefficient was 5 per cent higher when fluidized solids were present than when absent.

5. Furnas (7) studied heat transfer from a gas stream to beds of broken solids and reported that at his highest velocities the whole bed was lifted. However, in answer to

5. Thomas, C.L. and Hoekstra Fluidized Fixed Beds, Ind. and Eng. Chem. 37:332-4, April 1945.
6. Parent, J.D., Yagol N. and Steiner, C.S. Some Basic Observations on the Fluidizing Process in Laboratory Scale Equipment, Chem. Eng. Progress 43:429-436, Aug. 1947.
7. Furnas, J.J. Heat Transfer from a Gas Stream to Beds of Broken Solids, U. S. Bureau of Mines Bulletin 361, 1932.

a letter about these experiments (8), he stated that he had not studied heat transfer under these conditions.

Although these are the only papers relating to heat transfer in beds of fluidized solids, as far back as 1878 a patent was granted to Frederic Luckenbach (9) for an improvement in apparatus for drying cereal grains. His apparatus consisted of a vessel with a conical false bottom through which hot or cold air or steam could be introduced into a bed of grain. This equipment was quite similar to that used today for fluidization. He pointed out that: "By this means, a powerful and rapid drying, heating and cooling action was produced, rendering the process very rapid..." Other patents (10, 11, 12) mentioned the uniformity of temperature but none gave any indication of experiments to measure heat transfer rate.

Papers in related fields were also investigated and some of them have been helpful in designing the equipment and in understanding the problem. Among these might be mentioned, in addition to that by Furnas, the following:

1. Schumann's (13) mathematical analysis of heat flow
8. Furnas, J.J. Letter to J.S. Walton, Dec. 3, 1947.
9. Luckenbach, Frederic U. S. Patent 210,793, Dec. 10, 1878.
10. Canon, Frank A. U. S. Patent 1,355,105, Oct. 5, 1920.
11. Chappell, Frank L. U. S. Patent 1,892,233, Dec. 27, 1932.
12. Odell, William W. U. S. Patent 1,984,380, Dec. 18, 1934.
13. Schumann, T.E.W. Heat Transfer from a Liquid Flowing through a Porous Prism, Journal Franklin Inst. 208:405-16, 1929.

to a bed of stationary solids from a liquid flowing through the bed. His results were in the form of time-temperature-position curves. Furnas used these curves in his work to calculate heat transfer coefficients from experimental data. However, Furnas' results were given in terms of volume coefficients* rather than the usual film coefficients..

2. Saunders and Ford (14) carried out experiments similar to Furnas' but with certain improvements, chiefly, reduction of wall effects and reduction of heat capacity of insulation. They plotted the generalized temperature difference, $\frac{t_g' - t_o}{t_g - t_o}$ against the dimensionless group $\frac{Vc\theta}{dc}$ for glass, steel and lead balls of several sizes and arrived, finally, at a value of $\alpha = 11.25$ Btu per hour-square foot-°F.

- d = particle diameter
- θ = time
- V = velocity in feet per second
- t_o = initial temperature of solid
- t_g = gas temperature in
- t_g' = gas temperature out
- c' = heat capacity of unit volume of gas

* Coefficient of heat transfer based on a cubic foot of loose solids rather than a square foot of solid surface.

14. Saunders, O.A. and Ford, H. Heat Transfer in the Flow of Gas through a Bed of Solid Particles, Iron and Steel Inst. Journal 141:291-328, #1 1940.

c = Heat capacity of unit volume of loose solids

3. Johnstone, Pigford, and Chapin (15) studied heat transfer to clouds of falling particles. They dropped particles in the 30 - 80 mesh range through a tube heated electrically and measured the heat absorbed by catching the particles in a calorimeter. They obtained coefficients of heat transfer by convection, from gas to solid, of 30 to 50 Btu per hour - square foot - $^{\circ}\text{F}$.
4. Frey (16) studied pressure drop through beds of fluidized solids in a glass tube and concluded, as did Parent et al, (17) that the 'net' pressure drop was almost exactly equivalent to the weight of solid. By 'net' pressure drop is meant the measured drop minus that due to friction loss of the gas passing through the tube.

Scope

The problem, then, of the transfer of heat in a bed of fluidized solids has not been investigated, except as indicated above. In this thesis, equipment was designed and constructed for this purpose. A technique was developed

15. Johnstone, H.F., Pigford, R.L. and Chapin, J.H. Heat Transfer to Clouds of Falling Particles, Illinois Univ. Engineering Experiment Station Bulletin 330, 1941, 55 pages.
16. Frey, John S. The Flow Characteristics of Flowing Vapors through an Agitated Fluid Catalyst Bed, unpublished M.S. Thesis, Chemical Engineering Department, Oregon State College, 1947.
17. Parent, loc. cit.

which permitted a general study of the behavior of fluidized beds with respect to heat flow; and the magnitude of the film coefficient of heat transfer from the upward flowing gas to the wall, with and without the presence of solid particles, was determined. In addition, the film coefficient of heat transfer between gas and solid was determined qualitatively.

PROCEDURE

Method of Attack

The Study of heat transfer in fluidized beds appeared to be a fairly simple problem - the most obvious procedure being to pass a gas into a bed of fluidized solids and measure the inlet and outlet temperatures. However, there were a number of complications, chief among which were correct measurement of temperature, heat losses, and unsteady state operation.

Two methods of attack suggested themselves:

1. Continuous feed into and discharge from a bed of solids heated and fluidized by hot air. This was rejected because of the difficulties of maintaining constant feed and discharge rates; a difficulty which does not preclude its use at a more advanced stage of knowledge of the behavior of such systems.
2. A batch process in which hot air would be introduced suddenly into a fluidized bed. This was selected as a more convenient method for laboratory study.

Equipment

The scale of operations was limited, on the small side, by the seriousness of wall effects on the fluidization and, on the large side, by the volume of air available. As a result, a four inch tube was selected as the fluidization

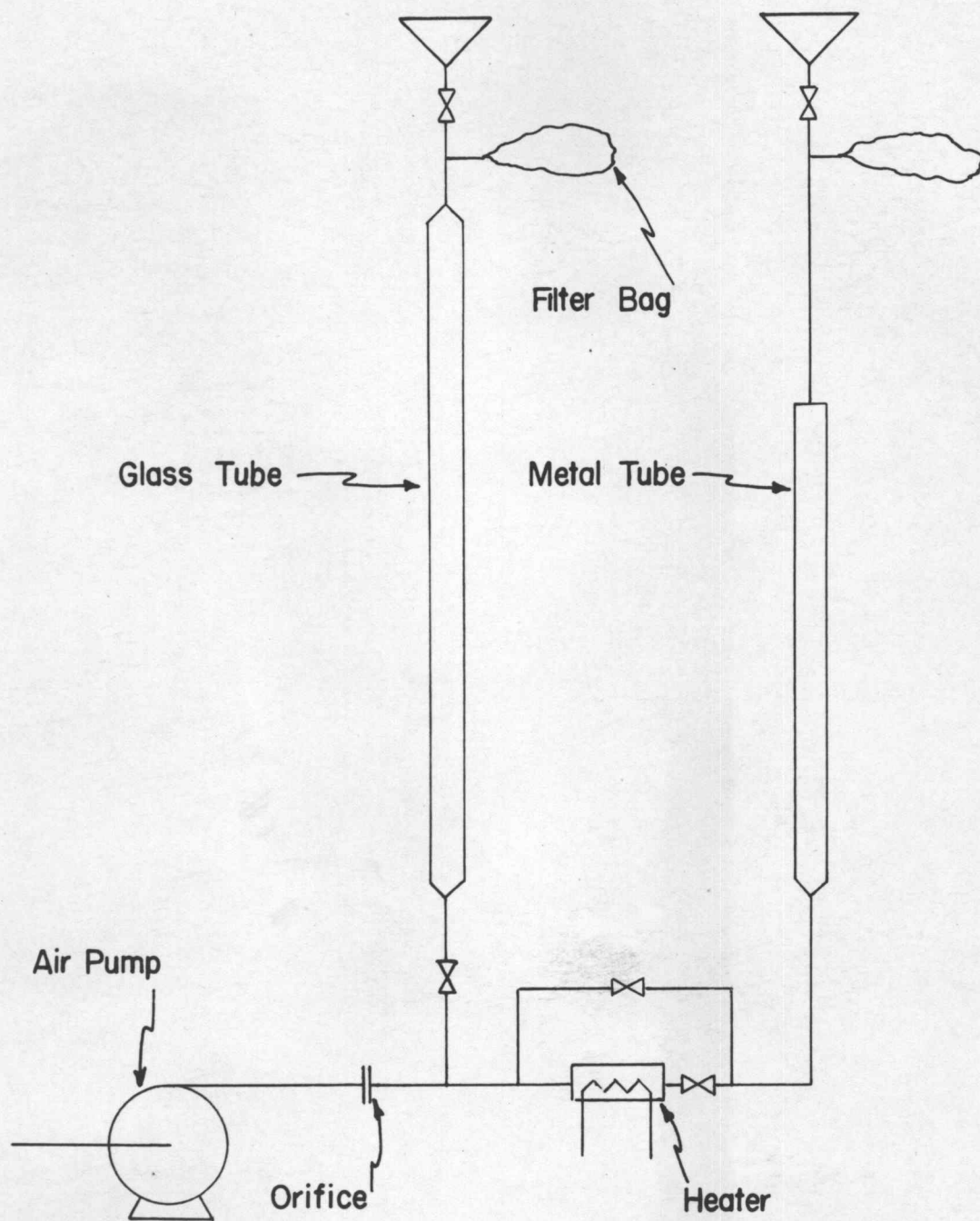
chamber.

The compressed air supply was of insufficient capacity and so a rotary vane air pump was used. This blower discharged a maximum of about 22 cubic feet per minute at atmospheric pressure, a value which corresponded to a linear velocity of $4\frac{1}{2}$ feet per second in the four inch tube. Air was used as the fluidizing gas throughout the experimental work. It was heated by an electric space heater and provision was made to by-pass the heater. The initial four inch tube was steel, $\frac{3}{32}$ inches thick and six feet high. In addition, a four inch glass tube, ten feet high, in parallel with the steel tube, was used for visual observation of materials in order that their behavior in the metal tube might be known. The air leaving the top of the tubes passed, in each case, through a cloth filter bag which trapped practically all solid carryover. See figures 1 and 2.

The metal tube was insulated with a one inch layer of 85 per cent magnesia pipe lagging. This was done in preference to either a steam jacket or electric resistance heating for reasons of simplicity both in construction and operation, although greater heat losses were suffered thereby.

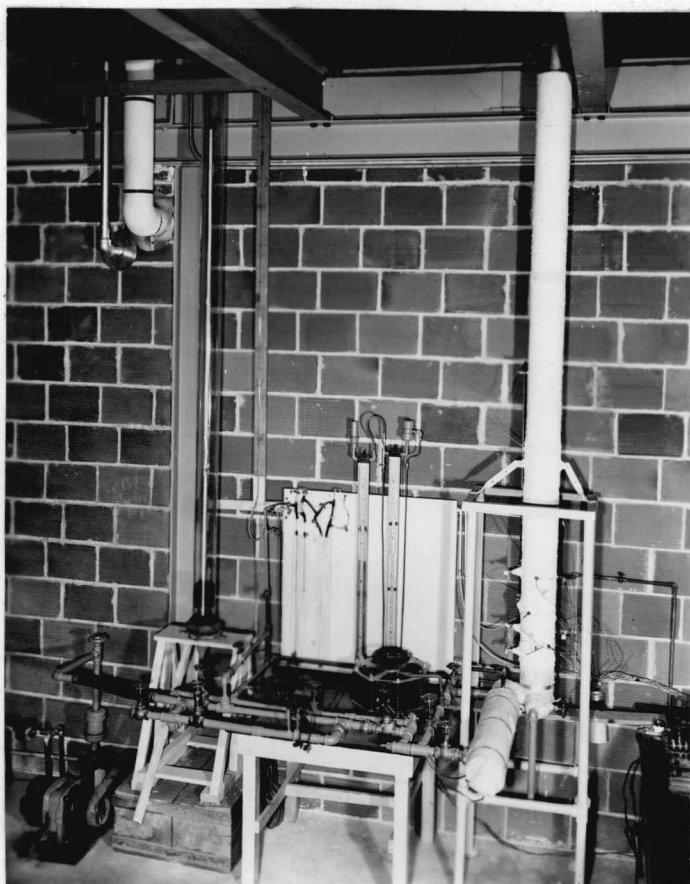
Measurements included velocity, pressure drop and temperature. Two calibrated thin-plate orifices were used to measure the air velocity. Pressure drop across part or

FIGURE 1



PROCESS FLOW DIAGRAM

FIGURE 2



PHOTOGRAPH OF APPARATUS

all of the bed could be measured. Temperatures were measured at a number of points in the system by means of iron-constantan thermocouples. Initially, three types of thermocouples were used:

1. Thermocouples brazed onto the outside of the tube to read the metal temperature.

2. Bare thermocouples to read the air temperature in the high velocity approach section between the heater and the fluidization tube. This same type of thermocouple gave incorrect readings of air temperature in the tube itself* with no solid present and a temperature, probably, somewhere between that of the solid and that of the air, when solid was present.

3. Suction thermocouples were used to determine the gas temperature in the fluidized bed. These were regular thermocouples inserted in wells through which the hot air could be drawn rapidly past the hot junction of the thermocouple[†]. The fine solids were prevented from being sucked into the well by means of a fine screen placed over the end of the well.

Preliminary Operations

A number of preliminary runs were made to determine the operability of the equipment and the behavior of several fine solids at various air velocities. Runs A-1, A-6,

*Due to the low air velocity past the hot junction.

†See appendix.

A-8, and A-13 were made in the glass tube using the following materials: Up to five pounds of 3A Catalyst, (a synthetic aluminum silicate, 60 per cent of which was - 200 mesh), a mixture of the largest 3A particles (10 per cent 50-100 mesh, 78 per cent 100-200 mesh, 12 per cent -200 mesh), and Ottawa Standard Silica Sand, (twice), respectively. This last material is a pure, white sand over 95 per cent of which is between 30 and 100 mesh in size. The individual grains are nearly spherical. These runs confirmed the conclusions of Parent et al (18) and Frey (19) that the pressure drop across a bed of fluidized solids is equal to the head of solids plus the friction loss through the empty tube at the same superficial velocity.*

Runs A-2, A-7, A-9, and A-14 were duplicates of the above runs except that they were made in the metal tube. It was found that bed depth and density could be estimated, approximately, by the difference in pressure between manometer taps. However, it was believed that the bed depth in the metal tube could be more accurately determined by comparison with the depth in the glass tube at the same mass velocity.

Runs A-3, A-5, A-10, A-11, A-12, and A-15 were tests of the heater, the thermocouples and the insulation. They were

18. Parent, loc. cit.

19. Frey, loc. cit.

* See Appendix

made at several voltages and various air velocities. These runs are summarized in Table I.

TABLE I
Preliminary Operations

Run	Material	Weight pounds	Tube	Mass Velocity lb per hr-sq ft	Superficial velocity fps	Purpose	Remarks
A-1	Ottawa Std. Sand	1	Glass	250-800	1.0-3.4	Behavior of solid	Good fluidiza- tion between 350 & 500 pounds/ hr-sq ft
A-6	Ottawa Std. Sand*	5	Glass	350-1100	1.5-4.5	Behavior of solid	Slugging [†] at all velocities
A-8	3A Catalyst	5	Glass	100-300	0.3-1.3	Behavior of solid	Good fluidiza- tion
A-13	3A Catalyst (screened) [‡]	5	Glass	90-230	0.25-0.9	Behavior of solid	Channels [†] up to 150 pounds/hr-sq ft better fluidi- zation above
A-2	Ottawa Std. Sand*	1&3	Metal	250-800	1.0-3.4	Behavior of solid	

* Screen Analysis of Ottawa Standard Sand

-16	+	30 mesh	2	±	2%
-30	+	50 "	70	±	5%
-50	+	100 "	26	±	2%

† These terms will be explained later

‡ Screen Analysis of Large Size 3A Catalyst

-50	+	100 mesh	10%
-100	+	150 "	39%
-150	+	200 "	39%
-200	+	270 "	10%
-270		"	2%

TABLE I CONTINUED
Preliminary Operations

Run	Material	Weight pounds	Tube	Mass Velocity lb per hr-sq ft	Superficial velocity fps	Purpose	Remarks
A-7	Ottawa Std. Sand	5	Metal	500-800	2.0-3.4	Behavior of solid	
A-9	3A Catalyst	5	Metal	110-180	0.36-0.66	Behavior of solid	
A-14	3A Catalyst (screened)	4-7/8	Metal	95-220	0.28-0.81	Behavior of solid	
A-3	--	--	Metal	660	3.0	Heater & TC operation	No preheat
A-5	--	--	Metal	700	3.1	" "	100v across heater
A-10	--	--	Metal	175	0.63	" "	Heater burnt out
A-11	--	--	Metal	180	0.63	" "	110v across heater
A-12	--	--	Metal	660	3.0	" "	110v across heater
A-15	--	--	Metal	660	3.0	" "	100v across heater

First Heating Runs

The first four unsteady state heating runs were preliminary runs to determine the general behavior of the equipment and the solids. These runs are summarized in Table II.

TABLE II
Heating Runs

Run	Material	Weight pounds	Mass Velocity lb per hr-sq ft	Remarks
1	3A Catalyst	5	180	Large % carry-over
2	3A Catalyst (screened)	4-7/8	175	Carryover still serious
3	Ottawa Std. Sand	5	230	Poor fluidization
4	Ottawa Std. Sand	5	810	Slugging

The first run was made using five pounds of 3A Catalyst at an intermediate air velocity (for this material). The chief difficulty was that, at the end of one hour, only about 50 per cent of the original five pounds was still in the tube. The other two and a half pounds had gradually been carried into the filter bag by the rising gas stream. Although the decrease in solid could be followed, roughly, by means of the pressure drop across the bed, it did introduce another variable which would be rather difficult to allow for in the calculations.

The second run was made on a fraction of 3A Catalyst, 78 per cent of which was between 100 and 200 mesh in size.

The carryover was reduced to about 9 per cent per hour which was still large but not excessive unless a run lasted for several hours. Throughout the heating period of this run, two bare thermocouples in the bed of solids (one near the bottom and one near the top) and two corresponding suction thermocouples in the bed all read the same temperature at any given time, within the accuracy of the readings. The two wall thermocouples at corresponding positions opposite the bed read two degrees lower. This indicated that the mixing in the bed was excellent and that the solid and air were very close to the same temperature (i.e. equilibrium) very shortly after the air entered the bed. This reasoning followed from the fact that the bare thermocouples, which gave a temperature between that of the gas and that of the solid, read the same as the suction thermocouples, which gave the true gas temperature.

Run 3 was made with five pounds of Ottawa Sand at a mass velocity of 210 pounds per hour per square foot. This velocity was so low that most of the solid was in the approach tube and in the cone connecting the one inch approach tube with the four inch main tube. Consequently, fluidization was poor.

Run 4 was also made with five pounds of Ottawa Sand but at a higher mass velocity namely, 810 pounds per hour per square foot. As in Run 2, the bare thermocouples and the suction thermocouples read the same temperature at any given time. However, the two wall thermocouples each read about

ten degrees lower. Losses due to carryover were less than $1\frac{1}{2}$ per cent per hour of operation.

These runs set limitations on the equipment and helped to determine the direction of later experimentation. Two reasons against the use of very fine particles appeared. Firstly, the drifting of appreciable quantities of solid out of the fluidization tube introduced an undesirable variable. Secondly, if the air and solid particles were close to equilibrium throughout most of the bed, it would be impossible to calculate a heat transfer coefficient between the air and the solid. Increasing the particle size, would decrease the area available for heat transfer and tend toward non-equilibrium in the bed. However, the heat transfer coefficient might be so large that it would be impossible to obtain a measurable temperature difference between air and solid within the limitations of the equipment. This did not apply to the heat transfer coefficient between the air and the wall of the tube for, as was mentioned above, the wall temperature was 2°F below the air temperature when material as fine as 100 to 200 mesh was fluidized.

The poor fluidization of the sand indicated a limit to the maximum size and/or density of particles which could be used. In order to decrease the heat transfer area and still fluidize, it was necessary to use a material of lower density.

Runs 5 to 8, inclusive, were heating runs on wood

charcoal (Douglas fir) of 8 to 28 mesh. The charcoal had an apparent density of 9 pounds per cubic foot as compared to 87 pounds per cubic foot for the sand. Carryover of solid was at a high rate and there was also a loss of weight due to the moisture or other volatile matter in the charcoal. This amounted to 6 per cent of the initial weight in Run 7. Another difficulty in the use of charcoal was the attrition resulting from the impacts between particles and between the particles and the wall. In the case of a hard material like sand, the attrition over the operating period of a run was negligible. The table below shows the reduction of size in Run 8, not including the material in the filter bag.

TABLE III

Attrition in Run 8

<u>Mesh</u>	<u>Per Cent at Start</u>	<u>Per Cent at End</u>
-14 + 20	100.0	51.6
-20 + 28	0.0	36.0
-28 + 35	0.0	9.2
-35 + 48	0.0	2.7
-48	0.0	0.5
	<u>100.0</u>	<u>100.0</u>

The four runs have been summarized below:

TABLE IV

Heating Runs on Charcoal

Run	Weight at Start in pounds	Mesh at Start	Mass Velocity lb per hr-sq ft	Remarks
5	1.0	-8 + 28	548	Operational difficulties
6	1.0	-8 + 20	535	Operational difficulties
7	1.0	-20 + 28	734	55% loss in weight
8	1.25	-14 + 20	523	36% loss in weight

Improved Apparatus

Preliminary calculations on Run 8 brought out a serious disadvantage in the use of charcoal namely, that the rate of heat transfer to the metal wall was several times as great as the rate of heat transfer to the solid. This was a result of the combination of a comparatively large weight of metal with a high coefficient of heat transfer to the metal, as indicated by a very rapid rise in metal temperature. However, this difficulty did not affect experimentation to determine the coefficient of heat transfer between air and tube wall but only obscured the heat transfer between air and solid.

Two solutions to this problem presented themselves:

1. The use of a solid of much greater heat capacity (i.e. weight) per unit volume. However, we have already seen that, in order to decrease the heat transfer area of the solid, it was necessary to go to a material of smaller

weight per unit volume. A compromise between these opposing demands was found in coal.

2. A decrease in the weight of metal. This was done by replacing the $3/32$ (0.094) inches thick tube by a sheet metal tube of the same diameter but 0.016 inches thick.

Another important change in the equipment was made at the same time. In the original apparatus, the bottom of the bed of solids was located somewhere in the cone or the approach tube, depending on the solid, the size of the particles and the air velocity. In order to fix the bottom of the bed and thus eliminate one unknown factor, a fine screen was placed near the bottom of the new sheet metal tube and in a similar position in the glass tube.

Three groups of runs were made on the improved apparatus. Runs A-25 to A-28 were steady state runs with an empty tube. The original purpose of these runs was to determine the conductivity of the insulation. However, it was discovered that, although the temperature difference between two radial points, for example, the inside of the insulation and one fourth of an inch out from the metal wall, could be determined easily (by movable thermocouples) and was appreciable, the drop in temperature of the air as it flowed up the tube was very small, amounting to about 4°F in the first twelve inches above the screen. This reduced the accuracy of the heat balance and resulted in

considerable variation in the calculated values of conductivity on either side of the value given in the literature (20). Consequently, it was decided to use the published conductivity of 85 per cent magnesia, namely, 0.041 Btu per hour per square foot per degree Fahrenheit per foot. Two other interesting points were brought out by these runs.

1. There was a very sharp temperature drop between the metal and the inside of the insulation. Pulling the insulation more tightly about the tube did not decrease this temperature difference. This corresponded to a film coefficient of heat transfer of between 0.4 and 0.7 Btu per hour per square foot per degree Fahrenheit.

2. The film coefficient of heat transfer between the air and the tube corresponded with the published value (21) and was a function of the mass velocity to the 0.8 power. This last relationship has also appeared in the literature (22).

Runs A-31 and A-32 were unsteady state runs with an empty tube. The purpose of these runs was to determine whether the calculations led to a heat balance. Run A-31 was a double run. When steady state had been reached, the air was by-passed around the heater and an unsteady state

20. McAdams, William H. Heat Transmission, Second Edition, New York, McCraw-Hill, 1942, p387.

21. Ibid. pl74.

22. Ibid. pl66

cooling run made.

Runs 9 through 12 were unsteady state runs using 14 to 28 mesh anthracite coal as the solid. Run 9 was both a heating and a cooling run. A summary of these runs appears below and a discussion follows in the next section.

TABLE V

Runs on Improved Apparatus

Run	Solid	Weight pounds	Mass Velocity lb per hr-sq ft	Type of Run
A-25	-	-	481	Steady State
A-26	-	-	485	Steady State
A-27	-	-	482	Steady State
A-28	-	-	481	Steady State
A-31	-	-	637	Unsteady State, Heating and Cooling
A-32	-	-	636	Unsteady State, Heating
9	Coal	2	630-636	Unsteady State, Heating and Cooling
10	Coal	2	638	Unsteady State, Heating
11	Coal	1	809	Unsteady State, Heating
12	Coal	$\frac{1}{2}$	635	Unsteady State, Heating

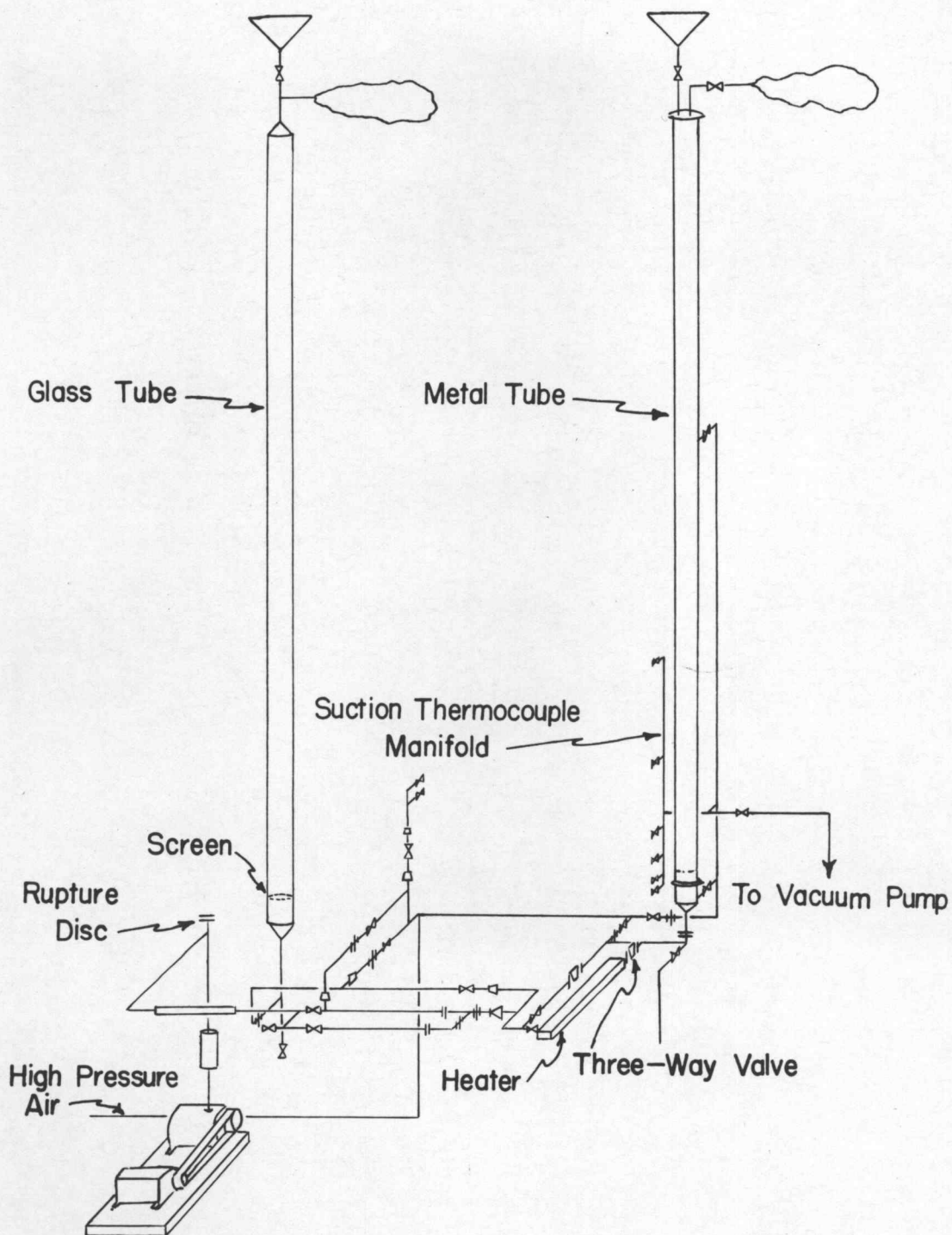
APPARATUS

Up to this point, the equipment and the changes made in it have been discussed only in outline. Inasmuch as some of the details were important to the operation and in the calculations, a more complete description of the final apparatus follows:

The air leaving the blower, which was driven by a one horsepower, variable-speed motor, passed through an oil mist filter consisting of a four inch length of three inch pipe filled with steel wool. A rupture disc made by clamping four sheets of waxed paper between the two halves of a flange union was located at an elbow just beyond this point. This part of the system was connected to the rest of the piping by a length of rubber hose in order to reduce vibration. Just above the orifice section was an air bleed which, in combination with the variable-speed motor, made possible control of the air flow at any rate between 80 and 1200 pounds per hour per square foot. Figure 3 is an isometric sketch of the piping and the layout.

To measure the velocity, two thin-plate orifices were used. The smaller was $9/32$ inches in diameter in a one inch iron pipe and was used up to about 350 pounds per hour per square foot (in the four inch tube). The larger was 0.500 inches in diameter in a one inch brass pipe. The former was

FIGURE 3



ISOMETRIC SKETCH OF PIPING AND LAYOUT

used by a previous experimenter (23) on fluidization. The latter was designed according to the rule of thumb that pressure drop in inches of water across the orifice should not exceed the upstream pressure in pounds per square inch absolute (24). Recommendations of the ASME Fluid Meter Committee (25, 26) were followed as closely as possible without elaborate measurements or construction.* Both orifices were calibrated by means of a dry gas meter. The meter was located on the pump suction in some cases and below the orifice at the very lowest rates. This was done because the pump was operating at its minimum limit and a bleed was necessary to decrease the volume of gas passing through the orifice. It was necessary to measure the gas temperature because the heat of compression was appreciable and was not all dissipated in the lines between the pump and the orifices. In operation, the temperature was measured at two points, at the air bleed and about a foot below the orifice, and an arithmetic average taken for the true

23. Frey, loc. cit.

24. Rhodes, Thomas J. Industrial Instruments for Measurement and Control, New York, McGraw Hill, 1941, p197.

25. American Society of Mechanical Engineers Power Test Codes Part 5, Chap. 4, Flow Measurement by Means of Standardized Nozzles and Orifice Plates, American Society of Mechanical Engineers, 1940, 64p.

26. Fluid Meters - Part 1, 4th ed. American Society of Mechanical Engineers, 1937, 139p.

* Since the recommendations were not followed exactly, the published values of the coefficients were not used. Instead, the coefficients were determined experimentally.

temperature at the orifice. The orifice calculations are shown in the appendix. A check valve was placed downstream of the orifices to prevent possible backflow of solids.

The air had three possible paths after it left the check valve:

(1) It could flow through a $3/4$ inch pipe to the bottom of the four inch diameter (4.055 inches average inside diameter) glass tube. From the top of this tube, the air flowed, via a $3/4$ inch pipe, to a cotton filter bag and then out into the room.

(2) It could flow through a one inch line to the electric heater and thence into the bottom of the four inch diameter (3.98 inch average inside diameter) sheet metal tube. From the top of the tube it flowed through a one inch pipe to a filter bag and then out to the room.

(3) The third path for the air was through a one inch pipe to the base of the tube, by-passing the heater. A two-way, quick-acting plug valve was located in this line.

The heater was a 1400 watt, finned space heater, and was enclosed in a 2 inch by 3 inch by $18\frac{1}{2}$ inch sheet iron box with three baffles to force the air to flow parallel to the fins. Electrical contact was made by means of two spark plugs. The spark plugs were brazed to the box and the central terminals were connected to the heater leads. The current to the heater was controlled by a 7.5 'Powerstat', variable transformer. A voltmeter and an

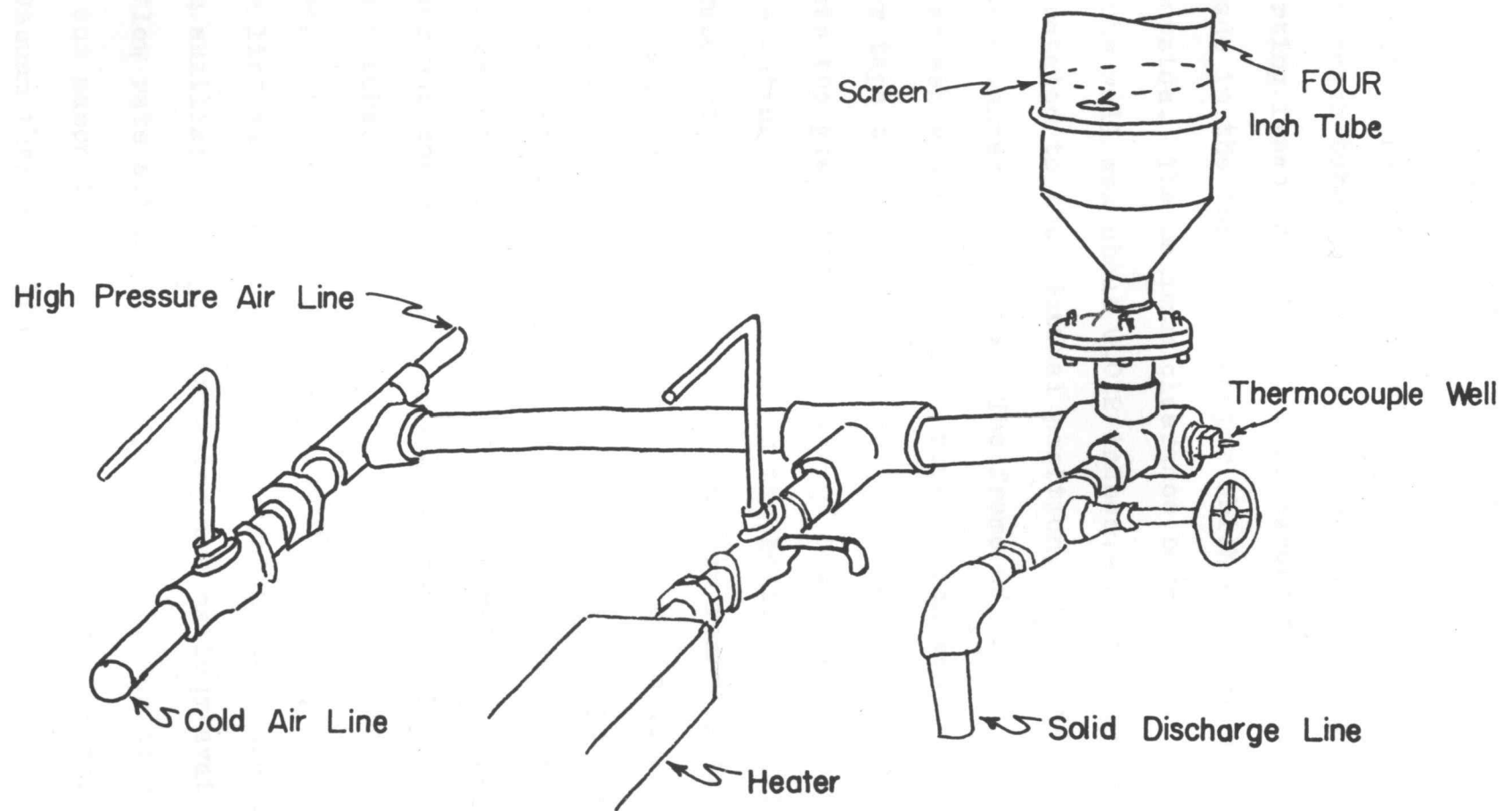
ammeter measured the power input.

Between the heater and the four inch tube, there was a one inch three-way valve made from a 'stop and waste' plug valve. The side opening was a bleed to allow preheat of the air without heating the tube. Because the valve was a plug type, it was quick-acting and eliminated lag in switching from bleed to tube. The connection between the one inch entrance pipe and the four inch tube was a sheet metal cone 2-3/8 inches high. When the 3/32 inches thick tube was replaced by the sheet metal tube, the former was cut off about 2 1/2 inches above the top of the cone and the connection to the sheet metal tube made by flanges. The two flanges were thermally insulated from one another by means of an asbestos paper gasket. The whole system from the heater entrance to the top of the four inch tube was insulated with one inch of 85 per cent magnesia. Figure 4 shows the piping at the base of the tube.

The solid was fed to the sheet metal tube from a hopper above the top of the tube and connected to it by a one inch pipe which extended about one foot into the tube. This was independent of the air exit line and so a small flow of air could be maintained during feeding to keep the bed from packing. In the case of the glass tube, the same pipe was used for feed and exit air and so this could not be done.

Before the screens were placed in the two tubes,

FIGURE 4



ISOMETRIC SKETCH OF PIPING AT BASE OF TUBE

discharge of particles, in each case, was through a tee in the approach tube a few inches below the tube itself. The supporting frame for the 100 mesh screen in the metal tube was made in the form of a damper which could be rotated from the outside. The maximum clearance between the frame and the tube wall was about 0.012 inches. After the screen had been rotated to the vertical position, discharge was made in the same manner as before. The frame of the 60 mesh glass tube screen was a brass ring around which was wrapped enough rubber tape to give a tight seal when the screen was forced up into the glass tube. The bed of solids was removed by disconnecting the glass tube at the bottom flange, lifting the tube onto a special frame, and then removing the screen.

Because a bed of fine solids packs quite tightly when air is not passing through it, air of several pounds pressure must be available to break it loose. Therefore, high pressure air from an eight cubic feet per minute compressor was connected into the line leading to the bottom of each tube. In addition, air from this source was used to keep the bed aerated during preheating operations. Another line was connected into the system above the orifices as an auxiliary supply, increasing the maximum available air flow rate slightly. High pressure air was also used to blow out manometer connections and to clear the screens on the vacuum thermocouples.

A pressure tap about $2\frac{1}{2}$ inches below the screen in the metal tube and another about five feet above the screen gave the combined pressure drop across the screen and the bed of solids. By subtracting the pressure drop at the same mass velocity with the tube empty, the 'net' pressure drop due to the bed was obtained. The pressure taps for the glass tube were located in the approach pipe and the air exit pipe. A water manometer was used to read the pressure drop and a second one gave the pressure drop across either orifice. A mercury manometer read the pressure at the upstream orifice tap.

Temperatures were measured by seventeen iron-constantan thermocouples. The thermocouple wires were number 20 gage, glass insulated. Lead wires were copper and extended from the cold junction to two multiple selector switches. The electromotive force was measured by a Type 8662 Leeds and Northup potentiometer. During calibration, the cold junction was located in an ice and water slush in a thermos bottle. During operation, the slush was replaced by water at 70°F.* All the thermocouples were calibrated against the freezing point of Bureau of Standards lead. Since the maximum deviation of any of the thermocouples was less than 3°F

*The water in the thermos was adjusted to 70°F before each run and would remain at that temperature for several hours.

over a temperature difference (between hot and cold junctions) more than twice as great as that occurring during operation, a straight line deviation was assumed.

The location and type of each thermocouple are listed in Table VI and shown schematically in Figure 5.

Before Run 12, the well of No. 4 was bent into an 'S' curve so that the end was only about $\frac{1}{4}$ inch below the screen. No. 9 was moved to a position about $\frac{1}{4}$ inch below the screen following Run 12.

Nos. 15 and 16 were used to measure insulation temperatures. During operation, they were forced through the insulation until they hit the metal wall. Since there was no actual contact between the wall and the thermocouples, the temperature read on the thermocouples was that of the inside of the insulation. This was confirmed in the steady state Runs A-25 to A-28. In these runs, insulation temperatures were determined every $\frac{1}{4}$ inch radially. When the temperatures were plotted against radial distance, the points fell on a smooth curve in every case.

Details of the several types of thermowells have been sketched in Figure 6. Following Run 12, the wells of thermocouples Nos. 5 and No. 7 were cut at a point just outside the tube wall and a piece of 'Micarta', a thermo-setting plastic, inserted for thermal insulation. This plastic insert replaced the brass fitting used to screw

FIGURE 5
LOCATION OF INSTRUMENTS

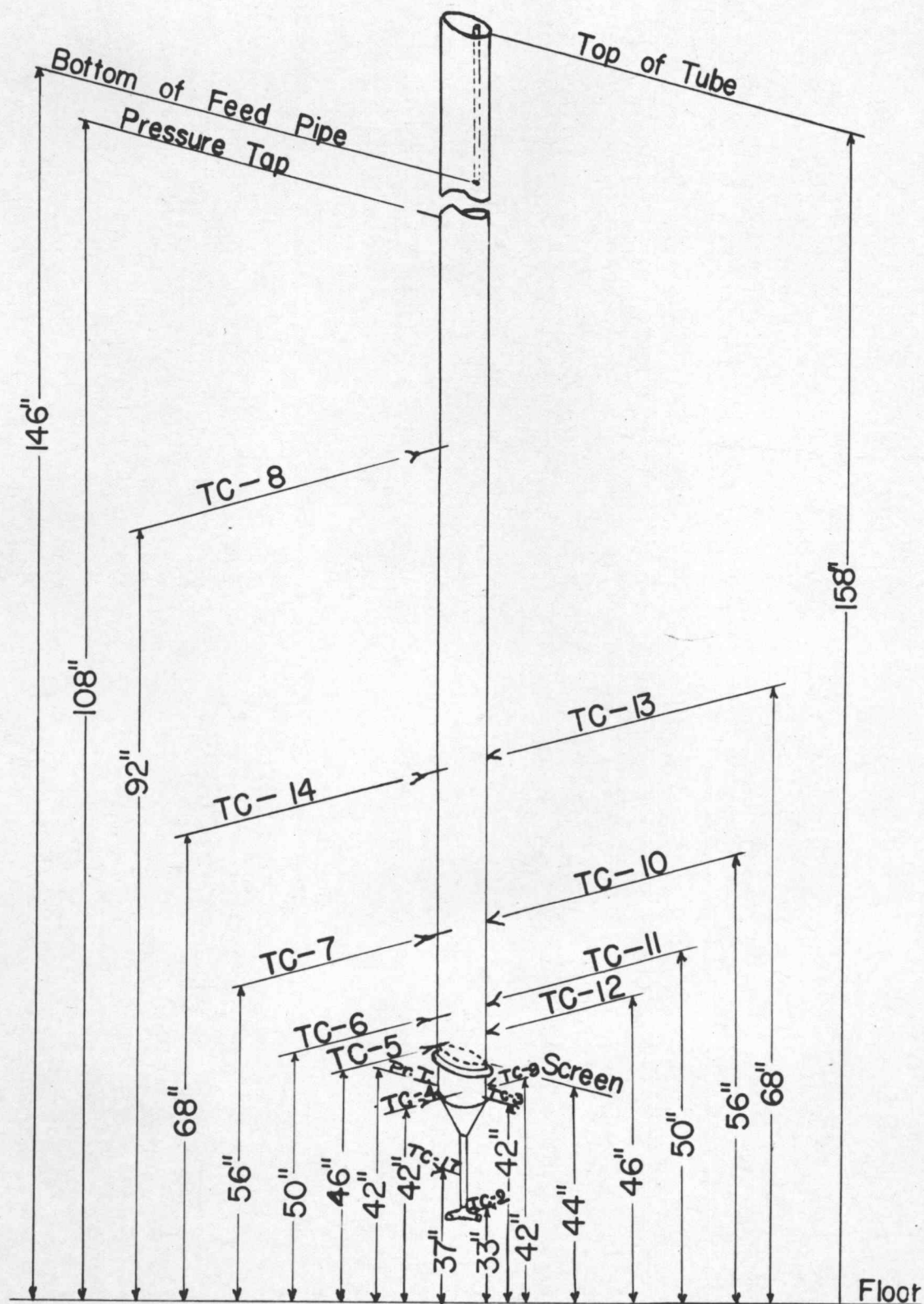


FIGURE 6
THERMOCOUPLE WELLS

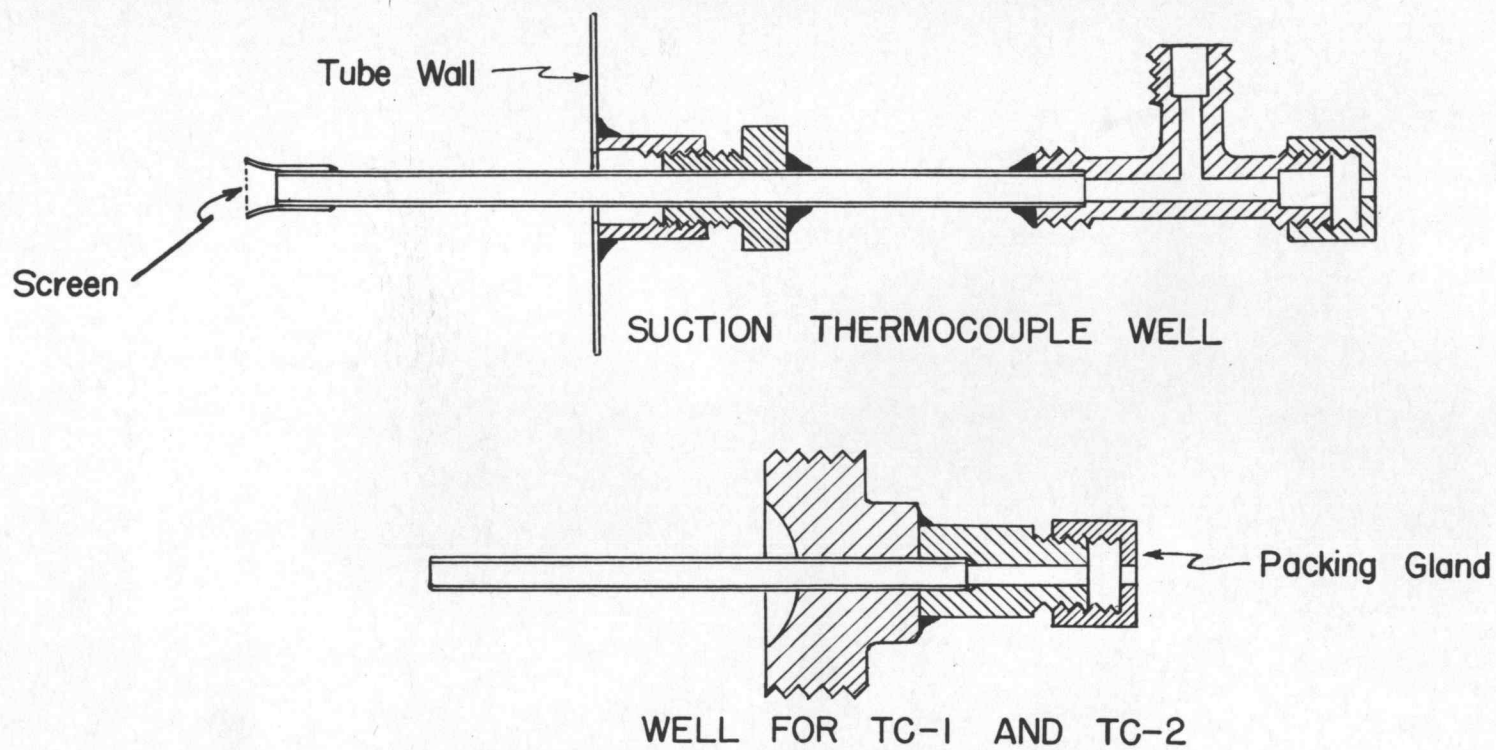


TABLE VI

Thermocouples

Thermocouple	Type	Location	Well*	Location of Hot Junction in Relation to End of Well
1	Bare	Below orifices	Open	$\frac{1}{8}$ " beyond
2	Bare	Approach tube downstream of heater	Open	$\frac{1}{2}$ " beyond
3	Bare	$2\frac{1}{2}$ " below screen	Open	$\frac{1}{4}$ " beyond
4	Suction	$2\frac{1}{2}$ " below screen	Open	$\frac{1}{8}$ " before
5	Suction	2" above screen	Screen†	$\frac{1}{8}$ " before
6	Suction	6" above screen	Screen	$\frac{1}{8}$ " before
7	Suction	12" above screen	Screen	$\frac{1}{8}$ " before
8	Suction	48" above screen	Open	$\frac{1}{8}$ " before
9	Wall‡	$2\frac{1}{2}$ " below screen	-	-
10	Wall	12" above screen	-	-
11	Wall	6" above screen	-	-
12	Wall	2" above screen	-	-
13	Wall	24" above screen	-	-
14	Suction	24" above screen	Screen	$\frac{1}{8}$ " before
15	Insulation	Varying distances above above screen	-	-
16	Insulation	Varying distances	-	-
17	Bare	Approach tube downstream of heater	Open	$\frac{1}{2}$ " beyond

* Wells were made of 3/16 inch outside diameter steel tubing.

† Screens were 80 mesh, brazed to flared opening of the well. See Figure 6.

‡ Brazed onto the outside of the metal tube.

the well into the wall fitting.

RESULTS AND DISCUSSION

Fluidization

Since the heat transfer studied in this thesis took place in fluidized beds, it will be desirable to discuss fluidization briefly.

When a stream of gas is passed upward through a bed of fine solids at a sufficient rate, the particles will be set in continuous motion of a rather complex pattern and the mass of solids will have the appearance of a boiling liquid. Carrying the analogy further, there is always some spraying of droplets above the surface of a rapidly boiling liquid. The same thing occurs in fluidization. The spray of fine solids is called the lean phase and the body of the bed, the dense phase. Entrainment of liquids corresponds to the carryover of solids which was mentioned earlier.

Three types of fluidization behavior have been recognized - channeling, 'slugging', and smooth fluidization. At very low gas velocities, particularly with very fine particles, channels are cut through the bed and relatively poor contact results. If the particles are too coarse, too closely sized, or of too high density, 'slugging' takes place, that is, a large number of the particles bridge across the whole tube and rise as a single body or 'slug' for quite a distance before breaking up. During

smooth fluidization, the particles move along twisting, ever-changing paths and excellent mixing occurs.

Each of these types of fluidization could be recognized in the metal tube by observing the action of the manometer connected across the bed. When channeling was occurring, the liquid levels in the manometer were stationary and the net pressure drop across the bed was smaller than the head of solids. When the bed was slugging, the manometer levels fluctuated widely. During smooth fluidization, the liquid levels had small rapid fluctuations and the net pressure drop was approximately equal to the head of solids.

Theory

It will be recalled that the method of attack was to introduce hot air, suddenly, into a bed of fluidized solids. The air was consequently reduced in temperature and the solid became warmer. If there were no heat losses, all the heat given up by the air would have gone to heat the solid. Expressed mathematically, the heat gained* by the air in time $d\theta$ would be

$$(1) \quad dQ_a = GA_T C_{p_a} (t_e - t_d) d\theta$$

and the heat gained by the solid would be

*Heat given up will be considered negative

$$(2) \quad dQ_s = W_s C_{p_s} dT$$

Rearranging equation (1)

$$(3) \quad q_a = \frac{dQ}{d\theta}^a = GA_T C_{p_a} (t_e - t_d)$$

and dividing both sides of equation (2) by $d\theta$

$$(4) \quad q_s = \frac{dQ}{d\theta}^s = W_s C_{p_s} \frac{dT}{d\theta}$$

If there were no losses, the equation would read

$$(5) \quad q_a + q_s = 0$$

However, this was impossible of attainment and so other terms were added to equation (5). The two main heat losses were to the metal wall and to the insulation. This made the heat balance

$$(6) \quad q_a + q_s + q_m + q_i = 0$$

The 'net' rate of heat flow to the metal can be expressed by an equation similar to that for the solid. By 'net' rate is meant rate at which heat is retained by the metal, i.e., not passed on through to the insulation.

$$(7) \quad q_m = W_m C_{p_m} \frac{dt_m}{d\theta}$$

The rate of heat flow into the insulation can be determined from the Fourier conduction equation.

$$(8) \quad q_i = -k_i A_i \frac{dt_i}{dl}$$

The total rate of heat flow to the metal is, then, the sum of q_i and q_m . When this sum is equated to the expression for rate of heat flow through a gas film, the following expression is obtained:

$$(9) \quad q_i + q_m = h_w A_w \Delta_w$$

In this equation, ' h_w ' is the film coefficient of heat transfer between the air and the metal wall.

Under steady state conditions, the net rate of heat transfer to the metal would be zero resulting in

$$(10) \quad q_i = h_w A_w \Delta_w$$

Similarly, when steady state prevails, equation (6) reduces to

$$(11) \quad q_a + q_i = 0$$

The rate of heat transfer to the solid (4) can be equated to an expression similar to equation (9).

$$(12) \quad q_s = U_s A_s \Delta_s$$

where

$$(13) \quad \frac{1}{U_s} = \frac{1}{h_s} + \frac{1_s A_s}{k_s A_i}$$

It will be proved, later, that, even for the largest

particles used in these experiments, the second term on the right hand side of equation (13) is negligible, making

$$(14) \quad q_s = h_s A_s \Delta_s$$

where h_s is the film coefficient of heat transfer between the air and the particles.

The above equations formed the theoretical background for the experiments. In order to determine the value of some of the terms, it was necessary to modify some of them and to make some assumptions.

All the factors on the right hand side of equation (3) were either measured or were available in the literature. In equation (4), however, the solid temperature could not be determined directly and so q_s was left as an unknown to be obtained by difference from equation (6). The metal temperature, on the other hand, was measured at several points and was known as a function of time. In the use of equation (7), the assumption was made that the measured metal temperature was indicative of the true temperature through the metal wall and at all points around the wall at that height. A calculation of the temperature drop through the wall under conditions of maximum heat flow gave about 0.01°F temperature drop. In view of the cylindrical shape, the latter part of the assumption also appeared to be quite reasonable.

In order to determine the rate of heat flow to the insulation, equation (8) was modified by changing the derivative, $\frac{dt_i}{dl}$, to the finite increment form $\frac{\Delta t}{\Delta l}$. Substituting in the correct area for cylindrical heat flow, i.e., the logarithmic mean area, the expression

$$(15) \quad q_i = -k_i 2\pi \left[\frac{r-r'}{\ln \frac{r}{r'}} \right] N \left[\frac{t-t'}{r-r'} \right]$$

was obtained. After changing to common logarithms and cancelling out the equality, the following equation resulted

$$(16) \quad q_i = \frac{2\pi N k_i (t' - t)}{2.30 \log \frac{r}{r'}}$$

where t' was the temperature at the inner surface of the insulation, that is, at a distance r' out from the center and t was the temperature which corresponded to another point, a small finite distance further out from the center of the tube. Two methods were available for the determination of t . It could be measured directly as was done in the steady state runs or could be calculated graphically. The latter was chosen in order to avoid taking additional sets of temperature readings. This allowed readings which could be determined only by the actual measurement to be taken more frequently.

E. Schmidt developed a graphical method for the approximate solution of complex problems in unsteady state

heat conduction. It was based on the use of finite increments in place of differentials in the basic conduction equation for an infinite slab

$$(17) \quad \frac{\Delta t}{\Delta \theta} = \alpha \frac{\Delta^2 t}{\Delta x^2}$$

where

$$(18) \quad \alpha = \frac{k}{C_p \rho}$$

Sherwood and Reed (27) discuss the method in some detail and Perry and Berggren (28) extend it to hollow cylinders. By the proper choice of the time increment, $\Delta \theta$, and the distance increment, Δx , the temperature at any point at any time becomes the arithmetic mean of the two temperatures x away on either side at a time $\Delta \theta$ previously. The relationship between Δx and $\Delta \theta$ which brings this about is

$$(19) \quad \alpha \frac{\Delta \theta}{(\Delta x)^2} = \frac{1}{2}$$

When the shape under consideration is a hollow cylinder, the abscissa scale is made logarithmic. An example of the method has been given in the Appendix.

27. Sherwood, Thomas K. and Reed, Charles E., Applied Mathematics in Chemical Engineering, New York, McGraw-Hill, 1939, pp241-255.
28. Perry, R.L. and Berggren, W.P., Transient Heat Conduction in Hollow Cylinders after Sudden Change of Inner-Surface Temperature, Univ. of Calif. Publications in Engineering Vol. 5, No. 3, pp59-88, 1944.

Typical Calculations

Run 11 has been selected in order to demonstrate the calculations. All the data on this run are given below:

TABLE VII

Run 11 - Heating Run on Dry Utah Coal

Material fluidized: Utah hard coal which had been heated at 300°F for several hours to drive off volatile matter and then cooled and kept in a desiccator.

Weight at start: 1.00 pounds

Weight at end: 1.00 pounds

Tyler standard screen analyses:

	<u>Start</u>	<u>End</u>
-8 + 14 mesh	0	0.005
-14 + 28 mesh	1.00	0.979
-28 + 48 mesh	0	0.019
-48 - mesh	0	0.005
	<u>1.00 pounds</u>	<u>1.008 pounds</u>

Room temperature: 70°F.

Vacuum pump flow when connected to one vacuum thermocouple: 0.18 cfm.

Duration of run: 83 minutes.

Fluidization: Good.

Orifice: 0.500 inch diameter.

Orifice and heater data:

Time minutes	Air Bleed, °F	TC - 1 - °F	P ₁ inches mercury	ΔP inches water	Heater Voltage
0	114	104	-	-	-
8	-	-	2.3	18.2	98
16	111	107	2.3	18.2	97
57	-	-	-	18.3	95
71	113	110	-	-	-

Temperatures:

TC-4		TC-5		TC-7		TC-12		TC-10		TC-15*	
Time	Temp	Time	Temp	Time	Temp	Time	Temp	Time	Temp	Time	Temp
0:20 [†]	213	1:45	166	3:15	207	1:30	150	3:40	149	2:45	95
4:20	253	6:00	235	7:30	238	5:00	217	9:20	197	6:40	119
10:00	259	10:50	248	9:00	241	10:30	236	15:50	216	11:20	140
13:00	262	14:00	252	11:50	246	13:30	242	21:40	223	14:30	147
17:20	263	19:10	255	15:10	250	19:50	246	29:05	229	20:30	153
22:40	265	24:20	259	21:00	254	23:30	248	43:10	233	25:00	156
26:50	266	28:30	259	25:50	257	27:50	249	52:30	237	31:15	161
33:10	266	34:10	260	29:50	257	33:40	251	70:30	238	35:30	163
38:00	265	40:40	260	32:20	258	39:20	250			41:40	164
45:10	268	47:00	262	36:20	258	50:10	254			46:15	165
48:50	268	50:40	262	42:30	260	53:50	254			55:40	166
53:10	269	55:00	262	51:50	260	59:30	254			62:45	168
59:00	267	60:20	262	56:50	260	67:40	254			69:10	168
66:50	268	63:30	262	64:50	260	73:50	254			74:50	168
73:00	268	74:10	262	65:00	260						
				76:00	261						

For the 0.500 inch orifice

$$(20) \quad G = 705 \sqrt{\rho_0 \Delta P}$$

where

$$(21) \quad \rho_0 = \frac{1.33(29.9 + P_1 - \frac{\Delta P}{13.6})}{t + 460}$$

*TC-15 located at inside of insulation 4 inches above the screen.

†Time in minutes and seconds after the start.

Using the arithmetic average of the air bleed temperature and TC-1 at 0 minutes

$$(22) \quad c_o = \frac{1.33(29.9 + 2.3 - \frac{18.2}{13.6})}{109 + 460} = 0.0721 \text{ lb per cu ft}$$

and

$$(23) \quad G = 705\sqrt{0.0721(18.2)} = 806 \text{ lb per hr-sq ft}$$

The data for other times are summarized in Table VIII.

TABLE VIII

Mass Velocity

Time min	Air Bleed °F	TC-1 °F	Average °F	c_o lb per cu ft	G lb per hr-sq ft
0	114	104	109	0.0721	806
16	111	107	109	0.0721	809
71	113	110	111	0.0718	810

The variation in the orifice temperature was due to the fact that the pipes had not been fully heated by the heat of compression of the pump. Actually, there was a variation in mass velocity from about 796 to 820 pounds per square foot because of variation in the motor speed.

Using 809 pounds per hour per square foot as the average over the run, the flow of air in pounds per hour was calculated.

$$(24) \quad G' = GA_T = \frac{809(3.97)^2 \pi}{4(144)} = 69.6 \text{ lb per hr}$$

From a run in the glass tube (Run A-30), the depth of the one pound bed at the above mass velocity was determined. See Figures 7 and 8. Because the cross-sectional area of the glass tube was 1.04 times as large as that of the metal tube, the depth equivalent to 1.04 pounds was used. This gave five inches for the depth of the dense phase and approximately six inches more for the lean phase.

To date, it has not been possible to separate the calculations of the lean phase from those of the dense phase and so the calculations below have been based on the total depth of dense phase and lean phase combined.

The weight of metal in contact with the bed was as follows:

$$(25) \text{ Weight of tube wall} = 0.0682 (11) = 0.75 \text{ pounds}$$

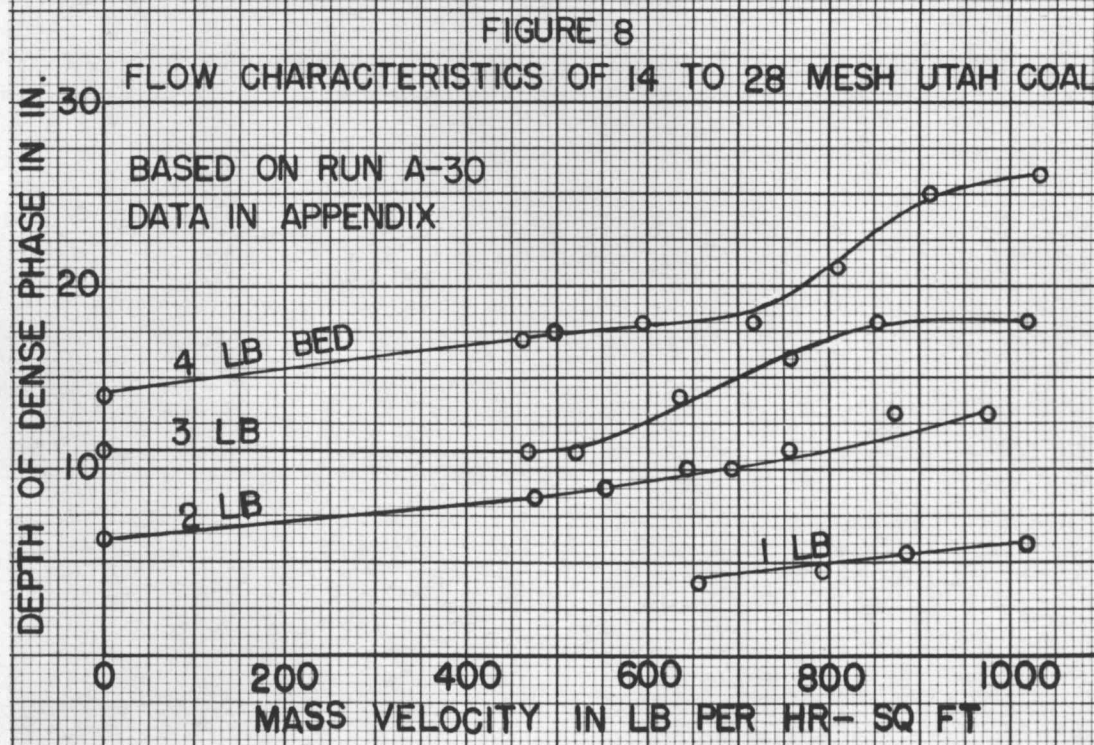
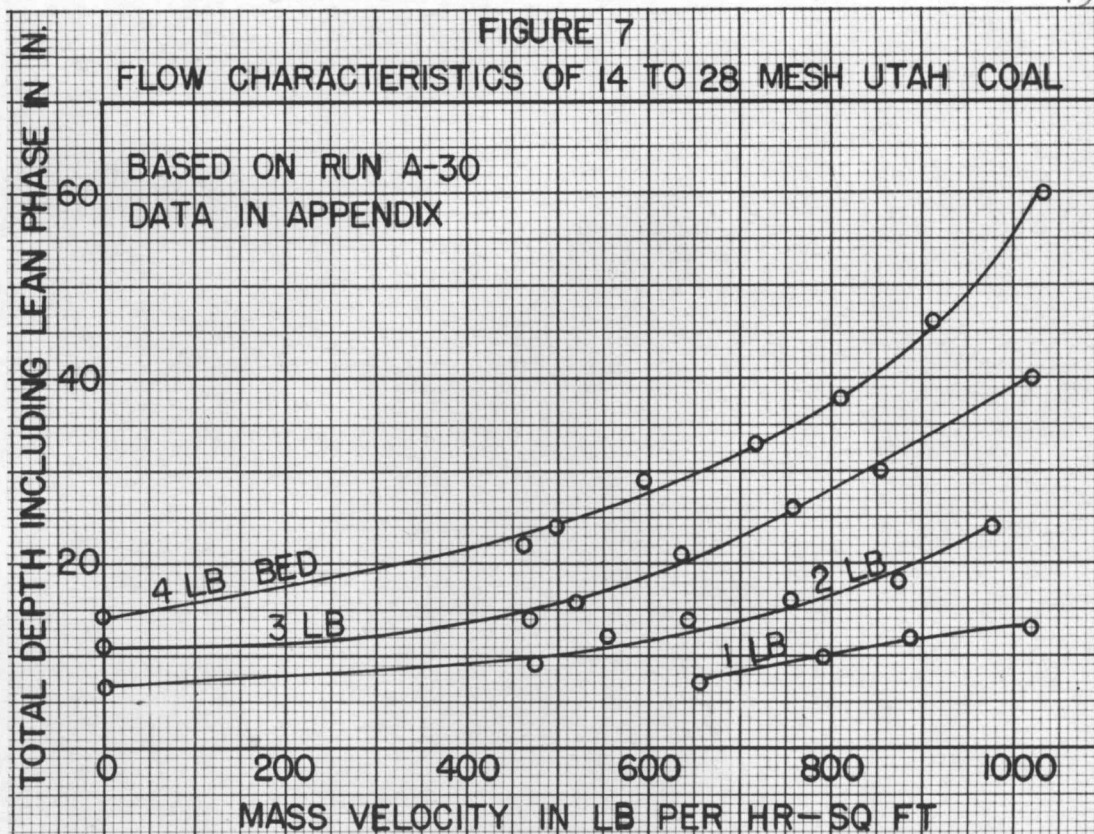
$$(26) \text{ Weight of two vacuum wells} = 0.044 (2) = 0.09 \text{ pounds}$$

$$(27) \text{ Weight of screen and frame} = 0.25 \text{ pounds}$$

The heat flow rate equations, based on equations (3), (4), (7), and (16), respectively, were:

$$(28) \quad q_a = 69.6 (0.240)(t_7 - t_4) = 17.4(t_4 - t_7)$$

The specific heat of air is a function of temperature but varies only slightly within the temperature limits employed (70°F to 320°F). Consequently, it has been considered a constant. The bed actually did not extend from TC-4 to TC-7. There was a space of about $2\frac{1}{2}$ inches between TC-4 and the screen which has since been eliminated



and the top of the lean phase was about 11 inches above the screen, an inch below TC-7. The temperature drop of the air in this one inch, as indicated by the runs with an empty tube, was negligible.

$$(29) \quad q_s = 1.00(0.300)\frac{dT}{d\theta} = 0.300\frac{dT}{d\theta}$$

The specific heat of the coal (0.300) was determined experimentally (See Appendix). This is also a function of temperature but was assumed constant.

$$(30) \quad q_m = \left[0.84(0.12) + 0.25(0.094) \right] \frac{dt_s}{d\theta} = 0.125\frac{dt_s}{d\theta}$$

The values of the specific heat of the metal were obtained from McAdams (29). The temperatures read on the thermocouple number 12 were assumed to be representative of the metal temperature at all points in contact with the bed of solids. This was justifiable because, in earlier runs, all wall thermocouples opposite the fluidized bed read the same or very close to the same temperatures at any given time. For example, as mentioned on page 18, in Runs 2, 3, and 4 two wall thermocouples about twelve inches apart read the same. In Run 9, the maximum difference between wall thermocouples ten inches apart was 5°F. In Run 10, the readings on the same two thermocouples were inseparable. Another assumption, implied in the weight of metal used in

29. Op. cit., p399.

equation (30), was that the longitudinal flow of heat in the metal was negligible compared to radial flow.* This same assumption was made regarding the insulation.

In applying the Schmidt method, room temperature was used as a base, inasmuch as the insulation was all at that temperature at the start of the run.

Inserting the constants into equation (16)

$$(31) \quad q_i = \frac{2\pi(11)(0.041)(t' - t)}{12(2.30) \log \frac{r(12)}{2.0}} = 0.1028 \frac{t' - t}{\log \frac{r(12)}{2.0}}$$

Before these equations could be used, time-temperature plots had to be drawn. See Figure 9.

The rate of heat flow to the air was obtained after determining the difference between t_4 and t_7 at various times. For example, five minutes after starting the run, the difference was 29°F and, therefore

$$(32) \quad q_a = -17.4(29) = -505 \text{ Btu per hr}$$

The values for other times are given in Table IX

TABLE IX
Rate of Heat Flow to Air

<u>Time minutes</u>	<u>$(t_4 - t_7)$ °F</u>	<u>$-q_a$ Btu per hr</u>
1	115	2000
2	74	1290
3	48	835
4	37	644
5	29	505

*See Appendix

TABLE IX CONTINUED
Rate of Heat Flow to Air

<u>Time minutes</u>	<u>$(t_4 - t_7)$ °F</u>	<u>$-q_a$ Btu per hr</u>
6	25	435
8	18	313
10	16	278
12	14.5	252
14	13.2	230
16	12.4	216
18	11.8	205
20	11.4	198
25	10.2	177
30	8.1	141
35	7.0	122
40	7.0	122
45	7.5	130
50	8.4	146
60	7.0	122
70	7.9	137

The rate of change of the metal temperature was determined by measuring the slope of the time-temperature curve of TC-12. The data are shown below:

TABLE X
Rate of Heating of Metal

<u>Time minutes</u>	<u>$(\frac{1}{60}) \frac{dt_{12}}{d\theta}$ °F/min.</u>	<u>q_m Btu per hr</u>
1	60.0	450
2	31.0	232
3	16.2	122
4	10.6	80
5	6.8	51
6	4.7	35
8	3.3	25
10	2.6	20
12	1.83	14
14	1.03	8

TABLE X CONTINUED
Rate of Heating of Metal

<u>Time</u> <u>minutes</u>	$(\frac{1}{60})\frac{dt}{d\theta}$ <u>°F/min.</u>	q_m <u>Btu per hr</u>
16	0.73	$5\frac{1}{2}$
18	0.48	$3\frac{1}{2}$
20	0.60	$4\frac{1}{2}$
25	0.38	3
30	0.21	$1\frac{1}{2}$
35	0.06	$\frac{1}{2}$
40	0.00	0
45	0.42	3
50	0.18	$1\frac{1}{2}$
60	0.00	0
70	0.00	0

Schmidt Method

The first step in finding the rate at which heat entered the insulation was to determine the value of the thermal diffusivity of the insulation. The density of the insulation was determined by weighing and measuring the volume of a piece of 85% magnesia. The value obtained was 12.5 pounds per cubic foot. The specific heat was taken from the literature (30).

$$(33) \quad \alpha = \frac{k_1}{Cp_1e_1} = \frac{0.041}{0.234(12.5)} = 0.0140 \text{ sq ft per hr}$$

Recalling that the key equation in the Schmidt method was

$$(19) \quad \alpha \frac{\Delta\theta}{(\Delta x)^2} = \frac{1}{2}$$

30. Perry, John H., ed. Chemical Engineers' Handbook, Second Edition, New York, McGraw-Hill, 1941, p543.

or, in terms of radial measurement,

$$(34) \quad \propto \frac{\Delta\theta}{(\Delta r)^2} = \frac{1}{2}$$

the size of the radial increment was arbitrarily selected as $\frac{1}{4}$ inch, a value which was small enough to insure accuracy and yet not so small as to make the graphical construction tedious. The time increment was then calculated using equation (34).

$$(35) \quad \frac{0.0140(\Delta\theta)}{\left[\frac{1}{4(12)}\right]^2} = \frac{1}{2}$$

$$(36) \quad \Delta\theta = 0.0155 \text{ hours} \sim 0.93 \text{ minutes}$$

The values of the abscissa corresponding to the $\frac{1}{4}$ inch increments were found.

TABLE XI

Values of Abscissa in Schmidt Method

Radial Distance - inches	2	$2\frac{1}{4}$	$2\frac{1}{2}$	$2\frac{3}{4}$	3
Log $\frac{r}{r_0}$	0.000	0.0512	0.0969	0.1383	0.1761

To account for the finite resistance to the flow of heat from the outside of the insulation to the room an additional increment was added. This increment had the following value (31):

$$(37) \quad \frac{k_i}{2.30h_r r_0}$$

where r_0 was the outside radius of the insulation and h_r had a value of 1.8 Btu per hour - square foot - $^{\circ}\text{F}$, a figure

obtained from the steady state runs, A-25 through A-28 (see Appendix). The numerical value of this term is not critical so that some inaccuracy in h_r is unimportant. The abscissa was, then

$$(38) \quad 0.1761 + \frac{0.041 (12)}{2.30 (1.80)(3.0)} \equiv 0.216$$

The temperature of the inside of the insulation which corresponded to the time increments (multiples of 0.93) was found next. The values listed in the third column of Table XII were taken from Figure 9. The graphical construction, the details of which are illustrated in the Appendix, was then carried out. Figure 10 shows the completed construction.

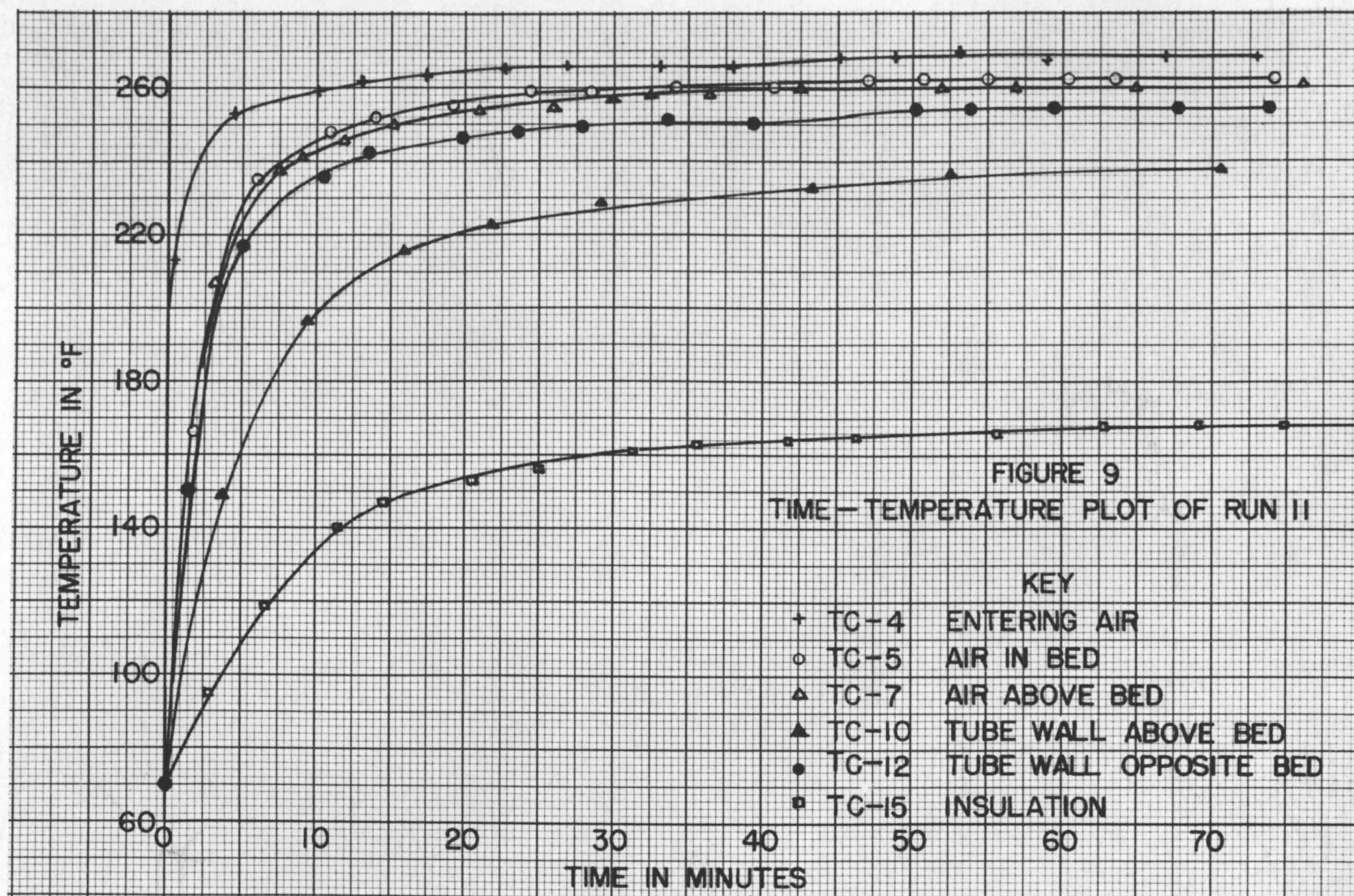
(31) Perry and Berggren, loc. cit.

TABLE XII

Flow of Heat into Insulation

Interval	Time minutes	t_1^* °F	t_2^\dagger °F	$t_1 - t_2$ °F	q_i Btu per hr
1	0.93	78	70	8	16
2	1.86	87.5	74	13.5	26
3	2.79	96	78.5	17.5	35
4	3.72	102	83.3	18.7	37
5	4.65	108	87.1	20.9	42
6	5.59	114	91.5	22.5	45
7	6.51	119	95.5	23.5	46
8	7.44	123	99.7	23.3	47
9	8.37	127.5	103.2	24.3	49
10	9.30	132	106.6	25.4	51
11	10.2	136	110.0	26.0	52
12	11.2	139	113.2	25.8	52
13	12.1	142	115.8	26.2	52
14	13.0	144	118.5	25.5	51
15	14.0	146	120.8	25.2	50
16	14.9	147	122.7	24.3	49
17	15.8	148	124.4	23.6	47
18	16.8	149	125.5	23.5	47
19	17.7	150	127.0	23.0	46
20	18.6	151	128.0	23.0	46
21	19.5	152	129.0	23.0	46
22	20.5	153	130.0	23.0	46
23	21.4	154	131.0	23.0	46
24	22.3	155	131.8	23.2	46
25	23.2	155.5	132.7	22.8	46
26	24.2	156.3	133.5	22.8	46
27	25.1	157	134.3	22.7	45
28	26.0	157.5	134.9	22.6	45
29	27.0	158.3	135.3	23.0	46
30	27.9	158.8	136.0	22.8	46
35	32.6	161	-	-	-
40	37.2	163	-	-	-
45	41.9	164.8	-	-	-
50	46.5	166	-	-	-
60	55.7	167	-	-	-
70	65.0	167.5	-	-	-
80	74.4	168	-	-	-
∞	∞	168.5	145.1	23.4	47

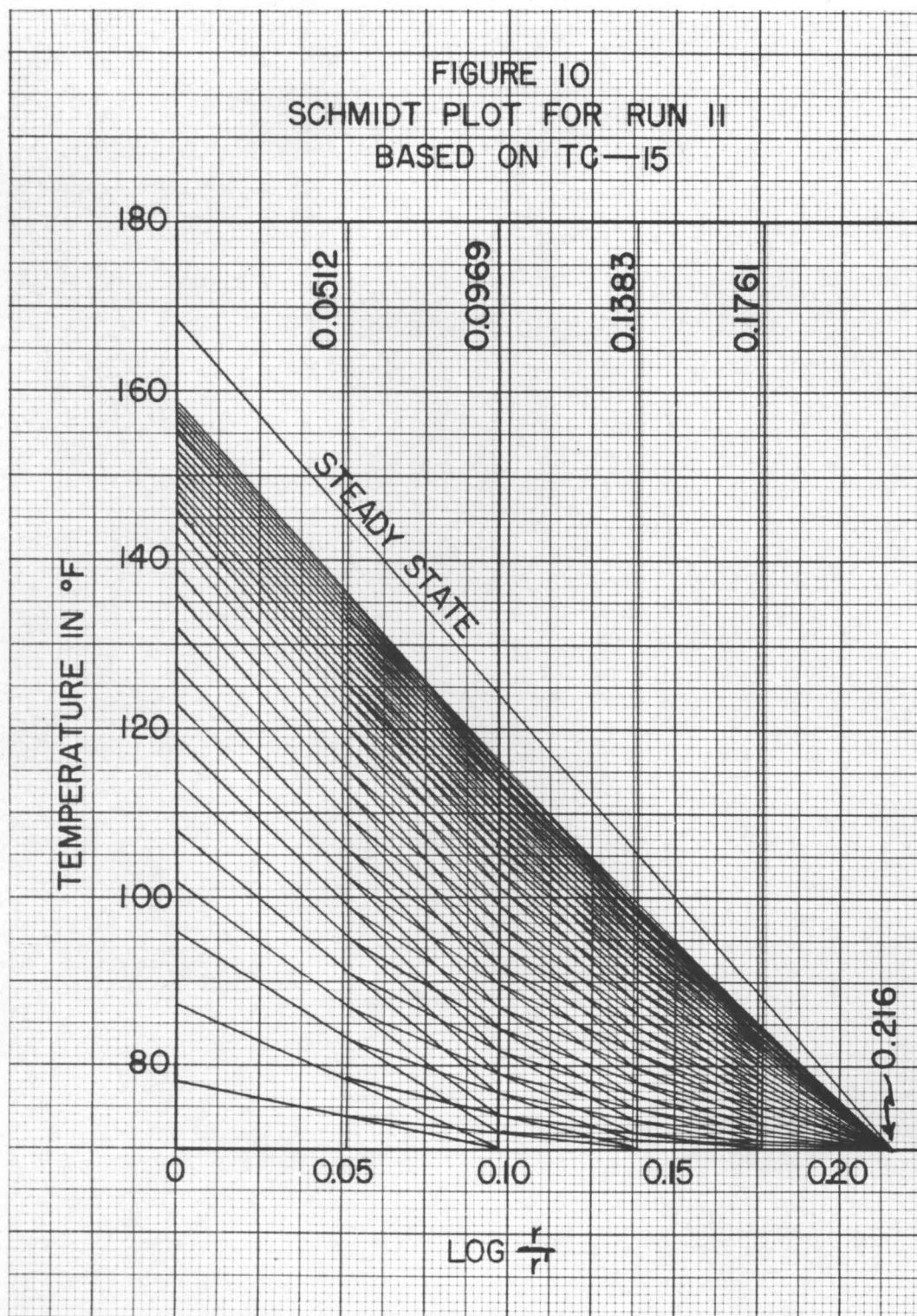
* $t_1 = t_{15}$ $^\dagger t_2$ was temperature $2\frac{1}{4}$ inches from center of tube.



The fourth column in Table XII was obtained from the point representing $\frac{1}{4}$ inch on the temperature distribution curves discussed above. The differences between the first two points on the distribution curves were calculated from columns 3 and 4 in the same table. Assuming that the slope of the chord connecting these two points does not differ very much from the slope of the distribution curve at the inside of the insulation,* these differences were substituted into equation (31) and the rate of heat flow to the insulation was calculated. For example, at 4.65 minutes,

$$(39) \quad q_1 = \frac{0.1028(20.9)}{\log \frac{2.25}{2.00}} = 42 \text{ Btu per hour}$$

*Perry and Berggren reported a maximum difference of 2% for the same number of increments.



The heat flow rates to the insulation are listed in Table XII and plotted against time in Figure 11. Note that after the sixth time interval, the rate of heat flow remained approximately constant. The extrapolation of the rate beyond the thirtieth time interval could be made, therefore, without difficulty.

Coefficient of Heat Transfer between Air and Tube Wall

Referring back to equation (9),

$$(9) \quad q_i + q_m = h_w A_w \Delta_w$$

it is seen that both the terms on the left hand side are now known. The wall area was calculated on the basis of the eleven inch bed depth.

$$(40) \quad A_w = \frac{3.97 \text{ II (11)}}{144} = 0.95 \text{ square feet}$$

The temperature difference between the air and the metal wall, Δ_w , was known at two points and was assumed to vary logarithmically. The value of Δ_w used in equation (9) was, then, the logarithmic mean of the two known differences.

$$(41) \quad \Delta_w = \frac{(t_4 - t_{12}) - (t_7 - t_{12})}{\frac{t_4 - t_{12}}{t_7 - t_{12}}}$$

For example, at eight minutes, $(t_4 - t_{12})$ was 27.7°F and $(t_7 - t_{12})$ was 9.5°F .

$$(42) \Delta_w = \frac{27.7 - 9.5}{\ln \frac{27.7}{9.5}} = 17.0 \text{ } ^\circ\text{F}$$

Substituting all the known values into equation (9)

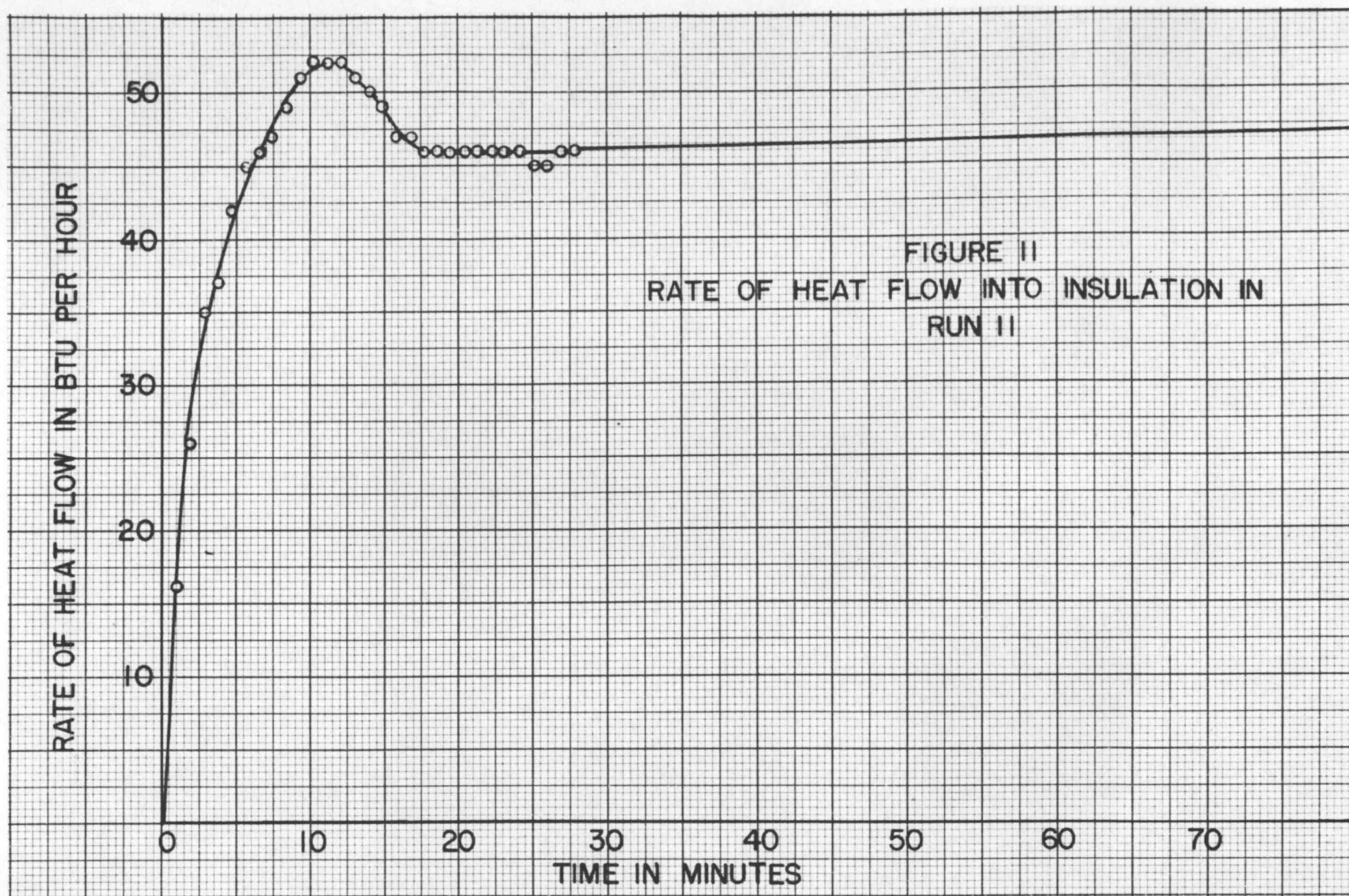


FIGURE II
RATE OF HEAT FLOW INTO INSULATION IN
RUN II

$$(43) \quad 50 + 25 = h_w (0.95)(17.0)$$

the coefficient of heat transfer from the air to the tube wall was found to be

$$(44) \quad h_w = 4.6 \text{ Btu per hr-sq ft} - ^\circ\text{F}$$

The values for other times are given in Table XIII

TABLE XIII

Run 11 - Coefficient of Heat Transfer
between Air and Tube Wall

Time minutes	$q_i + q_m$ Btu_per hr	$(t_4 - t_{12})$ $_{\text{OF}}$	$(t_7 - t_{12})$ $_{\text{OF}}$	Δ_w $_{\text{OF}}$	h_w Btu per hr- sq ft - $_{\text{OF}}$
2	259	77.5	4.0	24.8	11.8
4	119	45.5	9.0	22.5	5.6
6	81	33.0	9.0	18.5	4.6
8	75	27.7	9.5	17.0	4.6
10	72	24.0	8.0	14.6	5.2
12	66	21.6	7.0	13.0	5.3
14	58	20.0	6.6	11.2	5.5
16	53	19.3	6.8	11.5	4.9
18	$49\frac{1}{2}$	19.0	7.0	12.0	4.3
20	$50\frac{1}{2}$	18.3	7.1	11.8	4.5
25	49	17.0	7.0	11.3	4.6
30	$47\frac{1}{2}$	15.2	7.2	10.7	4.7
35	$46\frac{1}{2}$	14.5	7.5	10.6	4.6
40	$46\frac{1}{2}$	16.0	9.0	12.2	4.0
45	$49\frac{1}{2}$	15.5	8.0	11.4	4.6
50	48	14.5	6.2	9.8	5.2
60	$46\frac{1}{2}$	13.0	6.0	9.1	5.4
70	47	14.0	6.0	9.5	5.2

Eliminating the value for two minutes which was subject to large error because of the very rapid change in air temperature in the first few minutes, the average coefficient of heat transfer between the air and the metal tube wall was 4.9 Btu per hour - square foot - $_{\text{OF}}$.

The same calculations were made on Runs 9, 10, and 12. The basic information on these runs is given in Table XIV and the complete data and calculations are presented in the Appendix.

TABLE XIV
Heating Runs on Utah Hard Coal

<u>Run</u>	<u>Weight pounds</u>	<u>Mesh Size</u>	<u>Mass Velocity lb per hr-sq ft</u>
9	2.00	-14+ 28	635
10	2.00	-14+ 28	638
11	1.00	-14+ 28	809
12	0.50	-14+ 28	636

Steady State Heat Flow

If the sole purpose of the above runs had been to find the coefficient of heat transfer between the air and the tube wall, the calculations could have been simplified somewhat by the use of equation (10),

$$(10) \quad q_1 = h_w A_w \Delta_w$$

which holds when steady conditions prevail. Using this equation, the rate of heat flow to the insulation can be calculated from the Schmidt plot. Taking the Schmidt plot of Run 11 (Figure 10) as an example, a straight line is drawn connecting the steady state value of inside insulation temperature, 168.5° F, with the maximum abscissa, 0.216, at 70° F. If $\log \frac{r(12)}{2.00}$ which represents distances along the abscissa, in equation (31)

$$(31) \quad q_i = 0.1028 \frac{(t' - t)}{\log \frac{r(12)}{2.00}}$$

is replaced by 0.216 and the corresponding values of temperature substituted in, q_i can be found.

$$(45) \quad q_i = 0.1028 \frac{(168.5 - 70)}{0.216} = 47 \text{ Btu per hour}$$

The coefficient of heat transfer between air and tube wall is then found as before.

Carrying out the same calculation on Runs 9 and 12 (Run 10 was not continued to steady state), the following results were obtained:

TABLE XV

Steady State Values of Coefficient of Heat Transfer between Air and Wall

Run	q_i Btu per hr	Δ_w °F	h_a Btu per hr-sq ft - °F
9	70	12.9	4.5
11	47	9.5	5.2
12	19½	12.6	4.5

Runs A-31 and A-32 were made with an empty tube at mass velocities of 637 and 636 pounds per hour per square foot, respectively. The only difference in the calculations from those made with solid present, was that the metal temperature varied, becoming lower higher up the tube. This caused a corresponding decrease in insulation temperatures. Consequently, averages had to be used for

the metal and insulation temperatures.

Using the steady state technique just discussed, calculations were made based on the following data:

TABLE XVI

Run A-31 - Steady State Temperatures

Thermocouple	5	12	7	10	15*	16 [†]
Temperature °F	310	275	308	234	174	153

The rate of heat flow through the insulation was

$$(46) \quad q_i = \frac{2 \pi (10)(0.041)(163-71)}{2.30 (12)(0.216)} = 40 \text{ Btu per hour}$$

and, substituting in equation (10),

$$(47) \quad 40 = h_w \left[\frac{3.97 \pi (10)}{144} \right] \left[\frac{(308-234) - (310-275)}{\ln \frac{(308-234)}{(310-275)}} \right]$$

from which

$$(48) \quad h_w = 0.89 \text{ Btu per hour-square foot} - ^\circ\text{F}$$

TABLE XVII

Run A-32 - Steady State Temperatures

Thermocouple	5	12	7	10	15	16
Temperature °F	306	268	303	227	189	150

The rate of heat flow through the insulation was

*Located at inside of insulation 4 inches above the screen.

†Located at inside of insulation 9 inches above the screen.

‡Located at inside of insulation opposite screen.

$$(49) \quad q_i = \frac{2 \pi (10)(0.041)(150-76)}{2.30 (12)(0.216)} = 36 \text{ Btu per hour}$$

The figure 159° F was obtained by assuming proportionality between t_{15} and t_{16} and calculating an inside insulation temperature halfway between TC-5 and TC-7.

$$(50) \quad 36 = h_w \left[\frac{3.97 \pi (10)}{144} \right] \left[\frac{(303-227)-(308-268)}{\ln \frac{303-227}{308-268}} \right]$$

$$(51) \quad h_w = 0.74 \text{ Btu per hour-square foot} - ^\circ\text{F}$$

Although insulation temperatures were not measured in the early runs, it was possible, by means of the resistance concept, to calculate roughly the heat flow rate under steady state conditions and from that a value of h_w . The resistance to the flow of heat from the air to the room was made up of the following parts:

1. The air film on the inside of the tube wall, $\frac{1}{h_w}$.
2. The metal wall, a resistance which was negligible compared to the others.
3. The air film between the outside of the tube and the insulation, a resistance which can be called $\frac{1}{h_g}$. As mentioned earlier, no matter how tightly the insulation fitted the tube, this resistance still existed.
4. The insulation itself.
5. The air film on the outside of the insulation, $\frac{1}{h_r}$.

The method used in the last few pages, in effect, was to determine the heat flow rate from the known resistances,

(4) and (5), and the measured temperature difference between the inside of the insulation and room temperature. Knowing the heat flow rate and the temperature difference between the air and the tube wall, the coefficient of heat transfer between the air and the wall could be calculated.

Since the insulation temperatures were not measured in the early runs, it was necessary to combine resistances (3), (4), and (5) in order to determine the heat flow rate. However, before this could be done, the value of the coefficient of heat transfer across the gap between the metal and the insulation had to be determined.

The following equation expressed the relationship mathematically.

$$(52) \quad q_i = h_g A_g \Delta_g$$

where Δ_g was the temperature difference between the metal and the inside of the insulation. The heat flow rates and the required temperatures either have already been given or appear in the appendix for Runs 9, 10, 11, and 12. Substituting these values into equation (52), we have, for Run 9

$$(53) \quad 70.5 = h_g \frac{4.00 \pi (14)(302-197)}{144}$$

$$(54) \quad h_g = 0.55 \text{ Btu per hour-square foot} - ^\circ\text{F}$$

For Run 10

$$(55) \quad 63 = h_g \frac{4.00 \pi (14)}{144} (285-188)$$

$$(56) \quad h_g = 0.54 \text{ Btu per hour-square foot} - ^\circ\text{F}$$

For Run 11

$$(57) \quad 47 = h_g \frac{4.00 \pi (11)}{144} (254-168.5)$$

$$(58) \quad h_g = 0.57 \text{ Btu per hour-square foot} - ^\circ\text{F}$$

For Run 12

$$(59) \quad 19.5 = h_g \frac{4.00 \pi (4)}{144} (288-186)$$

$$(60) \quad h_g = 0.54 \text{ Btu per hour-square foot} - ^\circ\text{F}$$

The average of these four values is 0.55 Btu per hour-square foot - $^\circ\text{F}$.

Using the same technique for this resistance as for that on the outside of the insulation, an increment which had the following value was added

$$(61) \quad \frac{k_i}{2.30 h_{gr}} = \frac{0.041(12)}{2.30(0.55)(2.00)} = 0.194$$

The three increments corresponding to resistances (3), (4), and (5) had, then, the following values: 0.194, 0.176, and 0.040, respectively. Their sum is 0.410. The equation for heat flow rate would then read

$$(62) \quad q_i = \frac{2 \pi N(0.041)(t_m - t_o)}{2.30 (0.410)}$$

In Run 2, five pounds of a fraction of 3A catalyst averaging about 150 mesh in size* were fluidized. The air had a mass velocity of 193 pounds per hour per square foot. Although steady state was not reached, it was approached close enough so that temperatures could be extrapolated to this condition. These temperatures were:

TABLE XVIII

Run 2 - Steady State Temperatures

Thermocouple Temperature °F	Vacuum 247	Wall 245	Room 74
--------------------------------	---------------	-------------	------------

For the twelve inches between the two sets of thermocouples

$$(63) \quad q_1 = \frac{2 \pi (12) (0.041) (245-74)}{2.30 (12) (0.410)} = 46 \text{ Btu per hour}$$

and

$$(64) \quad 46 = h_w \frac{4.00 \pi (12)}{144} (247-245)$$

$$(65) \quad h_w = 22 \text{ Btu per hour-square foot} - ^\circ\text{F}$$

In Run 4, five pounds of Ottawa Standard Silica Sand were fluidized. This material had an average particle size of about 40 mesh.** The air had a mass velocity of 813 pounds per hour per square foot. The steady state temperatures were as follows:

*See Table I

**See Table I and Appendix

TABLE XIX

Run 4 - Steady State Temperatures

Thermocouple	Vacuum	Wall	Room
Temperature °F	287	283	75

For the twelve inches between the two sets of thermocouples

$$(66) \quad q_i = \frac{2 \pi (12)(0.041)(283-75)}{2.30 (12)(0.410)} = 56 \text{ Btu per hour}$$

$$(67) \quad 56 = h_w \frac{4.00 \pi (12)}{144} (287-283)$$

$$(68) \quad h_w = 13 \text{ Btu per hour-square foot} - ^\circ\text{F}$$

At the end of Run 5, there was approximately 0.8 of a pound of wood charcoal, which averaged about 20 mesh in size,* in the tube. The mass velocity of the air was 548 pounds per hour per square foot. The steady state temperatures were as follows:

TABLE XX

Run 5 - Steady State Temperatures

Thermocouple	Vacuum		Wall		Room
	(1)	(2)	(1)	(2)	
Temperature °F	256	247	235	241	81

For the twelve inches between the two sets of thermocouples

$$(69) \quad q_i = (0.269)(238-81) = 41 \text{ Btu per hour}$$

and

$$(70) \quad 41 = h_w \frac{\pi}{3} \left[\frac{(256-235) - (247-241)}{\ln \frac{256-235}{247-241}} \right]$$

*See Appendix

$$(71) \quad h_w = 3.2 \text{ Btu per hour-square foot} - ^\circ\text{F}$$

All the steady state values of the heat transfer coefficient between the fluidizing air and the tube wall are presented in Table XXI.

TABLE XXI
Steady State Values of h_w

Material Fluidized	Approximate Avg. Particle Size	Mass Velocity lb per hr-sq ft	h_w Btu per hr-sq ft - $^\circ\text{F}$
3A Catalyst	150 mesh	193	22
Sand	40 "	813	13
Coal	20 "	809	5.2
Coal	20 "	636	4.5
Coal	20 "	635	4.5
Charcoal	20 "	548	3.2
Empty Tube	-	637	0.89
Empty Tube	-	636	0.74

The data are not extensive enough to derive equations relating the film coefficient to the mass velocity and the particle size. However, some qualitative conclusions can be drawn:

1. The film coefficient of heat transfer between the air and the tube wall is much greater when fluidized solids are present than when the tube is empty.

2. The film coefficient increases with increasing mass velocity. In fact, it increases at about the same rate as the mass velocity. This can be expressed mathematically as

$$(72) \quad h_w = f(G)^m \qquad m \sim 1$$

3. The film coefficient increases with decreasing particle size. The increase is at least inversely proportional to the particle size and may be much greater than that. In equation form

$$(73) \quad h_w = f' (D_p)^{-n} \quad n > 1$$

Combining (72) and (73)

$$(74) \quad h_w = \phi (G)^m (D_p)^{-n}$$

Coefficient of Heat Transfer between Air and Solid

Referring back to equation (6),

$$(6) \quad q_a + q_s + q_m + q_i = 0$$

it was believed that the rate of heat flow to the solid, q_s , could be calculated by difference and originally it was hoped that such rates could be calculated with sufficient accuracy to determine the coefficient of heat transfer between the air and the solid particles (Equation 14). However, as will be seen below, unaccountable losses made this method too inaccurate.

When the third column of Table IX, the rate of heat flow to the air, q_a , was combined with the third column of Table X, the rate of heat flow to the metal, q_m , and the sixth column of Table XII, the rate of heat flow to the insulation, q_i , a series of values was obtained which should have, in the absence of other losses, given the rate of heat flow to the bed of fluidized solids. These data are given in Table XXII and plotted in Figure 12.

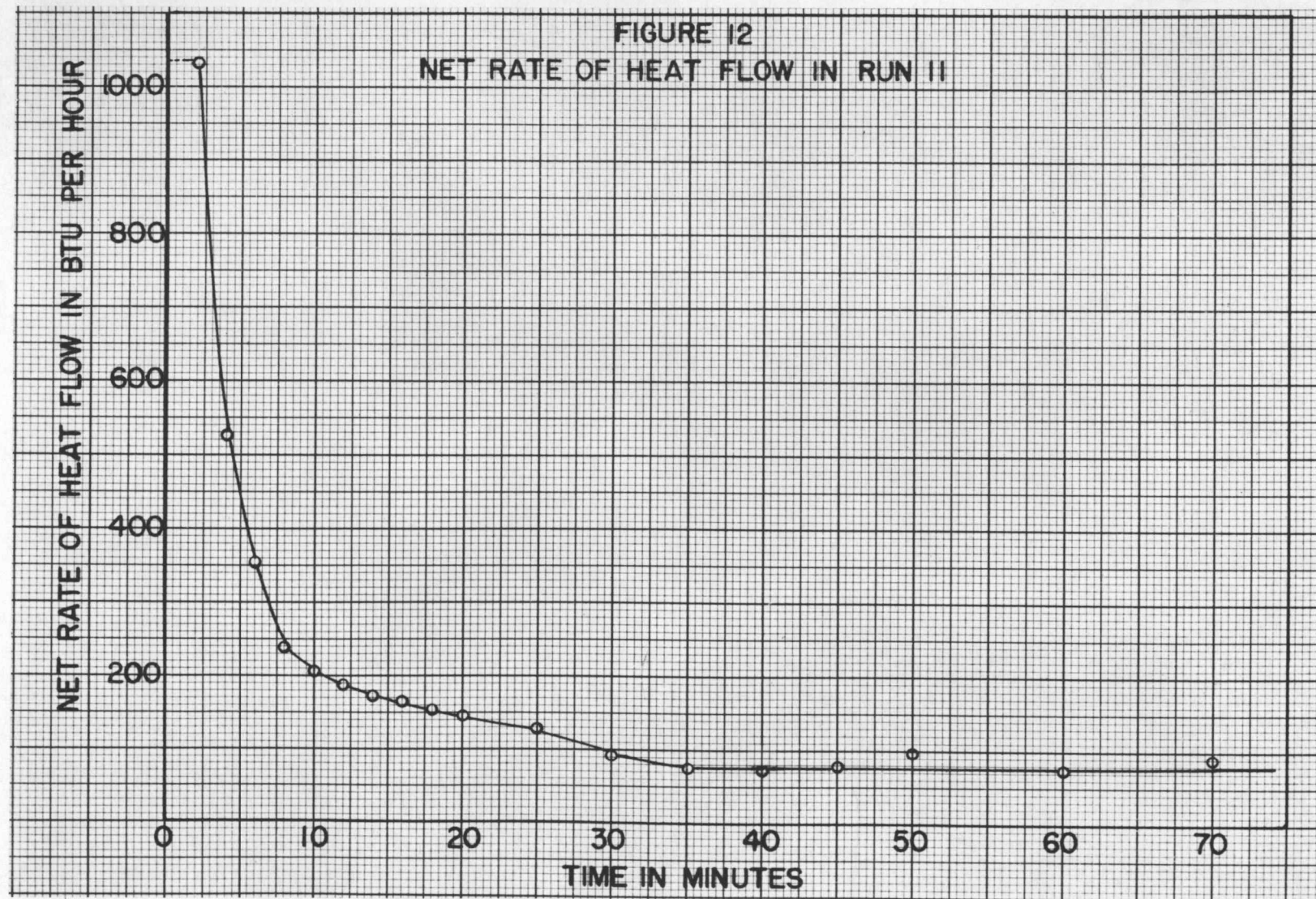


TABLE XXII

Run 11 - Net Rate of Heat Flow

<u>Time</u> <u>Minutes</u>	<u>$-q_a - (q_i + q_m)$</u> <u>Btu per hr</u>	<u>q_s^*</u> <u>Btu per hr</u>
2	1031	559
4	525	195
6	354	90
8	238	54
10	206	34
12	186	24
14	172	20
16	163	17
18	155	13
20	147	9
25	128	7
30	93	4
35	75	$2\frac{1}{2}$
40	75	$4\frac{1}{2}$
45	80	4
50	98	0
60	75	0
70	90	0

The ordinate in Figure 12 is q , which equals $\frac{dq}{d\theta}$, and the abscissa is time, θ . The area under the curve can be expressed as

$$(75) \int_0^{\theta} \frac{dq}{d\theta} d\theta = Q$$

If there were no losses besides those to metal and insulation, Q would represent the heat absorbed by the solid and, from the known weight and specific heat, the average solid temperature could be calculated.

$$(76) Q_s = W_s C_{ps} (T - t_0)$$

*Based on equilibrium at top of bed

For the case under consideration, at the end of 70 minutes the area under the curve amounted to 189 Btu, assuming a constant value of q from the start to two minutes. Setting the known values in (76)

$$(77) \quad 189 = 1.00(0.300)(T-70)$$

from which

$$(78) \quad T = 700^{\circ} \text{ F}$$

a temperature which is obviously too high, inasmuch as the maximum entering gas temperature was only 268° F . Assuming that the solid was in equilibrium with the air leaving the bed at all times and that mixing was so rapid that the particles throughout the bed were all at the same temperature, an approximate rate of heat flow to the solid, q_s , was calculated using equation (29)

$$(79) \quad q_s = 0.300 \frac{dt_g}{dt}$$

The values obtained are shown in the third column of Table XXII. It can be seen from the table that the approximate curve of q_s had the same shape as the curve plotted in Figure 12. The difference between the two curves, that is, the rate of heat flow to the unaccountable losses also had the same general shape, high in the first few minutes and decreasing rapidly with time.

In attempting to isolate the unaccountable losses, two unsteady state runs were made with an empty tube. These runs, A-31 and A-32, have already been discussed from the

standpoint of h_w under steady state conditions. A resumé of the data and calculations on Run A-31 is given below. Run A-32 was similar to Run A-31.

TABLE XXIII

Run A-31 - Unsteady State Run with Empty Tube

Duration of Heating Cycle: 140 minutes
Average mass velocity: 637 lb per hr-sq ft

TABLE XXIV

Run A-31 - Heat Flow Rate Equations

$$(80) \quad q_a = \frac{637(12.40)(0.240)}{144} (t_{14} - t_4) = -13.2(t_4 - t_{14})$$

$$(81)^* \quad q_m = \left[0.66(0.12) + 0.25(0.094) \right] \frac{dt_{12}}{d\theta} + \left[0.82(0.12) + \frac{0.084}{4} \right] \frac{dt_{10}}{d\theta} \\ + \left[0.41(0.12) + 0.25(0.094) \right] \frac{dt_{13}}{d\theta} \\ = 0.103 \frac{dt_{12}}{d\theta} + 0.110 \frac{dt_{10}}{d\theta} + 0.061 \frac{dt_{13}}{d\theta}$$

$$(82)^{\dagger} \quad q_i = \frac{2\pi(13)(0.041)(t_{15}' - t_{15}'')}{2.30(12) \log \frac{2.25}{2.00}} + \frac{2\pi(11)(0.041)(t_{16}' - t_{16}'')}{2.30(12) \log \frac{2.25}{2.00}} \\ = 2.37(t_{15}' - t_{15}'') + 2.00(t_{16}' - t_{16}'')$$

*This equation given in three parts because of the variation in metal temperature.

†This equation given in two parts because of the variation in insulation temperature.

TABLE XXV

Run A-31 - Heat Flow Rates

<u>Time Minutes</u>	<u>q_i Btu per hr</u>	<u>q_m Btu per hr</u>	<u>$q_i + q_m$ Btu per hr</u>	<u>$-q_a$ Btu per hr</u>
2	22	270	292	340
5	52	148	200	240
10	68	85	153	160
15	70	26	96	115
20	71	19	90	105
30	72	11	83	80
40	74	8	82	80
60	76	3	79	80

The unbalance ($q_i + q_m - q_a$) was small in the first few minutes and decreased to approximately zero after 30 minutes. The early unbalance can be traced to the weight of metal wall between TC-4 and the screen. As mentioned earlier, this difficulty has been corrected by locating the hot junction of TC-4 just below the screen. These calculations eliminated a number of possible sources of error such as incorrect measurement of mass flow rate, an air leak between the orifice and the tube, incorrect method of calculation, too large a volume of air flowing through the vacuum thermocouple wells, incorrect rate of heat flow to the metal, or incorrect rate of heat flow to the insulation.

From the shape of the curve of the rate of heat flow to the unaccountable losses, the fact that the rates balanced in the run with the empty tube, and the much more rapid rate of heat transfer to the metal when solid was present, it was believed that the greater part of these

losses was due to the various metal fittings which extended through the insulation.* As pointed out earlier (p33), plastic pieces were inserted to thermally insulate the thermocouple wells from the metal wall and from the outside. However, before trying out these changes, it was decided to make a calculation based on an assumed coefficient of heat transfer between the air and the particles of 5.2 Btu per hour-square foot - $^{\circ}\text{F}$, the value obtained in Run 11 for h_w .

Assuming that the particles have a surface area 1.75^{**} times as large as spheres of the same average size, the total surface area of one pound of 14 to 28 mesh coal would be in the neighborhood of 50 square feet. Substituting into equation (14)

$$(14) \quad q_s = h_s A_s \Delta_s$$

the value of q_s for two minutes in Table XXII

$$(83) \quad 559 = 5.2(50)\Delta_s$$

the mean value of Δ_s was found to be 2°F . Inasmuch as the temperature difference between air and solid--assuming the solid temperature was very close to the outgoing air temperature--was about 74°F at the entrance to the bed, the temperature difference would have to have been about 10^{-80}F to satisfy the logarithmic mean, i.e.,

*See Appendix

**Personal communication from Prof. J. Schulein, Aug. 1948.

$$(84) \quad 2 = \frac{74 - \Delta_e}{\ln \frac{74}{\Delta_e}}$$

at the top of the fluidized bed. It can be seen from this that, if the film coefficient between air and particles is of the same order of magnitude as the coefficient between air and tube wall, the temperature difference between air and solid will be extremely small at the top of the bed. Therefore, even if all the heat could be accounted for, the method of determining the solid temperature by means of the area under the curve of q_s versus time would not lead to a correct value of Δ_s .

Despite the failure of the attempt to determine the coefficient of heat transfer between the air and the fluidized particles, it was felt that it was worth while to describe the calculations for unsteady state heat flow. Extension of the experiments to higher temperatures or larger particles might serve to break the equilibrium between the air leaving the bed and the solid particles.

Before closing this section it might be well to mention the relative resistances of the air film around the particle and the particle itself. The conductivity of coal is 0.111 Btu per hour (square foot) ($^{\circ}\text{F}$) per foot (31) and half the diameter of the average particle in the 14 to 28 mesh range is about 0.0173 inches. If h_s were 5, the

(31) National Research Council, Chemistry of Coal Utilization, Volume I, John Wiley, 1945, pp320-6.

respective resistances would be

$$(85) \quad \frac{1}{K} = \frac{0.0173}{12(0.111)} = 0.013$$

$$(86) \quad \frac{1}{h_s} = \frac{1}{5} = 0.20$$

The resistance due to the particle itself is,
therefore, only a small fraction of the total resistance.

CONCLUSIONS

The following values of the heat transfer coefficient between the air stream and the tube wall were obtained:

TABLE XXVI

Steady State Values of Coefficient of Heat Transfer between Air and Wall

<u>Material Fluidized</u>	<u>Approx. Avg. Particle Size</u>	<u>Mass Velocity lb per hr-sq ft</u>	<u>Heat Transfer Coefficient Btu per hr-sq ft - °F</u>
3A Catalyst	150 mesh	193	22
Sand	40 "	813	13
Coal	20 "	809	5.2
Coal	20 "	636	4.5
Coal	20 "	635	4.5
Charcoal	20 "	548	3.2
Empty Tube	-	637	0.89
Empty Tube	-	636	0.74

From the above values, the following conclusions are drawn:

1. The film coefficient of heat transfer between an air stream and the containing tube wall is much larger when fluidized solids are present than when the tube is empty.

2. The film coefficient of heat transfer between the air and the tube is a function of the mass velocity to some power approximately equal to one.

3. The film coefficient of heat transfer between the air and the tube is an inverse function of the particle size to some power which is probably greater than one.

4. The rate of heat transfer between a bed of

fluidized solids and the fluidizing gas is very rapid. One factor which brings this about is the large area available for heat transfer.

RECOMMENDATIONS

It is recommended that:

1. Further extensive experimental work be carried out on the coefficient of heat transfer between the air stream and the tube wall. The effect of the following factors should be investigated: mass velocity, particle size, type of fluidization, material fluidized, and particle concentration. These experiments can be done batchwise, with steady state heat flow.

2. An attempt to determine the coefficient of heat transfer between the air and the fluidized particles be made using continuous feed and discharge of solid particles. However, before this is attempted, a thorough study should be made of the various flow rates to determine whether the coefficient can be determined by this method.

Weight of

Thickness

Average

Average

Cross-section

Cross-section

Cross-section

APPENDIX

Weight

Thickness

Average

Average

Cross-section

Cross-section

Cross-section

Cross-section

Cross-section

Cross-section

Cross-section

Cross-section

Cross-section

Cross-section

Cross-section

Cross-section

Cross-section

Cross-section

Cross-section

ADDITIONAL EQUIPMENT DATA

Length of sheet metal tube: 9 feet $7\frac{1}{2}$ inches

Weight of sheet metal tube: 7 pounds 14 ounces

Thickness of sheet metal tube: 26 gage

Average inside diameter of sheet metal tube: 3.97 inches

Average inside diameter of glass tube: 4.055 inches

Cross-section area of metal tube: $\frac{\pi}{4} (3.97)^2 = 12.90$ sq in.

Cross-section area of glass tube: $\frac{\pi}{4} (4.055)^2 = 12.90$ sq in.

Cross-section area of vacuum thermocouple well:

$$\frac{\pi}{4} (0.140)^2 = 0.0154 \text{ sq in.}$$

Density of insulation

$$\text{Volume of test piece: } \frac{\pi[(8.5)^2 - (5.75)^2](36)}{4(2)(1728)} = 0.321 \text{ cu ft}$$

Weight of test piece: 4 lb 0 ounces

$$\text{Density: } \frac{4}{0.321} = 12.5 \text{ lb per cu ft}$$

ORIFICE CALIBRATION

TABLE XXVII

Nomenclature for Orifice Calibration

G	= mass velocity; lb per hr-sq ft
U _o	= velocity in orifice, feet per second
U _m	= superficial velocity in metal tube, feet per second
U _g	= superficial velocity in glass tube, feet per second
T	= gas temperature, °R
T _o	= gas temperature in orifice, °R
T _R	= room temperature, °R
ρ	= gas density, pound per cu ft
ρ _o	= gas density in orifice, lb per cu ft
CFM	= cu ft of gas metered per min
P ₁	= upstream orifice pressure, inches mercury
ΔP	= pressure drop across orifice - inches water
ΔP'	= pressure drop across orifice @ 70° F and 30.2 in. mercury downstream pressure
D _o	= orifice diameter - inches
C	= orifice coefficient
h	= pressure drop across orifice, feet of fluid flowing

For metal tube 3.81 in. I.D.*

$$(87) \quad G = \frac{(\text{cfm})(60)(4)(144)(29)(492)}{\pi(3.81)^2(359)T_R} = \frac{30000(\text{cfm})}{T_R}$$

$$(88) \quad \rho_o = \frac{29(492)(29.9 + P_1 - \frac{\Delta P}{13.6})}{(359)T_o(29.9)} = \frac{1.33(29.9 + P_1 - \frac{\Delta P}{13.6})}{T_o}$$

$$(89) \quad U_o = \frac{C\sqrt{2gh}}{\sqrt{1 - (\frac{D_o}{1.049})^2}} = \frac{C\sqrt{2(32.2)(62.4)\Delta P}}{\sqrt{1 - (\frac{D_o}{1.049})^2}} \cdot \frac{12\rho_o}{12\rho_o}$$

For 0.500 inch orifice

$$(90) \quad U_o = 20.8C\sqrt{\frac{\Delta P}{\rho_o}}$$

*Orifices were calibrated with original 4 inch o.d. (3/32 in. thick tube. Conversion to sheet metal tube and glass tube is given on p93.

For 9/32 inch orifice

$$(91) \quad U_o = 19.0C \sqrt{\frac{\Delta P}{\rho_o}}$$

$$(92) \quad G = 3600U_o \rho_o \left(\frac{D_o}{3.81}\right)^2$$

For 0.500 inch orifice

$$(93) \quad G = 1290C \sqrt{\rho_o \Delta P}$$

For 9/32 inch orifice

$$(94) \quad G = 372C \sqrt{\rho_o \Delta P}$$

TABLE XXVIII

CALIBRATION OF 0.500 inch ORIFICE

Upstream Pressure P_1 in. mercury	Pressure Drop ΔP in. water	Gas Flow cfm	Room Temp T_R °R	Orifice Temp T_o °R	Density of Air - ρ_o lb per cu ft	Corrected Press. Drop $\Delta P'$	Mass Velocity G - lb per hr-sq ft	Remarks
0.3	0.7	2.7	536	537	0.0749	0.69	151) Not used in) calculations) ΔP - too small
0.4	1.3	3.8	536	536	0.0750	1.29	212	
0.5	2.3	5.2	536	536	0.0751	2.28	291	
0.5	3.0	6.4	536	537	0.0749	2.96	358	
0.5	3.0	6.5	528	528	0.0760	3.01	369	
0.6	3.8	7.2	528	551	0.0730	3.66	409	
0.6	4.6	8.2	528	539	0.0745	4.52	465	
1.9	5.1	8.6	528	539	0.0775	5.22	488	
1.0	7.8	10.1	528	533	0.0757	7.79	574	
1.0	7.5	10.0	528	551	0.0737	7.28	568	
1.2	9.4	11.4	532	534	0.0760	9.42	643	
1.3	11.5	12.1	528	535	0.0756	11.48	687	
1.5	12.6	13.1	528	553	0.0735	12.20	744	
1.5	12.9	13.3	528	553	0.0735	12.50	755	
1.7	15.2	14.8	528	538	0.0755	15.15	840	
2.05	18.3	16.0	528	540	0.0755	18.23	909	
2.1	18.8	16.0	528	553	0.0737	18.30	909	
2.2	19.6	16.4	528	553	0.0740	19.13	931	
2.3	19.8	16.8	528	543	0.0753	19.7	955	
2.5	22.3	17.7	532	540	0.0758	22.3	1000	
2.55	22.8	17.8	532	537	0.0763	22.9	1004	
2.75	25.1	18.8	528	550	0.0745	24.7	1068	
3.2	29.2	19.8	528	530	0.0764	29.4	1123	
3.0	27.0	19.4	528	553	0.0745	26.5	1101	
5.6	32.5	21.2	528	543	0.0811	34.8	1204	

TABLE XXVIII CONTINUED

CALIBRATION OF 0.500 inch ORIFICE

Upstream Pressure P_1 in. mercury	Pressure Drop ΔP in. water	Gas Flow cfm	Room Temp T_R °R	Orifice Temp °R	Density of Air - ρ lb per cu ft	Corrected Press. Drop $\Delta P'$	Mass Velocity G - lb per hr-sq ft	Remarks
3.0	27.5	19.8	528	553	0.0745	27.0	1124	
3.4	31.6	20.8	528	543	0.0760	31.7	1181	
3.6	34.1	21.75	528	550	0.0750	33.8	1235	

TABLE XXIX

CALIBRATION OF 9/32 inch ORIFICE

Upstream Pressure P_1 in. mercury	Pressure Drop ΔP in. water	Gas Flow cfm	Room Temp T_R °R	Orifice Temp T_O °R	Density of Air - ρ_o lb per cu ft	Corrected Press. Drop $\Delta P'$	Mass Velocity G - lb per hr-sq ft	Remarks
0.4	3.4	2.2	536	536	0.0746	3.35	123	Not used in calculations
0.4	3.2	1.8	536	536	0.0746	3.15	101	
0.6	6.0	2.5	536	536	0.0746	5.90	140	
0.8	8.8	3.0	536	536	0.0746	8.67	168	
0.8	9.0	3.2	536	536	0.0746	8.86	179	
1.0	11.5	3.6	536	537	0.0748	11.35	201	
1.4	17.4	4.4	536	539	0.0744	17.10	246	
2.0	17.5	4.6	530	540	0.0755	17.45	260	
1.6	19.3	4.6	536	538	0.0747	19.03	257	
2.1	19.5	4.9	530	540	0.0755	19.45	277	
2.0	24.8	5.3	536	538	0.0746	24.4	296	
2.6	25.7	5.9	530	540	0.0755	25.6	334	
2.4	29.0	6.2	530	541	0.0744	28.4	351	

In order to put all the data on the same basis:

Base temperature 70° F

Base downstream orifice pressure - 30.2 in. mercury

$C_o = 0.0758$ under these conditions

$$(95) \quad C_o \Delta P = 0.0758 (\Delta P^1)$$

$$(96) \quad G = K_1 (\Delta P^1)^{\frac{1}{2}}$$

$$(97) \quad U_m = \frac{G}{3600 e}$$

Using method of residual summation

$$(98) \quad \log G = \log K_1 + \frac{1}{2} \log (\Delta P^1)$$

$$(99) \quad \sum \log G = N \log K_1 + \frac{1}{2} \sum \log (\Delta P^1)$$

From the data on the 0.500 inch orifice:

$$(100) \quad 74.8505 = 26 \log K_1 + \frac{1}{2}(28.7658)$$

$$(101) \quad K_1 = 211.7$$

$$(102) \quad K_1 = 1290 C \sqrt{0.0758}$$

$$(103) \quad C = 0.597$$

$$(104) \quad G = 1290 (0.597) \sqrt{C_o \Delta P} = 770 \sqrt{C_o \Delta P}$$

From the data on the 9/32 inch orifice:

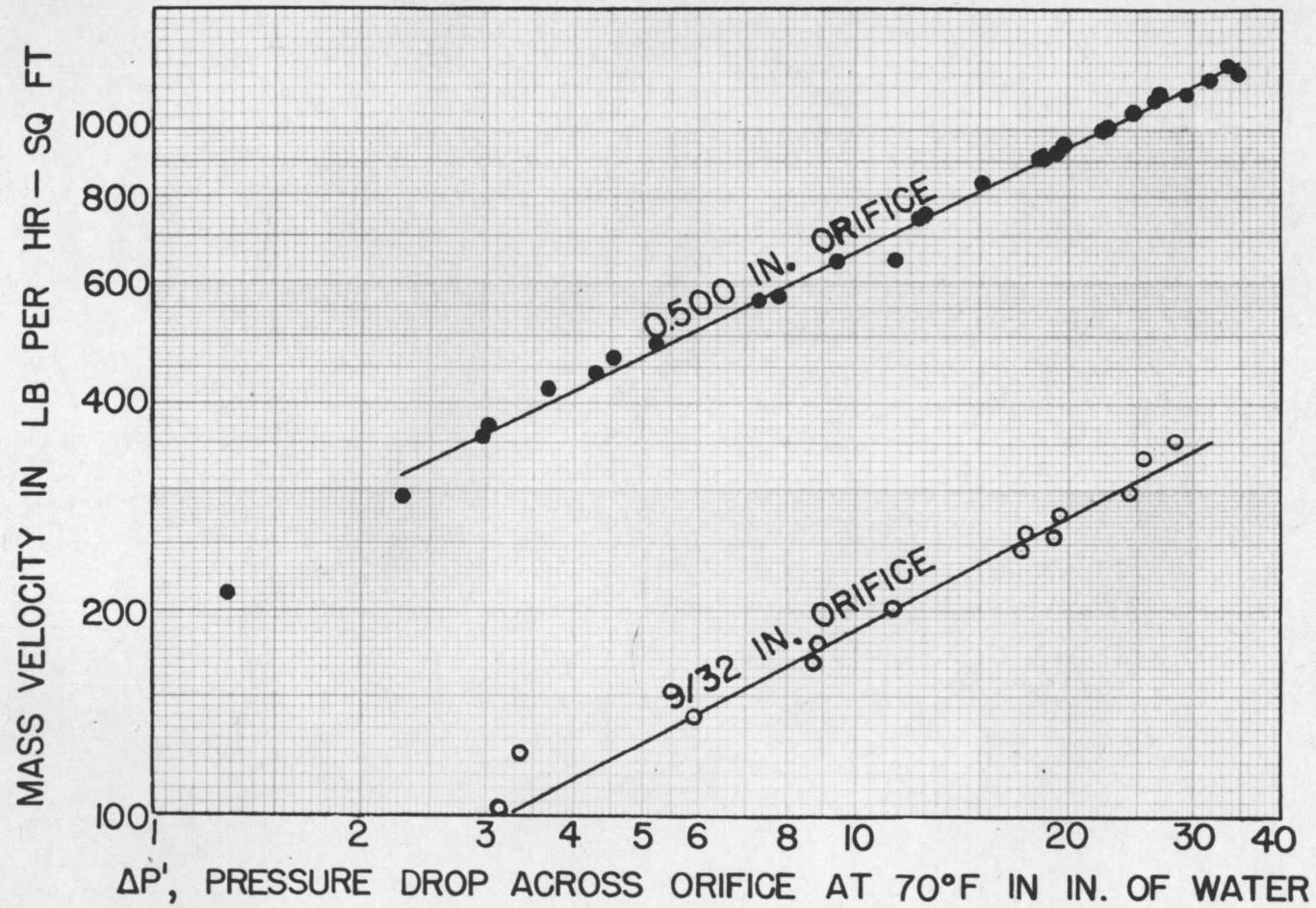
$$(105) \quad 28.1304 = 12 \log K_2 + \frac{1}{2}(13.3017)$$

$$(106) \quad K_2 = 61.7 = 372 C \sqrt{0.0758}$$

$$(107) \quad C = 0.604$$

$$(108) \quad G = 372 (0.604) \sqrt{C_o \Delta P} = 224 \sqrt{C_o \Delta P}$$

FIGURE 13
MASS VELOCITY IN 3.81 INCH DIAMETER METAL TUBE VS.
PRESSURE DROP ACROSS ORIFICES



Conversion of mass velocities in original 3/32 inch tube to new sheet metal tube and glass tube:

$$\text{Ratio of cross-section area of old tube to new tube: } \frac{11.36}{12.40} = 0.915$$

Ratio of cross-section area of old tube to glass tube:

$$\frac{11.36}{12.90} = 0.880$$

TABLE XXX

Mass Velocity Equations

	<u>Sheet Metal</u>	<u>Glass</u>
0.500 inch orifice	705 $\sqrt{e_o \Delta P}$	675 $\sqrt{e_o \Delta P}$
9/32 inch orifice	206 $\sqrt{e_o \Delta P}$	197 $\sqrt{e_o \Delta P}$

THERMOCOUPLE CALIBRATION

Calibration against Bureau of Standards Lead, the freezing point of which is 17.81 millivolts when the cold junction is at 32°F.

TABLE XXI

Thermocouple Calibration

<u>Thermocouple</u>	<u>Readings in Millivolts</u>	<u>Average Deviation Millivolts</u>
1	17.80	-0.005
	17.81	
2	17.79	-0.04
	17.75	
3	17.78	-0.01
	17.81	
	17.82	
4	17.81	0.00
	17.81	
5	17.82	-0.01
	17.76	
	17.81	
6	17.81	0.00
	17.81	
7	17.79	+ 0.04
	17.84	
	17.84	
8	17.79	0.00
	17.83	
9	17.81	0.00
	17.81	
10	17.76	-0.06
	17.74	
11	17.74	-0.08
	17.72	
12	17.74	-0.045
	17.79	
13	17.74	-0.05
	17.78	
14	17.75	-0.06
	17.78	
	17.74	
	17.74	

TABLE XXXI CONTINUED

Thermocouple Calibration

<u>Thermocouple</u>	<u>Readings in Millivolts</u>	<u>Average Deviation Millivolts</u>
15	17.83	+ 0.02
	17.83	
16	17.81	0.00
	17.80	
17	17.77	-0.04
	17.77	

TEMPERATURE vs MILLIVOLTS FOR IRON-CONSTANTAN
THERMOCOUPLE WITH COLD JUNCTION AT 70°F

TABLE XXXII

	0	100	200	300	400
°F	<u>Millivolts</u>				
0		0.86	3.82	6.85	9.92
5		1.01	3.97	7.00	10.08
10		1.16	4.12	7.16	10.22
15		1.30	4.27	7.31	10.38
20		1.45	4.43	7.46	10.53
25		1.60	4.58	7.62	10.69
30		1.75	4.73	7.77	10.84
35		1.90	4.88	7.92	10.99
40		2.04	5.03	8.08	11.15
45		2.19	5.18	8.23	11.30
50		2.34	5.34	8.38	11.45
55		2.49	5.48	8.54	11.61
60		2.64	5.64	8.69	11.76
65		2.78	5.79	8.84	11.92
70	0	2.93	5.94	9.00	12.07
75	0.14	3.08	6.09	9.15	12.22
80	0.28	3.23	6.24	9.30	12.38
85	0.43	3.38	6.40	9.45	12.53
90	0.57	3.52	6.55	9.61	12.68
95	0.72	3.67	6.70	9.76	12.84
100	0.86	3.82	6.85	9.92	12.99

TABLE XXXIII

FLUIDIZATION CHARACTERISTICS OF 14 to 28 MESH UTAH COAL

The data below were taken in Run A-30, using the glass tube.

<u>Weight pounds</u>	<u>Mass Velocity lb per hr-sq ft</u>	<u>Depth of Dense Phase - inches</u>	<u>Total Depth* inches</u>	<u>Type of Fluidization</u>
1	656	4	7	Smooth
1	792	$4\frac{1}{4}$	10	"
1	886	$5\frac{1}{2}$	12	"
1	1020	6	13	"
2	475	$8\frac{1}{2}$	9	Channeling
2	552	9	12	Smooth
2	642	10	14	"
2	754	11	16	"
2	871	13	18	"
2	978	13	24	Slugging infrequently
3	469	11	14	Channeling
3	520	11	16	Slugging infrequently
3	635	14	21	Slugging, more frequently
3	758	16	26	Slugging, frequently
3	854	18	30	Slugging, frequently
3	1020	18	40	Slugging
4	461	17	22	Slugging
4	499	$17\frac{1}{2}$	24	"

*Including maximum depth of lean phase.

TABLE XXXIII CONTINUED

<u>Weight pounds</u>	<u>Mass Velocity lb per hr-sq ft</u>	<u>Depth of Dense Phase - inches</u>	<u>Total Depth inches</u>	<u>Type of Fluidization</u>
4	594	18	29	Slugging
4	716	18	33	"
4	810	21	38	"
4	911	25	46	"
4	1033	26	60	"

NET PRESSURE DROP

It was stated earlier (p13) that the 'net' pressure drop across a bed of fluidized solids is approximately equal to the head of solids. For example, in Run A-30, the following data were obtained:

Weight of bed: 3.0 pounds

Pressure drop across 0.500 inch orifice: 17.0 inches of
water

Pressure drop across bed: 9.0 inches of water

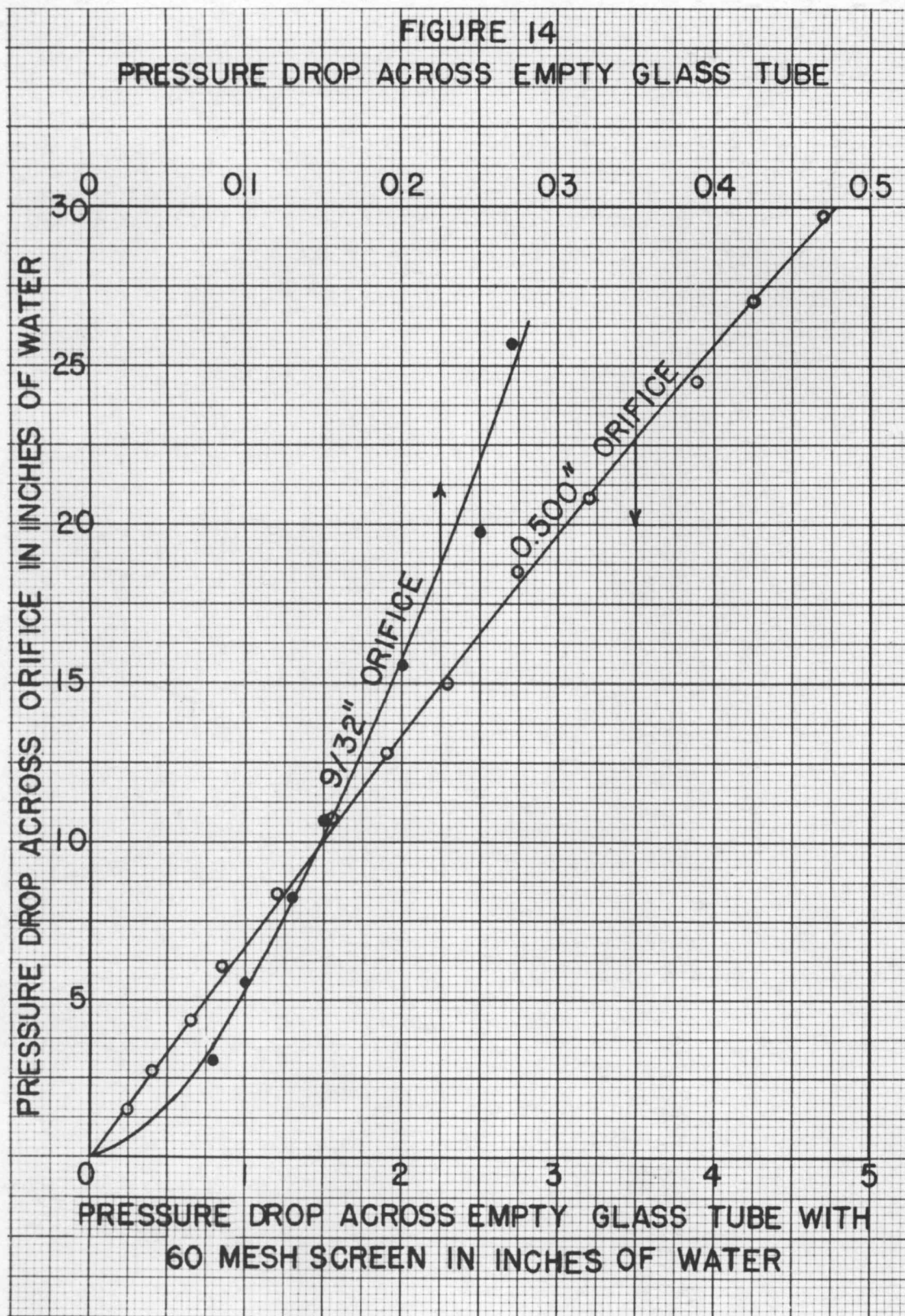
Mass Velocity: 758 lb per hr-sq ft

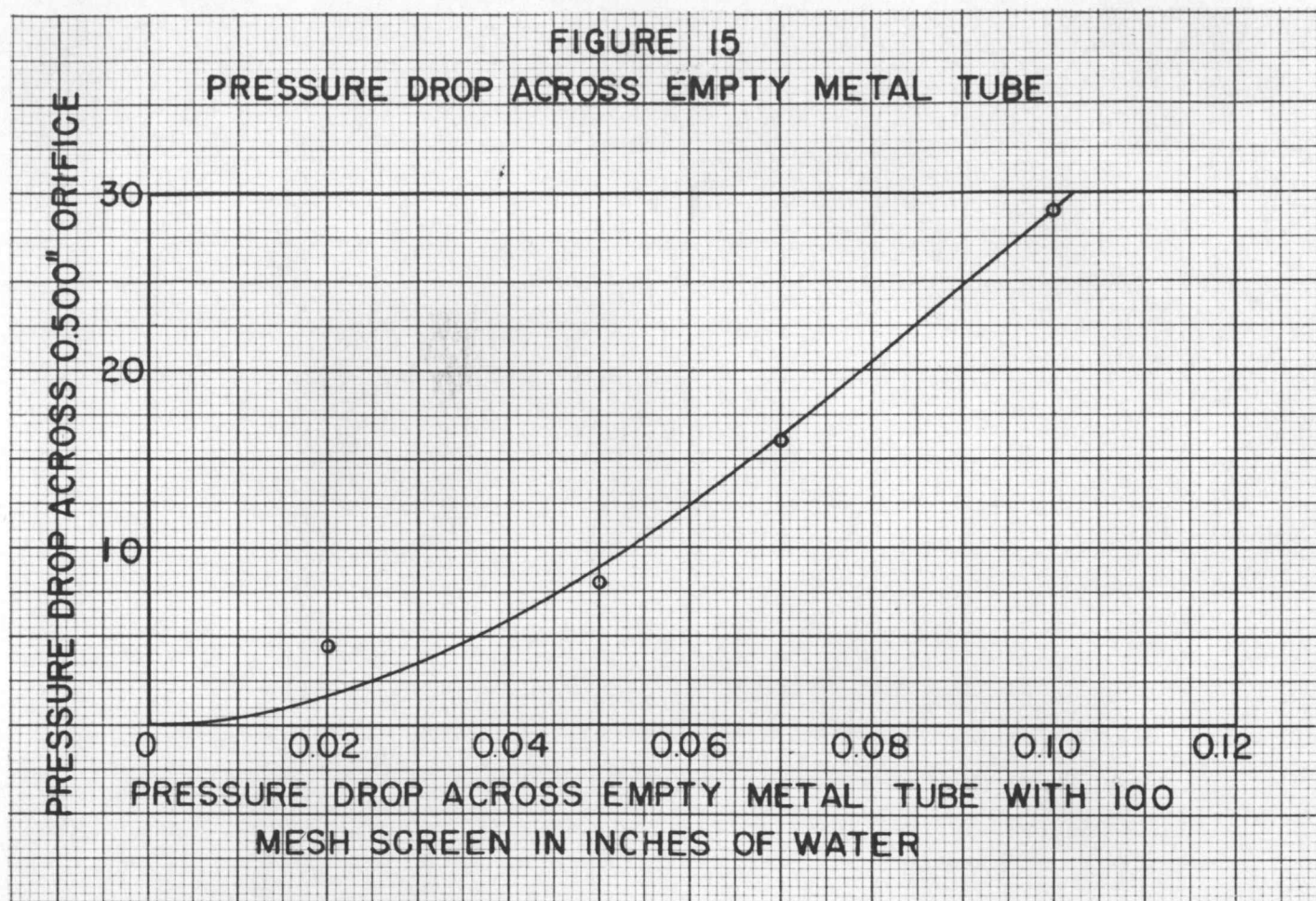
Referring to Figure 14, the pressure drop across the empty glass tube at this mass velocity was 2.6 inches of water. The net pressure drop was, therefore, 6.4 inches of water. One inch of water is equivalent to 0.0361 pounds per square inch of pressure or

$0.0361 (12.90) = 0.465$ pounds in the glass tube

The 6.4 inches of water was equivalent to

$6.4 (0.465) = 3.0$ pounds of solid in the tube





TYLER STANDARD SIEVES

TABLE XXXIV

<u>Mesh</u>	<u>Opening inches</u>
3	0.263
4	0.185
6	0.131
8	0.093
10	0.065
14	0.046
20	0.0328
28	0.0232
35	0.0164
48	0.0116
65	0.0082
100	0.0058
150	0.0041
200	0.0029

DENSITY OF PARTICLES

The density of the various solid particles was determined roughly by water displacement in a graduated cylinder. When the density was less than that of water, the particles were held beneath the surface by a piece of wire gauze.

TABLE XXXV

Material	Weight grams	Volume of Water before Particles Added - ml	Volume of Water after Particles added - ml	Density g per ml
Sand	74.0	43.0	71.7	2.58
Charcoal	8.1	45	67	0.37
Coal	30.0	51.2	76.8	1.17

APPARENT DENSITY OF PARTICLES

The apparent density of the various solid particles was determined by pouring them into a graduated cylinder slowly.

TABLE XXXVI

Material	Mesh	Volume ml	Weight grams	Apparent Density g per ml
3A Catalyst	-50+100	100	60.6	0.606
	-100+150	100	59.3	0.593
	-150+200	100	55.4	0.554
	-200+270	100	53.5	0.535
	-270	100	48.5	0.485
Sand	-20+28	4	5.6	1.40
	-28+48	100	153.8	1.54
	-48+65	100	147.0	1.47
	-65+80	15.5	22.0	1.42
	-80+100	17.7	24.9	1.41
	-100+150	5.8	7.9	1.36
	-150	1.3	1.3	1.0
Charcoal	-14+20	56	8.1	0.145
Coal	-4+8	100	67.4	0.674
	-8+14	100	68.7	0.687
	-14+28	100	63.1	0.631
	-28+48	100	58.2	0.582

AVERAGE PARTICLE SIZE

The average particle size was determined by the following formula:

$$(109) \quad x = \frac{100}{\sum \frac{f}{n}}$$

where

x = average particle size

f = volume per cent between two sieves

n = arithmetic average of adjacent sieve sizes

For example, Ottawa Standard Silica Sand had the following analysis

TABLE XXXVII

Average Size of Sand Particles

Mesh	Weight Grams	Volume* ml	f per cent	n inches	f/n
-20+28	5.6	4.0	0.7	0.0280	25
-28+48	611.9	398.5	70.6	0.0174	4060
-48+65	179.1	122.0	21.6	0.0099	2180
-65+80	22.0	15.5	2.8	0.0076	368
-80+100	24.9	17.7	3.1	0.0063	492
-100+150	7.9	5.8	1.0	0.0050	200
-150	1.3	1.3	0.2	0.0035	57
Totals	852.7	564.8	100.0		7380

The average particle size was

$$(110) \quad x = \frac{100}{7380} = 0.0135 \text{ inches}$$

which is equivalent to about 40 mesh.

*Using apparent density values from Table XXXVI

TABLE XXXVIII

Average Size of Charcoal Particles at Start of Run 5

Mesh	Weight grams	Volume* ml	f per cent	n inches	f/n
-8+10	5	37	1.1	0.079	14
-10+14	118	861	26.7	0.056	480
-14+16	164	1198	37.1	0.043	860
-16+20	134	930	28.8	0.036	800
-20+28	31	194	6.0	0.028	210
-28	2	10	0.3	0.012	25
Totals	454	3230	100.0		2390

$$(111) \quad x = \frac{100}{2390} = 0.042 \text{ inches}$$

TABLE XXXIX

Average Size of Charcoal Particles at End of Run 5

Mesh	Weight grams	Volume* ml	f per cent	n inches	f/n
-8+10	0	0	0	0.079	0
-10+14	13.0	95	15.4	0.056	280
-14+16	25.8	189	30.9	0.043	720
-16+20	27.2	189	30.9	0.036	860
-20+28	21.5	135	22.0	0.028	790
-28+50	0.7	3.6	0.6	0.017	35
-50	0.3	1.4	0.2	0.009	22
Totals	88.5	613.0	100.0		2710

$$(112) \quad x = \frac{100}{2710} = 0.037 \text{ inches}$$

The average at the end was equivalent to about 20 mesh.

*Using apparent density values from Table XXXVI

SPECIFIC HEAT OF UTAH COAL

The specific heat of coal was determined roughly by measuring the change in temperature when a weighed quantity of coal was added to a weighed quantity of hot water in a thermos bottle. The data are given below

TABLE XL

<u>Weight of</u> <u>Coal Grams</u>	<u>Temp of</u> <u>Coal °C</u>	<u>Weight of</u> <u>Water grams</u>	<u>Temp of</u> <u>water °C</u>	<u>Temp of</u> <u>Mixture °C</u>	<u>Specific</u> <u>Heat</u>
100.0	33.4	277.9	52.8	50.9	0.302
150.0	32.8	196.4	66.65	60.4	0.297

STEADY STATE RUNS WITH EMPTY TUBE

TABLE XLI

Run A-26

Room temperature: 72° F

Orifice: 0.500 inch diameter

Pressure drop across orifice: 6.3 in. of water

Pressure upstream of orifice: 0.9 in. of mercury

Potentiometer readings:

Thermocouple	1	2	4	5	6	7	8
Millivolts	0.12	9.11	8.41	8.29	8.13	8.09	7.44
Thermocouple	9	10	11	12	13	14	17
Millivolts	7.26	-	-	7.04	4.99	7.87	8.63
Thermocouple	16 ^a	0"	$\frac{1}{4}$ "	$\frac{1}{2}$ "	$\frac{3}{4}$ "	1"	
Millivolts		3.39	2.15	1.52	0.93	0.64	
Thermocouple	16 ^{b†}	0"	$\frac{1}{4}$ "	$\frac{1}{2}$ "	$\frac{3}{4}$ "	1"	
Millivolts		2.34	1.79	1.22	0.80	0.60	

*Measurements made six inches above the screen and at each $\frac{1}{4}$ inch through the insulation radially, from the metal wall (0") to the outside (1").

†Measurements made 24 inches above the screen.

TABLE XLII

Run A-27

Room temperature: 76° F

Orifice: 0.500 inch diameter

Pressure drop across orifice: 6.2 in. of water

Pressure upstream of orifice: 0.9 in. of mercury

TABLE XLII CONTINUED

Potentiometer readings:

Thermocouple	1	2	4	5	6	7	8
Millivolts	0.18	9.71	-	8.89	8.87	8.86	7.84
Thermocouple	9	10	11	12	13	14	17
Millivolts	7.79	5.72	6.45	7.18	5.15	8.61	8.94
Thermocouple	16a*	0"	$\frac{1}{4}$ "	$\frac{1}{2}$ "	$\frac{3}{4}$ "	1"	
Millivolts		3.30	2.43	1.74	1.13	0.91	
Thermocouple	16b [†]	0"	$\frac{1}{4}$ "	$\frac{1}{2}$ "	$\frac{3}{4}$ "	1"	
Millivolts		3.04	2.30	1.57	1.04	0.79	
Thermocouple	16c [‡]	0"	$\frac{1}{4}$ "	$\frac{1}{2}$ "	$\frac{3}{4}$ "	1"	
Millivolts		2.73	1.99	1.40	0.86	0.63	

*Measurements made four inches above the screen.

†Measurements made nine inches above the screen.

‡Measurements made eighteen inches above the screen.

TABLE XLIII

Run A-28

Room temperature: 73° F

Orifice: 0.500 inch diameter

Pressure drop across orifice: 6.2 inches of water

Pressure upstream of orifice: 0.9 inches of mercury

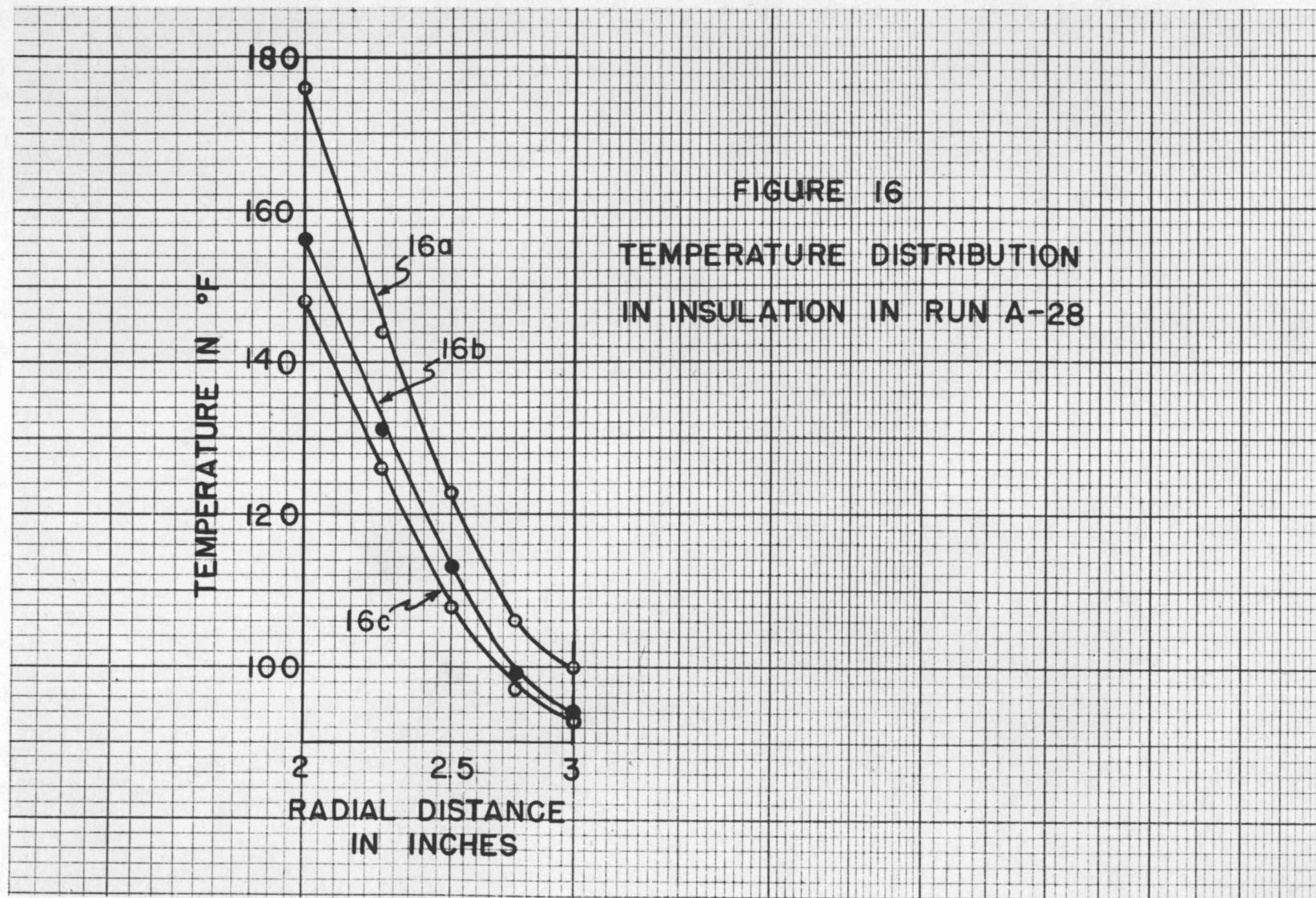
TABLE XLIII CONTINUED

Potentiometer readings:

Thermocouple	1	4	5	6	7	8
Millivolts	0.19	7.78	7.72	7.64	7.64	6.79
Thermocouple	9	10	11	12	13	14
Millivolts	6.60	4.89	5.54	6.26	4.57	7.41
Thermocouple	16 _a *	0"	$\frac{1}{4}$ "	$\frac{1}{2}$ "	$\frac{3}{4}$ "	1"
Millivolts		3.11	2.17	1.53	1.04	0.85
Thermocouple	16 _b [†]	0"	$\frac{1}{4}$ "	$\frac{1}{2}$ "	$\frac{3}{4}$ "	1"
Millivolts		2.52	1.79	1.24	0.84	0.70
Thermocouple	16 _c [‡]	0"	$\frac{1}{4}$ "	$\frac{1}{2}$ "	$\frac{3}{4}$ "	1"
Millivolts		2.29	1.63	1.10	0.77	0.66

Figure 16 is a plot of the insulation temperatures in Run A-28. The radial distances are plotted on a logarithmic scale.

* † ‡ Same location as Run A-27



CALCULATION OF FILM COEFFICIENT BETWEEN THE OUTSIDE OF THE INSULATION AND THE ROOM

Under steady state conditions, the heat which flows into the insulation flows into the room. Expressed in equation form

$$(113) \quad h_r A_r \Delta_r = \frac{K_i A_i \Delta_i}{1}$$

where Δ_r is the temperature difference between the outside of the insulation and room temperature and Δ_i is the temperature difference between the inside of the insulation and some point in the insulation, in this case the point. Using the data of 16c in Run A-28 as an example:

$$(114) \quad h_r = \frac{0.041(12)(2.5-2.0)(148-108)}{\frac{1}{2}(3) \ln \left(\frac{2.5}{2.0} \right) (93-73)}$$

$$= 1.47 \text{ Btu per hr-sq ft} - ^\circ\text{F}$$

The results for the other two points of Run A-28 and for Runs A-26 and A-27 are presented below:

TABLE XLIV

Film Coefficient between Outside of Insulation and Room

<u>Run</u>	<u>16a</u>	<u>16b</u>	<u>16c</u>
A-26	2.35	1.51	-
A-27	1.56	1.84	2.21
A-28	1.45	1.51	1.47

The average was 1.8, the figure used in earlier calculations.

UNSTEADY STATE RUN WITH EMPTY TUBE

TABLE XLV

RUN A-31

Room temperature: 71° F

Duration of heating cycle: 140 minutes

Orifice: 0.500 inch diameter

Orifice and heater data:

<u>Time</u> <u>Minutes</u>	<u>Air Bleed</u> <u>°F</u>	<u>TC-1</u> <u>°F</u>	<u>P₁ in.</u> <u>mercury</u>	<u>ΔP in.</u> <u>water</u>	<u>Heater</u> <u>Voltage</u>
0	107	93	-	-	99
6	-	-	-	11.4	-
20	107	101	1.4	11.4	99
50	108	103	-	-	-
90	108	104	-	-	-
146	109	105	-	-	-

Potentiometer readings:

TC-4		TC-5		TC-7		TC-10		TC-11	
<u>Time</u>	<u>mv</u>	<u>Time</u>	<u>mv</u>	<u>Time</u>	<u>mv</u>	<u>Time</u>	<u>mv</u>	<u>Time</u>	<u>mv</u>
2:55*	7.51	1:30	7.26	4:20	7.34	4:55	2.28	35:40	5.14
8:50	7.29	7:45	7.27	9:50	7.21	10:20	3.30	47:20	5.28
14:15	7.20	12:55	7.20	15:15	7.08	16:10	3.80	74:30	5.31
30:00	7.14	25:20	7.09	28:00	7.07	32:00	4.34		
47:50	7.19	43:10	7.16	45:00	7.07	45:50	4.58		
70:50	7.19	69:00	7.14	58:20	7.22	53:30	4.68		
87:30	7.12	85:00	7.15	72:20	7.11	72:50	4.76		
109:20	7.19	108:10	7.15	89:00	7.01	88:30	4.80		
137:10	7.19	136:10	7.16	110:40	7.11	104:50	4.81		
				139:00	7.14	138:20	4.84		

* Time in minutes and seconds after the start

TABLE XLV CONTINUED

TC-12		TC-13		TC-14		TC-15*		TC-16†	
Time	mv	Time	mv	Time	mv	Time	mv	Time	mv
2:07	3.64	0:59	0.74	0:23	5.09	3:30	0.44	5:20	0.51
8:30	5.29	7:25	2.64	6:45	6.87	9:25	1.14	10:50	0.95
13:45	5.54	12:20	3.08	11:40	6.89	14:50	1.53	16:30	1.25
29:00	5.76	26:30	3.63	23:30	6.80	30:40	2.00	32:30	1.61
43:10	5.95	39:30	3.86	24:40	6.85	44:30	2.20	46:20	1.80
52:10	6.01	51:20	4.04	40:30	6.96	52:40	2.26	54:00	1.89
70:00	6.00	68:30	4.19	66:30	6.93	71:30	2.37	73:20	1.99
84:30	6.04	82:40	4.25	83:30	6.96	87:00	2.41	89:50	2.06
103:30	5.99	101:30	4.23	107:10	6.92	104:10	2.44	105:40	2.07
132:30	6.07	131:20	4.31	135:10	6.98	133:00	2.46	133:40	2.10

*Located at inside of insulation four inches above the screen.

†Located at inside of insulation nine inches above the screen.

UNSTEADY STATE RUNS WITH COAL

TABLE XLVI

Run 9 - Heating Run on Utah Coal

Material Fluidized: Utah hard coal

Weight at start: 2.00 pounds

Weight at end: 1.93 pounds (The loss was apparently by volatilization).

Tyler Standard Screen Analyses:

	<u>Start</u>	<u>End</u>
-14 + 28 mesh	2.00	1.87
-28 + 48 mesh	0	0.05
-48 mesh	0	0.01
	<u>2.00 lb</u>	<u>1.93 lb</u>

Room temperature: 82° to 83° F

Duration of heating cycle: 90 minutes

Duration of cooling cycle: 47 minutes

Average weight of coal in bed during heating cycle: 1.98 lb

Approximate depth of dense phase: 10 inches

Approximate depth of lean phase: 4 inches

Fluidization: Infrequent slugging

Orifice and heater data:

<u>Time</u> <u>minutes</u>	<u>Air Bleed</u> <u>°F</u>	<u>TC-1</u> <u>°F</u>	<u>P₁ in.</u> <u>mercury</u>	<u>ΔP in.</u> <u>water</u>	<u>Heater</u> <u>Voltage</u>
7	-	-	1.8	11.4	99
16	119	111	-	-	-
25	119	111	-	11.4	100
47	122	113	1.8	11.4	99
81	126	115	-	-	-

Potentiometer readings:

TC-4		TC-5		TC-7		TC-10		TC-11	
Time	mv	Time	mv	Time	mv	Time	mv	Time	mv
1:30	6.77	3:20	3.71	4:45	4.34	0:20	0.48	15:00	5.90
9:50	7.34	11:20	5.84	5:55	4.79	9:20	5.10	33:50	6.62
19:30	7.39	20:40	6.58	12:40	5.98	18:45	6.08	54:15	6.76
28:40	7.49	30:30	6.91	21:45	6.57	27:50	6.47	76:00	6.92
37:45	7.25	39:25	6.87	31:45	6.88	37:15	6.57		
48:25	7.42	49:30	6.97	40:45	6.83	47:50	6.65		
60:20	7.53	61:45	7.13	50:50	6.98	59:40	6.76		
68:20	7.57	71:50	7.17	62:50	7.09	69:30	6.85		
72:40	7.57	85:10	7.22	86:20	7.19	84:00	6.89		
82:00	7.58								

TC-12		TC-13		TC-14		TC-15*		TC-16 [†]	
Time	mv	Time	mv	Time	mv	Time	mv	Time	mv
2:50	3.00	17:30	4.13	8:40	4.58	2:15	0.30	5:10	1.23
12:10	5.52	35:05	5.00	14:05	5.91	10:40	2.16	13:20	2.20
21:10	6.19	54:50	5.29	23:25	6.44	20:10	2.91	22:45	2.74
31:15	6.54	73:40	5.49	33:10	6.64	29:30	3.25	32:15	3.04
40:10	6.51			43:00	6.64	38:45	3.40	41:50	3.19
50:10	6.65			53:40	6.82	49:00	3.52	52:00	3.29
62:20	6.75			64:40	6.92	61:10	3.61	63:45	3.39
72:40	6.81			87:50	7.03	74:00	3.71	74:30	3.44
77:00	6.84					84:30	3.71	88:40	3.36
86:00	6.85								

*TC-15 located at inside of insulation four inches above the screen.

†TC-16 located at inside of insulation nine inches above the screen.

TABLE XLVII

Run 9 - Heat Flow Rate Equations

$$(115) \quad q_a = \frac{635(12.40)(0.240)(t_7 - t_4)}{144} = -13.1(t_4 - t_7)$$

$$(116) \quad q_s = 1.98(0.300) \frac{dT}{d\theta} = 0.594 \frac{dT}{d\theta}$$

$$(117) \quad q_m = [1.08(0.12) + 0.25(0.094)] \frac{dt_{10}}{d\theta} = 0.153 \frac{dt_{10}}{d\theta}$$

$$(118) \quad q_i = \frac{2 \pi (14) (0.041) (t' - t'')}{12 (2.30) \log \frac{2.25}{2.00}} = 2.55 (t' - t'')$$

$$(119) \quad q_i + q_m = h_w \frac{3.97 \pi (14) \Delta_w}{144} = h_w (1.21) \Delta_w$$

TABLE XLVIII

Run 9 - Rate of Heating of Metal

<u>Time minutes</u>	<u>(1) $\frac{dt_{10}}{d\theta}$ $\frac{60}{F}$ per min</u>	<u>q_m Btu per hr</u>
1	28.0	258
2	23.5	216
3	21.4	196
4	18.2	167
5	15.8	145
6	13.7	126
8	10.3	95
10	7.2	66
12	4.4	40
14	3.0	28
16	2.15	20
18	2.10	19
20	1.73	16
25	1.18	11
30	0.62	$5\frac{1}{2}$

TABLE XLVIII CONTINUED

Run 9 - Rate of Heating of Metal

Time minutes	$\frac{(1)}{(60)} \frac{dt_{10}}{dt}$ °F per min	q_m Btu per hr
35	0.135	1
40	0.24	2
45	0.32	3
50	0.36	$3\frac{1}{2}$
55	0.35	3
60	0.33	3
65	0.29	$2\frac{1}{2}$
70	0.22	2
75	0.14	$1\frac{1}{2}$
80	0.10	1
85	0.07	$1\frac{1}{2}$
90	0.05	$1\frac{1}{2}$

TABLE XLIX

Run 9 - Flow of Heat into Insulation

Interval	Time minutes	t' °F	t'' °F	$t' - t''$ °F	q_i Btu per hr
1	0.93	81	81	0	0
2	1.86	85	81	4	10
3	2.79	98	83	15	38
4	3.72	108	89.2	18.8	48
5	4.65	114	94.2	19.8	50
6	5.59	120	98.7	21.3	54
7	6.51	125	103.0	22.0	56
8	7.44	130	106.9	23.1	59
9	8.37	134	110.5	23.5	60
10	9.30	138	114.0	24.0	61
11	10.2	142	117.3	24.7	63
12	11.2	146	120.2	25.8	66
13	12.1	150	123.6	26.4	67
14	13.0	154	126.7	27.3	70
15	14.0	158	129.8	28.2	72
16	14.9	160	132.9	27.1	69
17	15.8	161	135.0	26.0	66
18	16.8	162.5	136.8	25.7	65
19	17.7	164	138.7	25.3	64

TABLE XLIX CONTINUED

Run 9 - Flow of Heat into Insulation

<u>Interval</u>	<u>Time minutes</u>	<u>t'*</u> °F	<u>t''</u> °F	<u>t'-t''</u> °F	<u>q_i</u> Btu per hr
20	18.6	165.5	140.0	25.5	65
21	19.5	167	141.7	25.3	64
22	20.5	169	143.0	26.0	66
23	21.4	170	144.6	25.4	65
24	22.3	171	145.4	25.6	65
25	23.2	172.5	146.9	25.6	65
26	24.2	174	148.1	25.9	66
27	25.1	175	149.2	25.8	66
28	26.0	176	150.2	25.8	66
29	27.0	177	151.1	25.9	66
30	27.9	178	152.0	26.0	66
35	32.6	183	-	-	-
40	37.2	185	-	-	-
45	41.9	187	-	-	-
50	46.5	189	-	-	-
60	55.7	192	-	-	-
70	65.0	194	-	-	-
80	74.4	195	-	-	-
90	83.7	196	-	-	-
∞	∞	197	169.5	27.5	70

*t' = t₁₅.

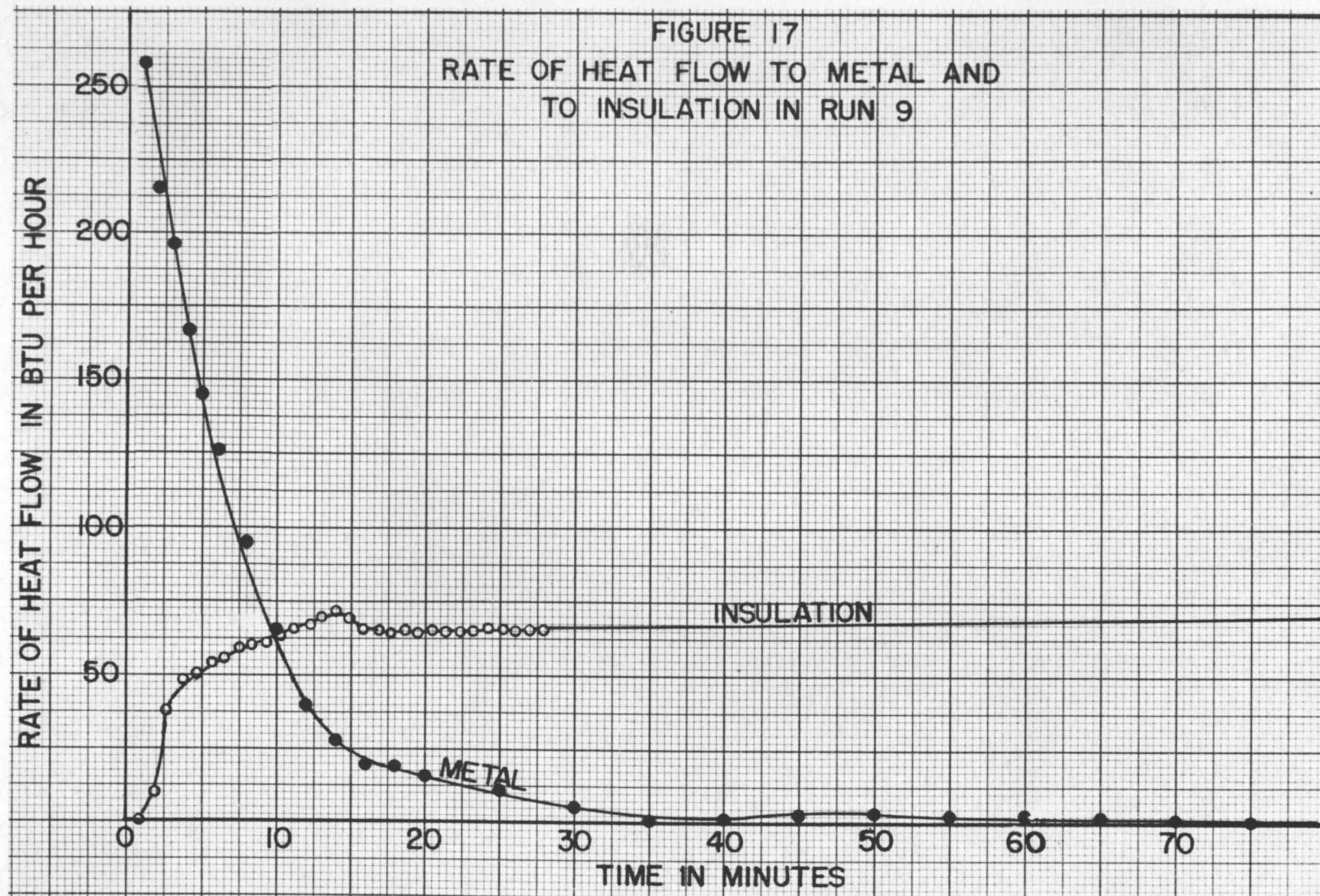


TABLE L

Run 9 - Coefficient of Heat Transfer between
Air and Tube Wall

Time minutes	$q_i + q_m$ Btu per hr	$t_4 - t_{12}^*$ °F	$t_7 - t_{10}$ °F	Δ_W °F	h_w Btu per hr- sq ft - °F
2	229	147	30	73.8	2.6
4	215	109	30	61.2	2.9
6	180	90	26	51.5	2.9
8	155	78	20	42.7	3.0
10	129	69	15	35.4	3.0
12	107	61	11	29.2	3.0
14	100	54	9	25.2	3.3
16	86	49	9	23.6	3.0
18	83	44.6	9.2	21.8	3.1
20	81	41.2	9.5	21.6	3.1
25	77	35.1	9.4	19.5	3.3
30	$71\frac{1}{2}$	31.4	9.5	18.4	3.2
35	67	24.3	9.5	15.7	3.5
40	68	25.8	7.5	14.8	3.8
45	69	28.2	7.6	15.7	3.6
50	71	28.5	8.2	16.3	3.6
55	$70\frac{1}{2}$	27.7	8.3	16.1	3.6
60	71	26.0	8.0	15.3	3.8
65	$71\frac{1}{2}$	24.9	7.5	14.5	4.1
70	71	24.3	7.1	14.0	4.2
75	71	23.3	7.0	13.6	4.3
80	71	22.5	6.8	13.1	4.5
85	$70\frac{1}{2}$	22.0	6.8	12.9	4.5
90	$70\frac{1}{2}$	21.7	6.8	12.9	4.5

Although there was an upward trend with time, the values of the coefficient of heat transfer between the air and the metal wall were generally lower than those in Run 11.

*Because of the small difference between t_{10} and t_{12} , the latter is used here.

TABLE LI

Run 10 - Heating Run on Utah Coal

Material fluidized: Utah hard coal

Weight at start: 2.00 pounds

Weight at end: 1.94 pounds (The loss was apparently due to volatilization)

Tyler standard screen analyses:

	<u>Start</u>	<u>End</u>
-8 +14 mesh	0	0.02
-14+28 mesh	2.00	1.87
-28+48 mesh	0	0.04
-48 mesh	0	0.01

Room Temperature: 84°F 2.00 lb 1.94 lb

Duration of heating cycle: 45 minutes

Average weight of coal in bed: 1.97 pounds

Approximate depth of dense phase: 10 inches

Approximate depth of lean phase: 4 inches

Fluidization: Some slugging but not severe

Orifice and heater data:

<u>Time</u> <u>minutes</u>	<u>Air Bleed</u> <u>°F</u>	<u>TC-1</u> <u>°F</u>	<u>P1 in.</u> <u>mercury</u>	<u>ΔP in.</u> <u>water</u>	<u>Heater</u> <u>Voltage</u>
0	116	104	-	-	-
9	-	-	1.9	11.3	98
20	116	111	-	11.4	98
30	-	-	1.9	11.4	97
36	116	112	-	11.4	97

Potentiometer readings:

TC-4		TC-5		TC-7		TC-10		TC-11	
Time	mv	Time	mv	Time	mv	Time	mv	Time	mv
2:45	5.57	3:50	3.09	1:30	1.59	11:05	4.56	0:30	0.52
6:30	6.11	7:45	4.38	5:20	3.64	17:45	5.39	4:50	3.13
14:35	6.68	15:45	5.57	13:35	5.30	28:00	6.03	13:05	4.99
20:40	6.97	24:45	6.26	22:30	6.10	43:40	6.35	22:00	5.80
32:00	7.10	33:10	6.56	30:50	6.47			30:30	6.19
39:40	7.10	40:40	6.66	38:50	6.58			39:20	6.34

TC-12		TC-13		TC-14		TC-15*		TC-16	
Time	mv	Time	mv	Time	mv	Time	mv	Time	mv
11:50	4.73	7:15	2.08	10:25	3.47	2:10	0.67	3:10	0.53
15:15	5.15	25:20	4.27	17:05	5.54	5:59	1.34	8:20	0.94
26:50	5.97	42:40	4.89	26:05	6.12	14:00	2.31	16:50	1.61
32:45	6.17			34:45	6.43	23:00	2.88	24:20	1.96
44:00	6.34			43:10	6.47	31:30	3.21	34:10	2.36
						40:20	3.39	41:30	2.47

*Located at inside of insulation four inches above the screen.

TABLE LII

Run 10 - Heat Flow Rate Equations

$$(120) \quad q_a = \frac{638(12.40)(0.240)(t_7 - t_4)}{144} = -13.2(t_4 - t_7)$$

$$(121) \quad q_s = 1.97(0.300) \frac{dT}{d\theta} = 0.591 \frac{dT}{d\theta}$$

$$(122) \quad q_m = [1.08(0.12) + 0.25(0.094)] \frac{dt_{11}}{d\theta} = 0.153 \frac{dt_{11}}{d\theta}$$

$$(123) \quad q_i = \frac{2\pi 14(0.041)(t' - t'')}{12(2.30) \log \frac{2.25}{2.00}} = 2.55(t' - t'')$$

$$(124) \quad q_i + q_m = h_w \frac{3.97\pi(14)}{144} \Delta_w = h_w(1.21) \Delta_w$$

TABLE LIII

Run 10 - Rate of Heating of Metal

Time minutes	$\left(\frac{1}{60}\right) \frac{dt_{11}}{d\theta}$ °F per min	q_m Btu per hr
1	19.7	181
2	26.5	244
3	19.5	179
4	16.8	155
5	14.1	130
6	11.6	117
8	8.1	$74\frac{1}{2}$
10	6.05	$55\frac{1}{2}$
12	5.35	49
14	3.80	35
16	3.25	30
18	2.76	$25\frac{1}{2}$
20	2.69	25

TABLE LIII CONTINUED

Run 10 - Rate of Heating of Metal

<u>Time minutes</u>	$\left(\frac{1}{60} \right) \frac{dt_{11}}{d\theta}$ <u>°F per min</u>	q_m <u>Btu per hr</u>
25	1.71	16
30	1.01	$9\frac{1}{2}$
35	0.53	5
40	0.37	$3\frac{1}{2}$
45	0.10	1

TABLE LIV

Run 10 - Flow of Heat into Insulation

<u>Interval</u>	<u>Time minutes</u>	t' <u>°F</u>	t'' <u>°F</u>	$t' - t''$ <u>°F</u>	q_i <u>Btu per hr</u>
1	0.93	86	84	2	5
2	1.86	91	85	6	15
3	2.79	95	87.3	7.7	20
4	3.73	102	89.5	12.5	32
5	4.65	108	93.2	14.8	38
6	5.59	115	96.8	18.2	46
7	6.51	119	101.0	18.0	46
8	7.44	124	104.0	20.0	51
9	8.37	128	107.5	20.5	52
10	9.30	133	110.6	22.4	57
11	10.2	136	114.4	21.6	55
12	11.2	139	117.0	22.0	56
13	12.1	142	120.0	22.0	56
14	13.0	145	122.3	22.7	58
15	14.0	149	124.9	24.1	62
16	14.9	151	127.5	23.5	60
17	15.8	153	129.8	23.2	59
18	16.8	155	131.6	23.4	60
19	17.7	157	133.5	23.5	60
20	18.6	159	135.3	23.7	60
21	19.5	161	137.3	23.7	60
22	20.5	163	139.0	24.0	61
23	21.4	165	140.5	24.5	62
24	22.3	167	142.2	24.8	63
25	23.2	168	144.0	24.0	61
26	24.2	170	145.1	24.9	63

TABLE LIV CONTINUED

Run 10 - Flow of Heat into Insulation

Interval	Time minutes	$t'_{\text{O F}}^*$	$t''_{\text{O F}}$	$t' - t''_{\text{O F}}$	q_i Btu per hr
27	25.1	172	147.0	25.0	64
28	26.0	173	148.0	25.0	64
29	27.0	175	149.1	25.9	66
30	27.9	176	150.4	25.6	65
35	32.6	180	151.7	-	-
40	37.2	183	155.5	-	-
45	41.9	185	158.5	-	-
∞	∞	188	163.4	24.6	63

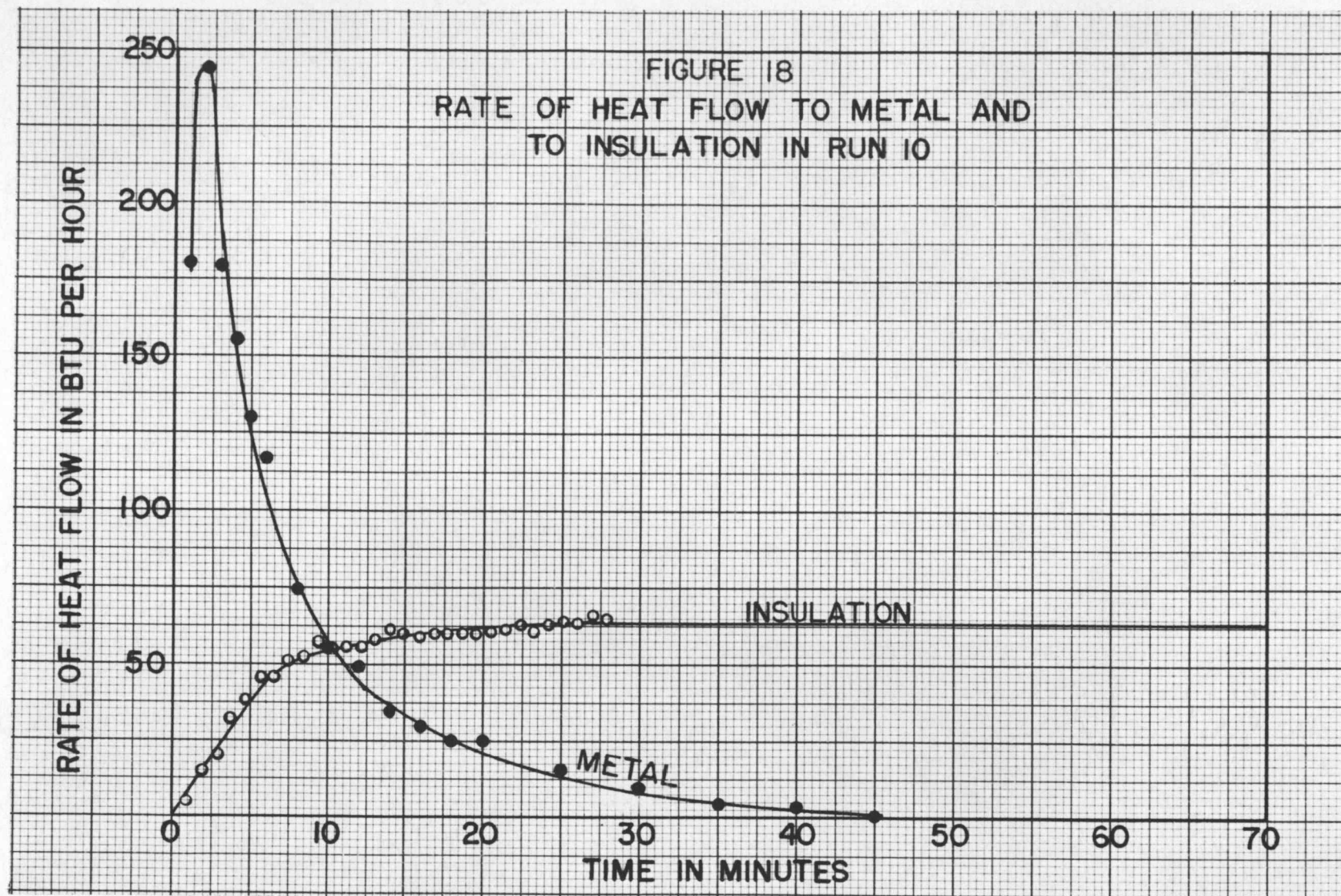
TABLE LV

Run 10 - Coefficient of Heat Transfer between
Air and Tube Wall

Time minutes	$q_i + q_m$ Btu per hr	$t_4 - t_{12}$ O F	$t_7 - t_{10}$ O F	Δ_w O F	h_w Btu per hr- sq ft - O F
2	261	127	11	47.5	4.5
4	188	101	11	40.6	3.8
6	162	87	14	39.7	3.4
8	126	69	8	29.3	3.6
10	111	62	8	26.4	3.5
12	$106\frac{1}{2}$	59.5	11.0	28.8	3.1
14	94	54.1	11.1	27.2	2.9
16	90	48.4	10.5	24.9	3.0
18	$87\frac{1}{2}$	45.5	10.8	24.1	3.0
20	$87\frac{1}{2}$	42.2	10.4	22.8	3.2
25	80	36.1	11.1	21.2	3.1
30	$74\frac{1}{2}$	31.7	10.4	19.1	3.2
35	70	28.5	10.0	17.7	3.3
40	$68\frac{1}{2}$	26.0	9.6	16.5	3.4
45	66	24.1	8.8	15.2	3.6

Runs 9 and 10 were duplicates except for slight variations in heater voltage and air preheat time. Comparison

* $t' = t_{15}$



of the values of h_w for the two runs shows excellent agreement.

TABLE LVI

Run 12 - Heating Run on Utah Coal

Material fluidized: Utah hard coal which had been heated at 300° F for several hours and then cooled and kept in a desiccator.

Weight at start: 0.500 pounds

Weight at end: 0.498 pounds

Tyler standard screen analyses:

	<u>Start</u>	<u>End</u>
-8 + 14 mesh	0	0.006
-14+ 28 mesh	0.500	0.479
-28+ 48 mesh	0	0.011
-48 mesh	0	0.002
	<u>0.500 lb</u>	<u>0.498 lb</u>

Room temperature: 74° F

Duration of heating cycle: 60 minutes

Approximate depth of dense phase: 2 inches

Approximate depth of lean phase: 2 inches

Fluidization: Good

Orifice and heater data:

<u>Time</u> <u>minutes</u>	<u>Air Bleed</u> <u>°F</u>	<u>TC-1</u> <u>°F</u>	<u>P₁ in.</u> <u>mercury</u>	<u>ΔP in.</u> <u>water</u>	<u>Heater</u> <u>Voltage</u>
0	115	102	1.5	11.4	97
13	114	106	1.5	11.4	97
26	-	-	-	-	96
55	115	108	-	11.4	96

Potentiometer readings:

TC-4		TC-5		TC-6		TC-7		TC-12		TC-15*	
<u>Time</u>	<u>mv</u>	<u>Time</u>	<u>mv</u>	<u>Time</u>	<u>mv</u>	<u>Time</u>	<u>mv</u>	<u>Time</u>	<u>mv</u>	<u>Time</u>	<u>mv</u>
0:30	3.15	1:30	2.49	2:25	2.82	3:20	3.39	1:10	1.62	1:50	0.57
4:20	4.92	5:30	4.55	6:50	4.54	7:50	4.88	5:10	3.91	6:20	1.53
9:10	5.86	10:50	5.55	12:10	5.56	13:20	5.64	10:30	5.01	11:20	2.17
15:10	6.39	16:20	6.06	18:40	6.12	19:30	6.10	15:50	5.59	17:50	2.65
21:00	6.66	22:10	6.37	23:50	6.23	24:45	6.32	21:40	5.94	22:40	2.86
26:50	6.83	27:30	6.54	28:40	6.44	30:30	6.48	27:10	6.12	28:00	3.05
32:50	6.93	34:00	6.68	36:10	6.60	37:20	6.59	33:30	6.29	35:40	3.23
42:45	7.04	44:00	6.80	46:00	6.70	41:20	6.66	44:50	6.44	45:30	3.36
50:00	7.05	51:30	6.80	53:20	6.69	48:00	6.73	51:00	6.44	52:30	3.44
						59:50	6.70				

* Located at inside of insulation two inches above screen.

TABLE LVII.

Run 12 - Heat Flow Rate Equations

$$(125) \quad q_a = \frac{636(12.40)(0.240)(t_6 - t_4)}{144} = -13.1(t_4 - t_6)$$

$$(126) \quad q_s = 0.50(0.300) \frac{dT}{d\theta} = 0.150 \frac{dT}{d\theta}$$

$$(127) \quad q_m = \left[0.32(0.12) + 0.25(0.094) \right] \frac{dt_{12}}{d\theta} = 0.0619 \frac{dt_{12}}{d\theta}$$

$$(128) \quad q_i = \frac{2\pi(4)(0.041)(t' - t'')}{12(2.30) \log \frac{2.25}{2.00}} = 0.730(t' - t'')$$

$$(129) \quad q_i \quad q_m = h_w \frac{3.97\pi(4)}{144} \Delta_w = h_w(0.346) \Delta_w$$

TABLE LVIII

Run 12 - Rate of Heating of Metal

Time minutes	$\left(\frac{1}{60} \right) \frac{dt_{12}}{d\theta}$ °F per min	q_m Btu per hr
1	42.5	158
2	24.6	108
3	18.2	74
4	15.1	51
5	11.5	45
6	8.4	40
8	6.7	31
10	4.2	17
12	3.7	16
14	3.1	12
16	2.9	9
18	2.0	7
20	1.61	6

TABLE LVIII CONTINUED

Run 12 - Rate of Heating of Metal

<u>Time</u> <u>minutes</u>	$(\frac{1}{60}) \frac{dt_{12}}{d\theta}$ <u>°F per min</u>	q_m <u>Btu per hr</u>
25	1.08	4
30	0.79	3
35	0.61	2
40	0.40	1
45	0.21	1
50	0.03	0

TABLE LIX

Run 12 - Flow of Heat into Insulation

Interval	Time minutes	t' °F	t'' °F	$t' - t''$ °F	q_i Btu per hr
1	0.93	82	74	8	6
2	1.86	90	78	12	9
3	2.79	98	81.8	16.2	12
4	3.72	105	86.3	18.7	$13\frac{1}{2}$
5	4.65	112	90.6	21.4	$15\frac{1}{2}$
6	5.59	118	95.2	22.8	$16\frac{1}{2}$
7	6.51	124	99.5	24.5	18
8	7.44	128	104.0	24.0	$17\frac{1}{2}$
9	8.37	132	107.3	24.7	18
10	9.30	136	110.8	25.2	$18\frac{1}{2}$
11	10.2	140	114.0	26.0	19
12	11.2	143	117.3	25.7	19
13	12.1	146	120.0	26.0	19
14	13.0	149	122.7	26.3	19
15	14.0	152	125.1	26.9	$19\frac{1}{2}$
16	14.9	154	127.8	26.2	19
17	15.8	156	129.6	26.4	$19\frac{1}{2}$
18	16.8	158	131.6	26.4	$19\frac{1}{2}$
19	17.7	160	133.4	26.6	$19\frac{1}{2}$
20	18.6	162	135.2	26.8	$19\frac{1}{2}$
21	19.5	163.5	137.0	26.5	$19\frac{1}{2}$
22	20.5	165	138.3	26.7	$19\frac{1}{2}$
23	21.4	166.5	139.6	26.9	$19\frac{1}{2}$
24	22.3	168	141.2	26.8	$19\frac{1}{2}$
25	23.2	169	142.3	26.7	$19\frac{1}{2}$
30	27.9	174	-	-	-
35	32.6	178	-	-	-
40	37.2	181	-	-	-
45	41.9	183	-	-	-
50	46.5	184.3	-	-	-
55	51.2	185	-	-	-
∞	∞	186	159.4	26.6	$19\frac{1}{2}$

* $t' = t_{15}$

FIGURE 19
RATE OF HEAT FLOW TO METAL AND
TO INSULATION IN RUN 12

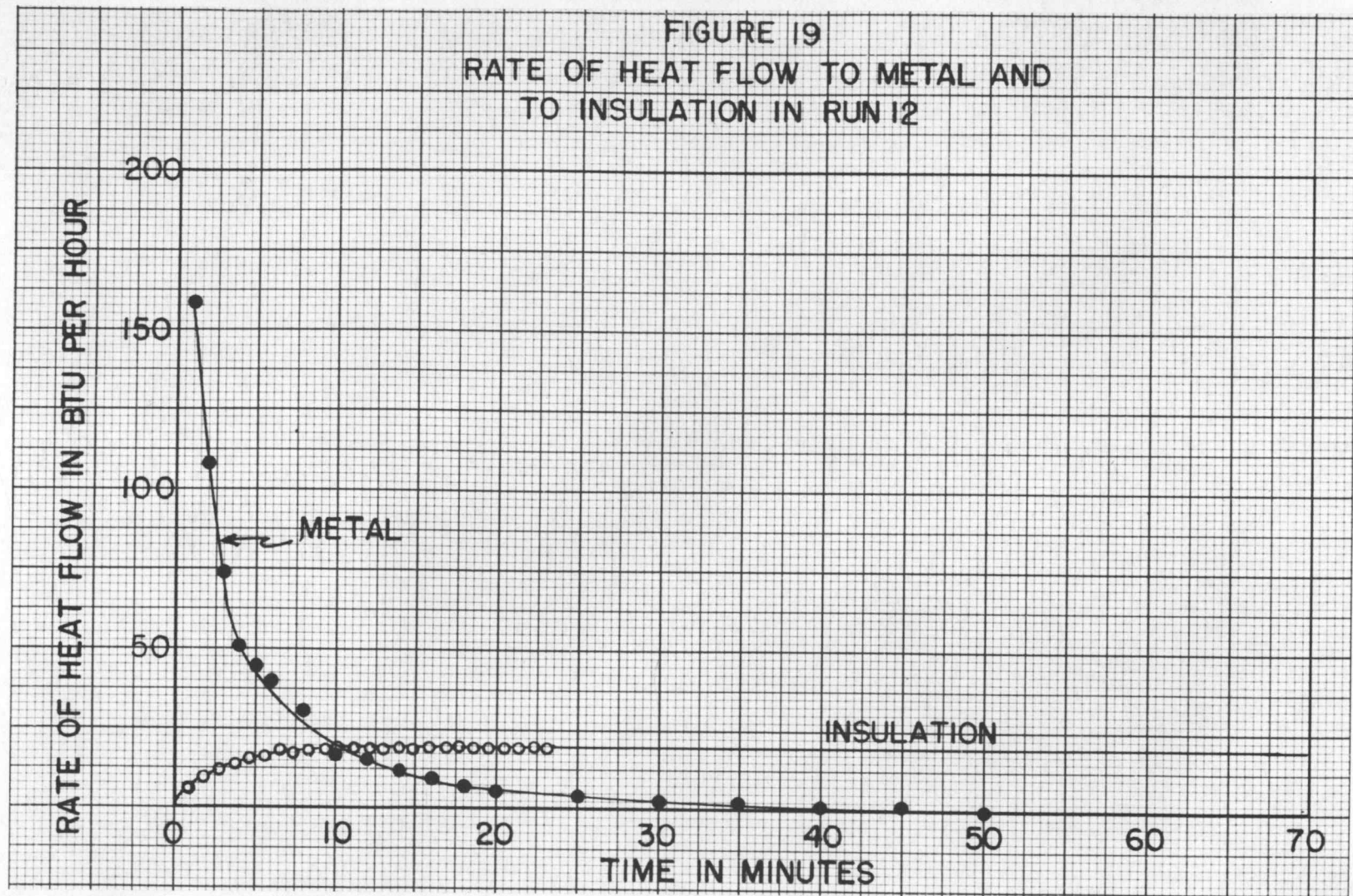


TABLE LX

Run 12 - Coefficient of Heat Transfer between
Air and Tube Wall

Time minutes	$q_i + q_m$ Btu per hr	$t_4 - t_{12}$ °F	$t_6 - t_{12}$ °F	Δ_w °F	h_w Btu per hr- sq ft - °F
2	118	55	5	20.9	16.3
4	66	42	7	19.6	9.7
6	57	38	7	21.9	7.5
8	49	38.3	9.5	20.7	5.8
10	36	32.5	8.0	17.5	5.9
12	35	31.2	10.0	17.8	5.7
14	31	29.0	10.4	18.1	4.9
16	$28\frac{1}{2}$	27.5	10.0	17.3	4.8
18	$26\frac{1}{2}$	25.5	9.0	15.9	4.8
20	$25\frac{1}{2}$	24.5	8.7	15.2	4.8
25	$23\frac{1}{2}$	23.2	8.5	14.7	4.6
30	$22\frac{1}{2}$	21.8	8.3	14.6	4.4
35	$21\frac{1}{2}$	21.1	8.0	13.4	4.6
40	$20\frac{1}{2}$	20.3	7.8	13.1	4.5
45	$20\frac{1}{2}$	19.5	7.5	12.6	4.7
50	$19\frac{1}{2}$	19.5	7.5	12.6	4.5

The large values of h_w in the first few minutes were probably due to inaccuracies resulting from the small weight of solids fluidized. However, the steady state value agreed with that found in Run 9, a run made at approximately the same mass velocity.

UNSTEADY STATE COOLING RUNS

In attempting to find the coefficient of heat transfer between the air and the solid particles, a cooling run was made, that is, after steady state had been reached in Run 9, cool air was introduced into the fluidized bed. Additional data not appearing in previous tables are given below.

TABLE LXI

Run 9 - Cooling Run on Utah Coal

Average mass velocity during cooling: 632 lb per hr-sq ft

Average weight of coal in bed during cooling: 1.94 lb

Potentiometer readings:

TC-4		TC-5		TC-7		TC-10		TC-11	
Time	mv	Time	mv	Time	mv	Time	mv	Time	mv
1:20	3.49	3:00	5.31	4:20	4.68	0:45	6.65	6:20	3.88
10:50	2.00	13:10	2.46	14:30	2.26	10:20	3.00	14:05	1.67
17:30	1.65	18:30	1.95	19:30	1.88	16:40	2.18		
25:00	1.46	26:40	1.61	28:00	1.54	24:30	1.71		
25:30	1.36	31:30	1.50	32:50	1.43	30:00	1.52		
40:05	1.26	42:10	1.34	42:40	1.28	40:30	1.32		

TC-12		TC-13		TC-14		TC-15		TC-16	
Time	mv	Time	mv	Time	mv	Time	mv	Time	mv
3:40	4.86	3:40	4.11	5:15	4.24	2:00	3.63	4:50	2.93
14:00	2.31	23:30	1.91	16:00	2.13	11:50	2.07	14:50	1.76
19:00	1.88			20:50	1.81	18:00	1.55	20:20	1.42
27:30	1.52			29:00	1.51	26:05	1.19	28:30	1.11
32:30	1.40			34:20	1.38	31:10	1.06	33:20	1.02
42:40	1.27			45:30	1.25	41:50	0.87	45:00	0.82

The heat flow rate equations were the same as for the heating part of the run except for the slight change in mass velocity and in the average weight fluidized, assuming that the small loss in weight was spread out over the entire run.

TABLE LXII

Run 9 - Heat Flow Rate Equations during Cooling

$$(130) \quad q_a = \frac{632(12.40)(0.240)(t_7 - t_4)}{144} = 13.1(t_7 - t_4)$$

$$(131) \quad q_s = 1.94(0.300) \frac{dT}{d\theta} = 0.582 \frac{dT}{d\theta}$$

$$(132) \quad q_m = 0.153 \frac{dt_{12}}{d\theta}$$

$$(133) \quad q_i = 2.55(t' - t'')$$

The method of calculation was the same as in the heating part of the run except that the Schmidt plot of insulation temperatures had the line representing steady state heat flow as a base, rather than room temperature. Tables LXIII, LXIV, and LXV give the values of q_a , q_m , and q_i , respectively, at various times. The last is also plotted in Figure 21.

TABLE LXIII

Run 9 - Rate of Heat Flow to Air during Cooling

<u>Time minutes</u>	<u>$t_7 - t_4$ °F</u>	<u>q_a Btu per hr</u>
1	83	1090
2	79	1035
3	72	930
4	63	825
6	48	630
8	36	470
10	28	370
12	22	290
14	17	220
16	14	185
18	11	145
20	9	120
25	7	90
30	6	80
35	4	50
40	2	25
45	0	0

TABLE LXIV

Run 9 - Rate of Heat Flow to Metal during Cooling

<u>Time minutes</u>	<u>$-\frac{1}{60} \frac{dt_{12}}{d\theta}$ °F per min</u>	<u>$-q_m$ Btu per hr</u>
1	20.2	185
2	17.8	163
3	16.0	147
4	14.2	130
6	11.3	104
8	7.8	71
10	5.8	53
12	4.7	43
14	4.0	37
16	3.2	29
18	2.6	24
20	2.0	18½
25	1.25	11½
30	0.90	8
35	0.70	6½
40	0.48	4½
45	0.05	½

TABLE LXV

Run 9 - Rate of Heat Flow to Insulation during Cooling

<u>Interval</u>	<u>Time</u> <u>minutes</u>	<u>t'*</u> <u>°F</u>	<u>t''</u> <u>°F</u>	<u>t'-t''</u> <u>°F</u>	<u>q_i</u> <u>Btu per hr</u>
1	0.93	186	161.4	24.6	63
2	1.86	183	161.4	21.6	55
3	2.79	180	160.0	20.0	51
4	3.72	175	158.8	16.2	41
5	4.65	172	155.8	16.2	41
6	5.59	167	154.2	12.8	33
7	6.51	163	151.9	11.1	28
8	7.44	159	148.6	10.4	26½
9	8.37	155	145.8	9.2	24
10	9.30	151	140.0	11.0	28
11	10.2	147	137.3	9.7	25
12	11.2	144	135.0	9.0	23
13	12.1	140	132.0	8.0	20
14	13.0	137	129.6	7.4	19
15	14.0	133	126.6	6.4	16
16	14.9	130	124.1	5.9	15
17	15.8	128	122.0	6.0	15
18	16.8	126	120.3	5.7	14½
19	17.7	124	118.6	5.4	14
20	18.6	122	116.7	5.3	13½
21	19.5	120	115.0	5.0	13
22	20.5	119	113.8	5.2	13
23	21.4	118	112.8	5.2	13
24	22.3	117	111.6	5.4	14
25	23.2	116	110.5	5.5	14
26	24.2	114	109.2	4.8	12
27	25.1	113	108.2	4.8	12
28	26.0	112	107.1	4.9	12½
29	27.0	111	106.2	4.8	12
30	27.9	110	105.5	4.5	11½
31	28.9	109	104.6	4.4	11
32	29.8	108	103.8	4.2	11
33	30.7	107.5	103.3	4.2	11
34	31.7	107	102.7	4.3	11
35	32.6	106	102.0	4.0	10

*t' = t₁₆, located at inside of insulation 9 inches above screen.

TABLE LXV CONTINUED

Run 9 - Rate of Heat Flow to Insulation during Cooling

<u>Interval</u>	<u>Time</u> <u>minutes</u>	<u>t'</u> <u>°F</u>	<u>t''</u> <u>°F</u>	<u>t' - t''</u> <u>°F</u>	<u>q_i</u> <u>Btu per hr</u>
40	37.2	103*	99	4	10
45	41.9	101*	97	4	10
50	46.5	99*	95	4	10

* Approximate values

On substituting into equation (6),

$$(6) \quad q_a + q_s + q_m + q_i = 0$$

the following values of q_s were obtained:

TABLE LXVI

Run 9 - Rate of Heat Flow to Solid during Cooling

<u>Time</u> <u>minutes</u>	<u>$-q_s$</u> <u>Btu per hr</u>
1	970
2	920
3	825
4	735
6	660
8	425
10	340
12	265
14	200
16	170
18	135
20	115
25	90
30	85
35	55
40	30
45	10

Figure 22 is a plot of Table LXVI. By taking the area under this curve, values of Q_s were obtained for various lengths of time. Substituting these into equation (76)

$$(134) \quad -Q_s = 1.94(0.300)(T-310)$$

the calculated average solid temperature, T , was found.

The results are given in Table LXVII.

Table LXVII

Run 9 - Solid Temperature during Cooling

<u>Time minutes</u>	<u>T °F</u>
2	255
4	206
6	165
8	134
10	112
12	95
14	81
16	70
18	61
20	$53\frac{1}{2}$
25	39
30	27
35	18
40	12
45	9
50	7

The temperatures are obviously too low although not as greatly in error as in the heating runs.

FIGURE 20
TIME - TEMPERATURE PLOT
OF COOLING CYCLE IN RUN 9

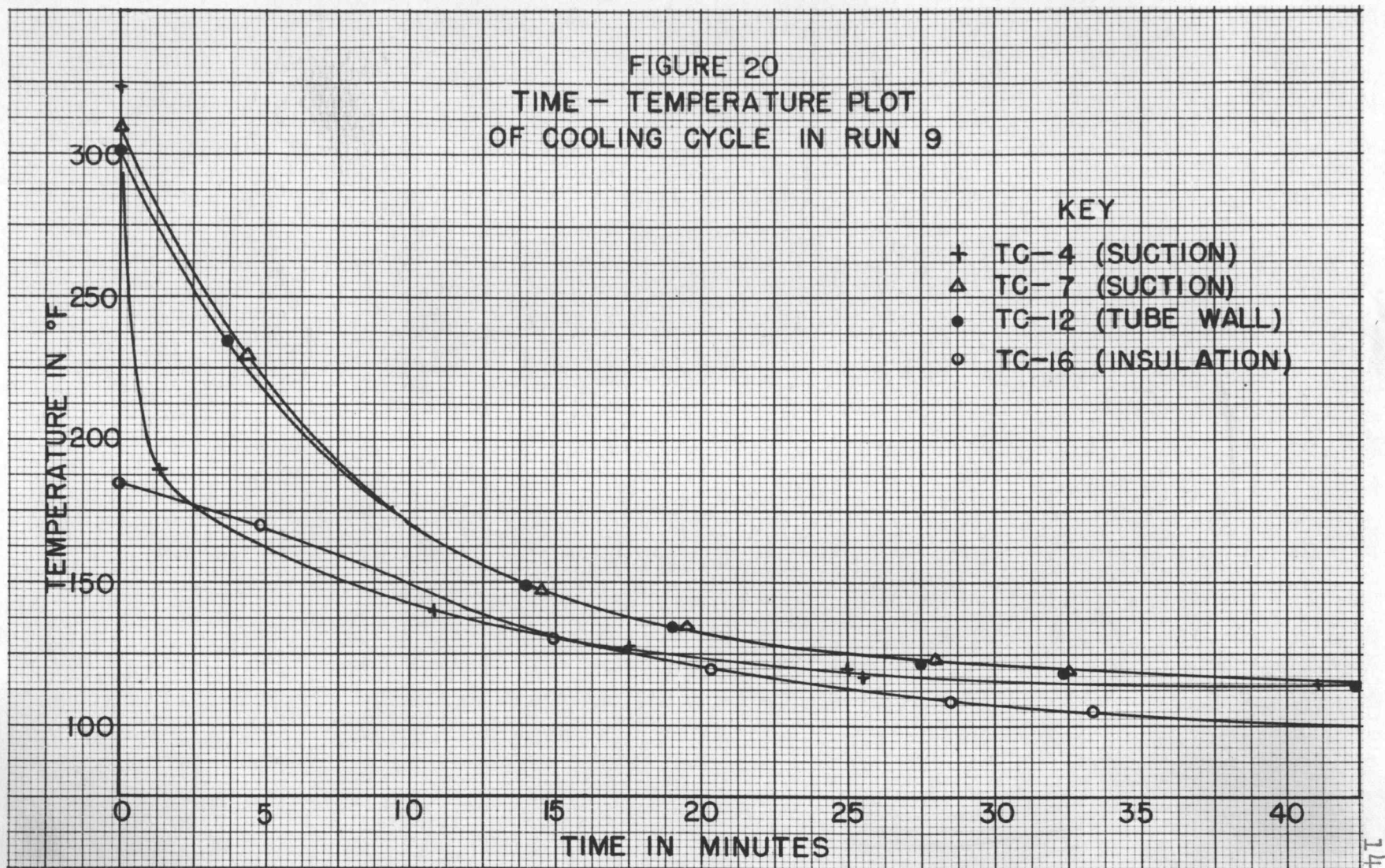


FIGURE 21
RATE OF HEAT FLOW TO INSULATION
DURING COOLING IN RUN 9

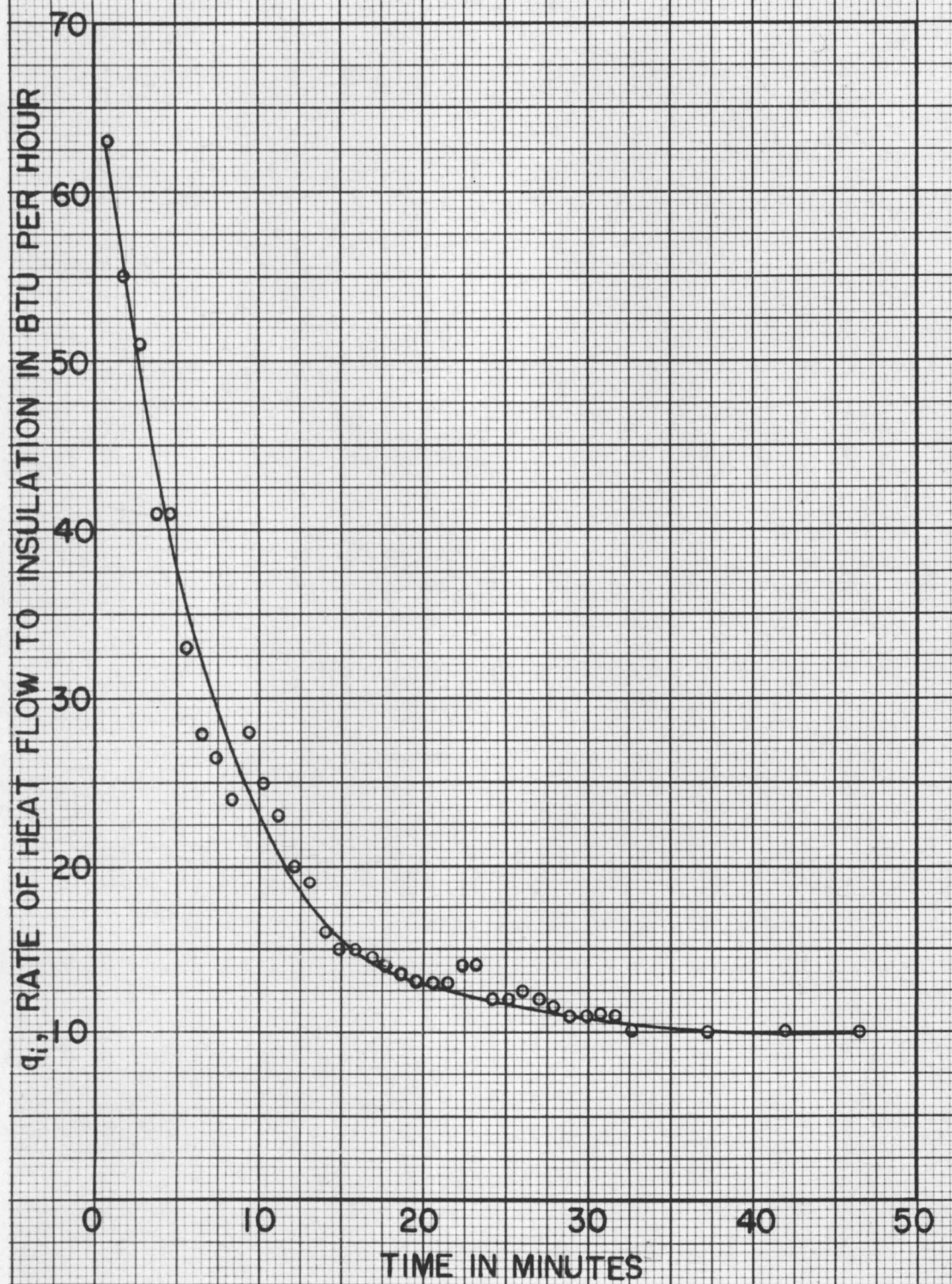
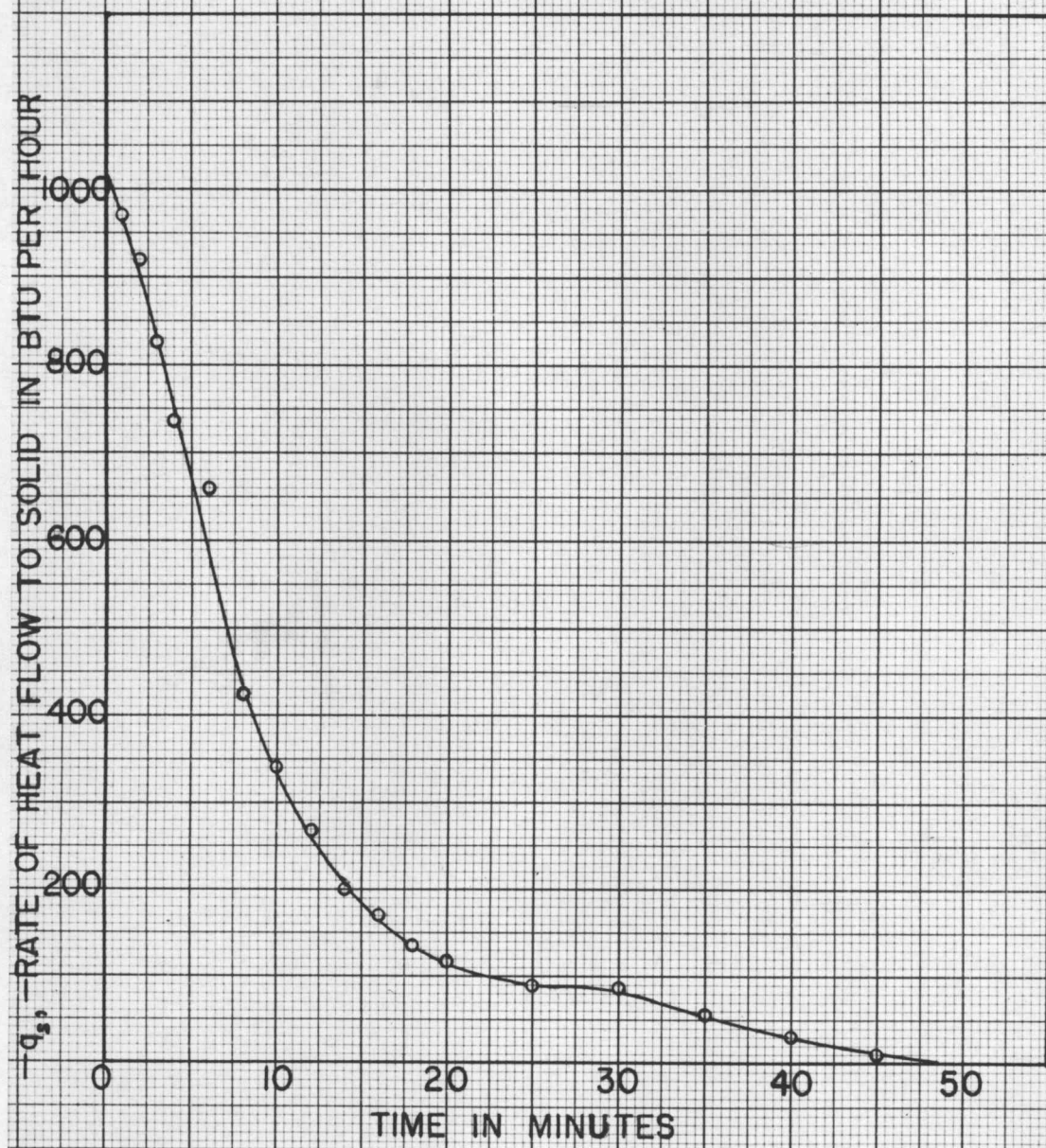


FIGURE 22
RATE OF HEAT FLOW TO SOLID
DURING COOLING IN RUN 9



SUCTION THERMOCOUPLE OPERATION

The air was drawn past the hot junction of the thermocouple at a rate which was high enough to reduce radiation errors to a negligible amount. Actually, the air velocity was probably higher than necessary. A rough calculation of this velocity follows using the vacuum pump flow rate of Run 11 and the area of the well given on p85.

$$(135) \quad \text{Velocity} = \frac{0.18(144)}{(60)(0.0154)} = 28 \text{ feet per second}$$

Although this quantity of air was small compared to the total mass velocity, it was cooled all the way to room temperature. As a result, the rate of heat loss was appreciable as shown below:

$$(136) \quad q = \frac{0.18(60)(0.075)(0.24)(300-70)}{3} = 15 \text{ Btu per hr}$$

This loss was calculated as if the suction were operating at all times whereas it was actually sucking air only about half the time. Note that three thermocouples are considered to be contributing to the loss.

TEMPERATURE DROP THROUGH THE METAL WALL

A calculation of the temperature drop, Δ , through the metal wall was made for a heat flow rate of 200 Btu per hour over a ten inch length of the tube.

$$(137) \quad q = \frac{-K 2 \pi r N \Delta}{1}$$

For iron, $K = 26$

The thickness of the sheet metal tube was 0.016 inches.

$$(138) \quad -200 = \frac{-26(2) \pi (2.0)(10) \Delta}{0.016(12)}$$

$$(139) \quad \Delta = 0.012^{\circ} \text{ F}$$

LONGITUDINAL FLOW OF HEAT

In Run 11, if it is assumed that all of the 16° temperature drop (steady state) between TC-10 and TC-12 occurred in the approximately one inch between the top of the lean phase and TC-10, the following longitudinal heat flow rate is obtained:

$$(140) \quad q = -\frac{K 2 \pi r l \Delta}{N}$$

$$(141) \quad q = \frac{+26(2) \pi (2.0)(0.016)(16)}{12 (1)} = 7.0 \text{ Btu per hr}$$

FLOW OF HEAT THROUGH FITTINGS

The order of magnitude of the rate of heat loss through fittings can be determined if some approximations are made. Taking a vacuum well as an example:

Cross-section area: $\frac{\pi}{4} \left[(0.1875)^2 - (0.140)^2 \right] = 0.0122 \text{ sq in}$

Length of section: $\frac{1}{2} \text{ inch}$

Approximate outside temperature: 120° F

Approximate inside temperature: 250° F

(142) $q = \frac{-26(0.0122)(12)(120-250)}{(144)(\frac{1}{2})} = 7 \text{ Btu per hr}$

SCHMIDT METHOD

The Schmidt plot shown in Figure 10 was constructed as follows

1. At the end of the first time increment (0.93 minutes), the temperature of the inside of the insulation was 78° F. This point was connected with 70° F at the abscissa corresponding with a point half way through the insulation, c. (See Figure 23).
2. At 1.86 minutes, the inside temperature was $87\frac{1}{2}^{\circ}$ F. This was connected with point c and intersected the abscissa corresponding to a point one fourth of the way through the insulation at h. Point f was connected with d, which indicated room temperature (70° F) three-fourths of the distance through the insulation. The temperature for points one-fourth of an inch apart, at the end of the first time interval, was, as follows: 78° (a), 70° (b), 70° (c), 70° (d), 70° (e). At the end of the second interval, the corresponding values were 87.5° (e), 73.8° (f), 70° (c), 70° (d), 70° (e).
3. The line ef intersected the halfway line at i. Continuing on, gi was drawn, intersecting the one-fourth line at K. The line hd was drawn next and intersected the halfway line at l. Points i and e were joined and intersected the three-fourths line at

m. The temperature distribution thus became ghide. Since d and e were at room temperature, the heat had not yet reached the outside of the insulation. It was stated earlier (p44) that the temperature at any point at any time is the mean of the two temperatures Δx ($\frac{1}{4}$ inch) away on either side at a time $\Delta \theta$ (0.93 minutes) previously. Thus, point h, located $\frac{1}{4}$ inch from the metal wall, is the mean of point e, which was the temperature of the inside of the insulation, one time interval earlier, and point c, which was located $\frac{1}{2}$ inch from the metal wall and also was the temperature one time interval before point h. This can be seen more readily in Tables LXVIII and LXIX.

4. At the end of the next time interval (3.72 minutes), the heat flow had just reached the outside of the insulation, i.e. the temperature distribution was jklme.

TABLE LXVIII

Temperature Distribution at Start of Schmidt Method Plot

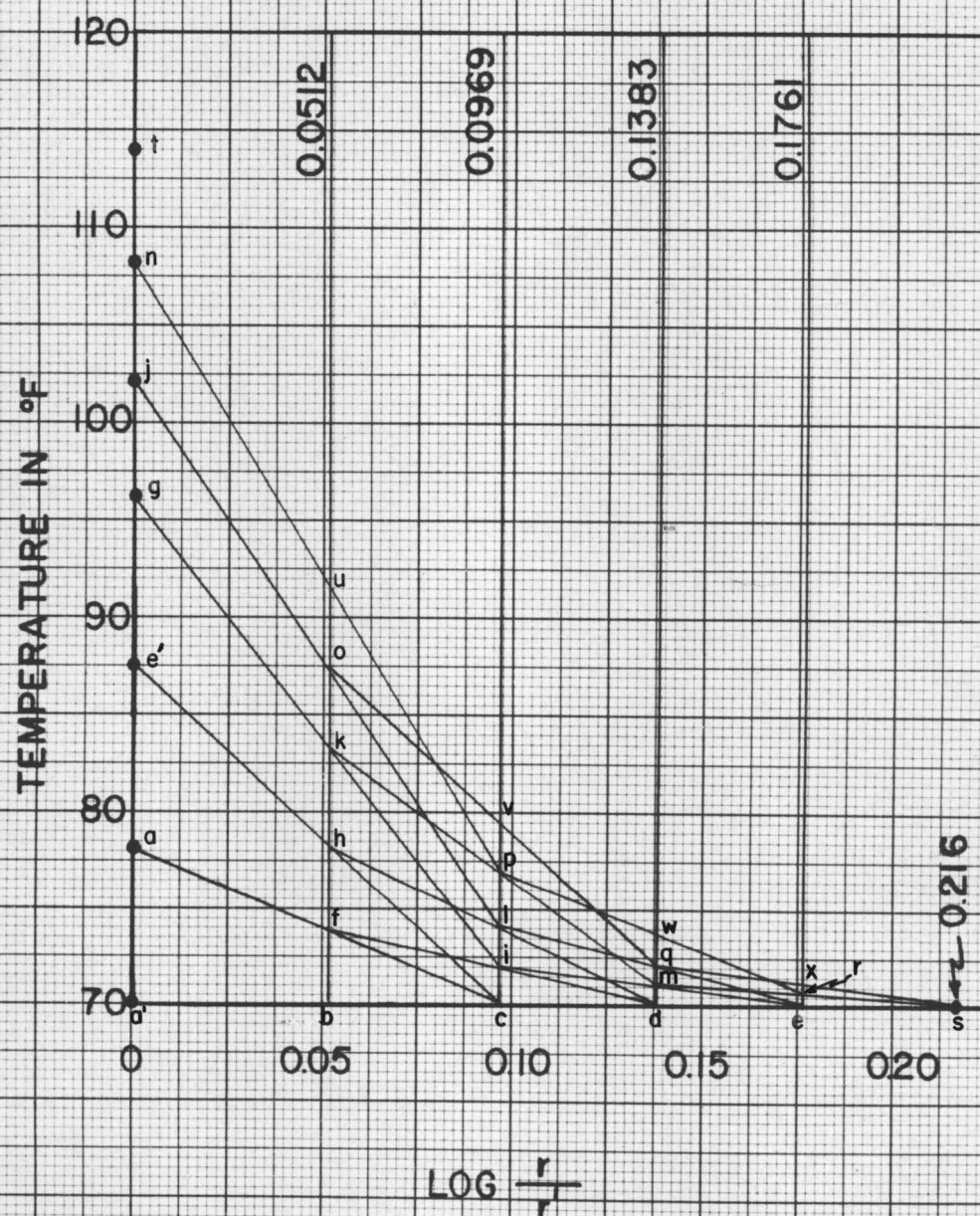
<u>Interval</u>	<u>2"(Inside)</u>	<u>2$\frac{1}{4}$"</u>	<u>2$\frac{1}{2}$"</u>	<u>2-3/4"</u>	<u>3"Outside)</u>
0	70	70	70	70	70
1	78	70	70	70	70
2	87.5	74	70	70	70
3	96	78.5	71.7	70	70
4	102	83.3	73.8	70.8	70
5	108	87.1	76.7	71.9	70.5
6	114	91.5	79.1	73.2	71.0

TABLE LXIX

Location of Points in Temperature Distribution Curves

<u>Interval</u>	<u>2" (Inside)</u>	<u>2$\frac{1}{4}$"</u>	<u>2$\frac{1}{2}$"</u>	<u>2-3/4"</u>	<u>3" (Outside)</u>
0	a'	b	c	d	e
1	a	b	c	d	e
2	e'	f	c	d	e
3	g	h	i	d	e
4	j	k	l	m	e
5	h	o	p	q	r
6	t	u	v	w	x

FIGURE 23
START OF SCHMIDT PLOT FOR RUN 11



5. If there were no resistance to the flow of heat from the outside of the insulation to the room ($h_r = \text{infinity}$), the temperature at the outside of the insulation would always remain 70° F and the graphical construction would pivot about this point. Because of the finite resistance, this pivot point was located at an abscissa of 0.216 (point s). The next temperature distribution was nopqrs. After the sixth time interval (5.59 minutes), the temperature distribution was tuvwx. The construction was continued through the thirtieth time interval. By that time, as seen in Figure 10, the succeeding lines were very close together. Inasmuch as the rate of heat flow to the insulation was nearly constant by this time interval, extrapolation was made without difficulty.

ACCURACY OF RESULTS

An approximation can be made of the maximum error in the values of the coefficient of heat transfer between the air and the tube wall by substituting the worst possible combination into the flow rate equations.

$$(143) \quad q_i = \frac{2\pi N K_i (t' - t_o)}{2.30 \left[0.176 + \frac{K_i}{2.30 h_r r_o} \right]} = h_w 2\pi N r' \frac{(t_7 - t_{12}) - (t_4 - t_{12})}{\ln \frac{(t_7 - t_{12})}{(t_4 - t_{12})}}$$

$$K = -0.041 \pm 0.004$$

$$h_r = 1.8 \pm 0.4$$

$$t' = \pm 10$$

$$t_7, t_{12}, t_4 = \pm 1$$

Taking Run 11 as an example, for

$$(144) \quad q_i = 47 \text{ Btu per hr}$$

$$\Delta_w = 9.5$$

$$\frac{K}{2.30 h_r r_o} = 0.040,$$

$$h_w = 5.2$$

If the following extreme values are assumed:

$$K_i = 0.041 - 0.004$$

$$t' = 168.5 - 10$$

$$h_r = 1.8 - 0.4$$

$$t_7 = 260 + 1$$

$$t_4 = 269 + 1$$

$$t_{12} = 254 - 1$$

$$(145) \quad \frac{K_i}{2.30 h_r r_o} = \frac{0.037(12)}{2.30(1.4)(3.0)} = 0.046$$

$$(146) \quad \Delta_w = \frac{(251-253) - (270-253)}{\ln \frac{261-253}{270-253}} = 11.5^\circ \text{ F}$$

and $h_w = 3.4$

The maximum error is

$$(147) \text{ Error} = \left(\frac{5.2 - 3.4}{5.2} \right) 100 = 35\%$$